Aus der Abteilung für Klinische Pharmakologie

Leiter: Prof. Dr. med. S. Endres

Medizinische Klinik Innenstadt

der Ludwig-Maximilians-Universität München

Direktor: Prof. Dr. med. M. Reincke

Erkennung immunstimulatorischer Nukleinsäuren durch das angeborene Immunsystem

Dissertation

zum Erwerb des Doktorgrades der Medizin

an der Medizinischen Fakultät der

Ludwig-Maximilians-Universität zu München

vorgelegt von

Andrea Ablasser

aus Bad Friedrichshall

2010

Mit Genehmigung der Medizinischen Fakultät

der Universität München

1. Berichterstatter:	Prof. Dr. med. Stefan Endres
2. Berichterstatter:	Prof. Dr. med. Gunther Hartmann
Mitberichterstatter:	Prof. Dr. med. Wolfgang Zimmermann
	PD Dr. med. Marion Subkleve
Mitbetreuung durch die	
Promovierten Mitarbeiter:	Prof. Dr. med. Gunther Hartmann,
	Prof. Dr. med. Veit Hornung
Dekan:	Prof. Dr. med. Dr. h. c. Maximilian Reiser, FACR, FRCR

Tag der mündlichen Prüfung: 11.03.2010

Meinen Eltern in Dankbarkeit

Inhaltsverzeichnis

1. Einleitung

Das Überleben jedes Organismus hängt in entscheidender Weise davon ab, eingedrungene Pathogene zu erkennen und eine Abwehrreaktion gegen sie einzuleiten. Diese Aufgabe obliegt den Zellen und Mechanismen, die unter dem Begriff „Immunsystem“ zusammengefasst werden. Im Angesicht der schnellen und steten Entwicklung und der immensen molekularen Vielfalt ist die zuverlässige Erkennung krankheitsverursachender Mikroben eine der faszinierendsten Eigenschaften unseres Immunsystems. Um dieser Herausforderung zu begegnen verfolgt das Immunsystem von Vertebraten unterschiedliche Strategien, die sich aus einer angeborenen und einer adaptiven Immunantwort zusammensetzen.

1. Grundlegende Konzepte des humanen Immunsystems

Die Funktionsweise des Immunsystems basiert auf seiner Fähigkeit „Selbst“ von „Nicht-Selbst“ zu unterscheiden. Anhand der dieser Differenzierung zugrunde liegenden Mechanismen lässt sich das Immunsystem von Säugetieren formell in zwei Komponenten aufgliedern: dem angeborenen und dem adaptiven Immunsystem. Das adaptive Immunsystem detektiert „Nicht-Selbst“ auf der Grundlage von Antigenen die von Antigen-Rezeptoren auf B-Zellen (B-Zell-Rezeptor, BCR) und T-Zellen (T-Zell-Rezeptor, TCR) erkannt werden. Das Spektrum dieser Antigen-Rezeptoren ist dabei nicht von vorne herein festgelegt, sondern entwickelt sich erst im Zuge der Lymphozytenreifung durch den Prozess der somatischen Rekombination. Darunter versteht man einen genetischen Umlagerungsprozess, worin einzelne Gensegmente des kodierenden Bereichs der Antigen-Rezeptoren zufällig miteinander kombiniert werden. Dieser Mechanismus führt zur Generierung von einem äußerst breiten Repertoire verschiedenster Rezeptoren, die spezifisch ein bestimmtes Antigen erkennen. Die Aktivierung eines Antigen-Rezeptors durch das zu ihm „passenden“ Antigen fördert die klonale Expansion des entsprechenden Lymphozyten und bewirkt durch die Produktion spezifischer Antikörper und durch die Reaktion spezifischer T-Zellen die Eliminierung des relevanten Erregers. Diese hochspezifische Erkennungsstrategie des adaptiven Immunsystems, welches sich ausschließlich in Vertebraten nachweisen lässt, birgt jedoch zwei entscheidende Nachteile. Erstens ist das adaptive Immunsystem mit seinen Antigen-Rezeptoren nicht in der Lage auf die Art des Erregers und den biologischen Kontext der Infektion zu schließen. Eine Fähigkeit, die jedoch von immenser Wichtigkeit ist, da intrazelluläre Erreger über andere Mechanismen eliminiert werden müssen als extrazelluläre Pathogene. Zweitens vollzieht sich die Adaption über einen Zeitraum mehrerer Tage und würde somit für die initiale Bekämpfung schnell replizierender Mikroben zu spät greifen. Das adaptive Immunsystem funktioniert jedoch nicht alleine bei der Abwehr von Infektionen. Vielmehr zeigte sich, dass nahezu alle Aspekte der adaptiven Abwehr durch Signale aus dem angeborenen Immunsystem

gesteuert und reguliert werden. Intensive Forschungsarbeiten lieferten innerhalb der letzten Jahrzehnte ein tief greifendes Verständnis darüber wie die Fremderkennung des angeborenen Immunsystems funktioniert. Eine theoretische Basis hierfür bildet das *pattern recognition* Modell. Dieses System der Pathogenerkennung ist über die Grenzen verschiedener Spezies verbreitet und lässt sich in Pflanzen, Invertebraten und Vertebraten nachweisen {Janeway, 2002}. Die Unterscheidung zwischen „Selbst" und „Nicht-Selbst" erfolgt dabei auf Grundlage einer begrenzten Anzahl invarianter, schon in der Keimbahn vorhandener *pattern recognition* Rezeptoren (PRR). Diese Rezeptoren erkennen aus dem mikrobiellen Metabolismus stammende, hoch konservierte Produkte, die ausschließlich in Pathogenen nicht aber im Wirt selbst akkumulieren. Diese Eigenschaft drückt sich auch in der Bezeichnung dieser Molekülklasse als *pathogen-associated molecular pattern* (PAMP) aus. Das angeborene Immunsystem besitzt eine ganze Reihe derartiger PRRs, die an der Zelloberfläche positioniert sind oder in bestimmten intrazellulären Kompartimenten sequestriert vorliegen. Hierzu zählen die *Toll-like* Rezeptoren und *C-type Lectins* {Takeda, 2005; Huysamen, 2009}. Andere wie die *RIG-I-like* Helikasen und *Nod-like* Rezeptoren lassen sich dagegen im Zytoplasma nachweisen {Yoneyama, 2007; Ting, 2006}.

Die Erkennung von PAMPs durch PRRs liefert die Grundlage für die Einleitung einer adaptiven Immunantwort, dadurch dass sie die Expression kostimulatorischer Faktoren auf Antigen-präsentierenden Zellen reguliert. Ferner bestimmt sie durch das Zusammenspiel sezernierter Zytokine die Art der sich anschließenden Effektorantwort. Die Funktion der Zellen des adaptiven Immunsystems ist somit absolut von den Signalen des angeborenen Systems abhängig. Zusammenfassend lassen sich angeborene und adaptive Immunantworten somit in ein gemeinsames System integrieren, in dem die Mechanismen der angeborene Immunität zunächst greifen und eine unabdingbare Voraussetzung für die sich anschließende adaptive Immunantwort darstellen.

Die Familie der Toll-like Rezeptoren

Unter den verschiedenen Klassen von PRRs bildet die Familie der *Toll-like* Rezeptoren (TLRs) die am besten charakterisierte Gruppe. Wenngleich die exakte Anzahl zwischen einzelnen Spezies variiert, so gilt dennoch, dass die meisten Säugetiere zwischen 10 und 15 TLRs besitzen. TLRs detektieren eine Vielzahl mikrobieller Bestandteile, einschließlich Peptidoglykan aus der Zellwand Gram-positiver Bakterien (erkannt durch TLR2), Lipopolysaccharid aus der Zellwand Gram-negativer Bakterien (erkannt durch TLR4), Flagellin, der Hauptbestandteil bakterieller Flagellen (erkannt durch TLR5), unmethylierte CpG-DNA aus dem Genom von Viren und Bakterien (erkannt durch TLR9) und doppel- bzw. einzel-strängige RNA aus dem Genom diverser Viren (erkannt durch TLR3, TLR7 und TLR8) {Takeda, 2007}. Innerhalb der Familie der TLRs bilden die Nukleinsäure erkennenden TLRs

eine eigene Untergruppe. Dabei grenzen sie sich von den anderen TLRs durch ihre intrazelluläre Lokalisation ab, TLR1, TLR2, TLR3, TLR5 sind demgegenüber an der Zelloberfläche exprimiert. Ein gemeinsames Kennzeichen ist ferner, dass sie zusätzlich zu der Induktion pro-inflammatorischer Zytokine, die von allen TLRs hervorgerufen wird, vor allem die Produktion von Typ I Interferonen vorantreiben {Kawai, 2007}. Eine Aktivierung von TLRs führt über Rezeptor- und Zell-spezifische Signaltransduktionskaskaden zur Aktivierung von *interferon regulatory factors* (IRFs) und NF-κB, die schließlich koordiniert die Induktion der Immunantwort transkriptionell regulieren {Kawai, 2007}.

Intrazelluläre *Pattern-Recognition*-Rezeptoren

Neben dem TLR-System wurden vor kurzem weitere invariante Rezeptor-Familien beschrieben, die bei der Erkennung von PAMPs maßgeblich beteiligt sind. Hierzu zählen die *NOD-like* Rezeptoren (NLR, auch *CATERPILLER*, *NOD-LRR* oder *NACHT-LRR* genannt) und die *Retinoid-acid inducible protein I (RIG-I) – like* Helikasen. Im Unterschied zu TLRs befinden sich Vertreter dieser Familien innerhalb des Zellzytoplasmas. Ihre Entdeckung suggerierte, dass Pathogene, die sich den Erkennungsmechanismen der TLRs entziehen, über einen komplementären, intrazellulären Rezeptorapparat aufgespürt werden können.

NOD-like* Rezeptoren und das *Inflammasom

Die Proteinfamilie der *NOD-like* Rezeptoren (NLRs) zeichnen sich durch eine gemeinsame Rezeptorarchitektur aus mit einer so genannten *nucleotide oligomerization domain* und einer *leucine-rich repeat domain* am C-Terminus. Anhand der Struktur der N-terminalen Domäne unterscheidet man drei Subfamilien: Proteine der NOD-Gruppe enthalten N-terminal eine *caspase recruitment domain* (CARD). Die NAIP-Subgruppe exprimiert am N-Terminus eine *baculoviral inhibitor-of-apoptosis-protein repeat-containing* (BIR) *domain* und eine *Pyrin domain* (PYD) findet sich am N-Terminus der NLRP-Subfamilie. Inzwischen ist erwiesen, dass die Gruppe der NLRs wichtige Aufgaben bei der Erkennung intrazellulärer Bakterien erfüllt. Beispielsweise detektieren Nod1 und Nod2 Substrate, die während der Synthese oder des Abbaus von Peptidoglykan entstehen und sowohl von Gram-negativen als auch Gram-positiven Bakterien produziert werden {Mariathasan, 2007}. Eine Bindung der entsprechenden Agonisten an Nod1 und Nod2 führt über die Aktivierung des Transkripitionsfaktors NF-κB zu der verstärkten Expression einer Vielzahl pro-inflammatorischer Zytokine. Demgegenüber sind andere NLRs, einschließlich IPAF, NLRP1 und NLRP3 an der Formierung eines multimeren, intrazellulären Proteinkomplexes beteiligt, dem sogenannten *Inflammasom* {Martinon, 2002}. Die Formierung dieses makromolekularen Proteinkomplexes bildet

das Gerüst für die Rekrutierung und Aktivierung des Zymogens Procaspase-1. Caspase-1 ist wiederum für die Spaltung von pro-Interleukin 1β (pro-IL-1β) und pro-IL-18 in deren biologisch aktive Formen verantwortlich. IL-1β steuert eine Vielzahl an Immunreaktionen, einschließlich der Rekrutierung von Entzündungszellen zum Ort der Infektion, während IL-18 zur Produktion von Interferon- γ und zur Stärkung der zytolytischen Aktivität Natürlicher Killerzellen beiträgt {Arend, 2008}. Drei Varianten des *Inflammasoms* wurden bis dato teilweise charakterisiert und entsprechend dem zugrundeliegendem NLR benannt (NLRP1, NLRP3, IPAF) {Franchi, 2009}. Es ist bekannt, dass einige Gram-negative Bakterien einschließlich Salmonella typhimurium, Legionella pneumophila, Pseudomonas aeruginosa und Shigella flexneri eine Aktivierung von Caspase-1 über IPAF induzieren {Franchi, 2009}. Demgegenüber wurde das NLRP1 Inflammasom mit der Erkennung von Muramyldipeptid (MDP) assoziiert {Faustin, 2007}. Darüber hinaus scheint NLPR1 für die pathologischen Prozesse im Rahmen einer Infektion mit Bacillus anthracis verantwortlich zu sein {Boyden, 2006}. Ein wesentliches Merkmal des NLRP3 Inflammasoms ist, dass es als Sensor für endogene Gefahrensignale, so genannte *danger-associated molecular patterns* (DAMPs) dienen kann. Harnsäure aus nekrotischen Zellen wurde beispielsweise als endogenes Gefahrensignal identifiziert und kann adaptive Immunantworten einleiten {Shi, 2003s}. Eine weitere Klasse an NLRP3 Agonisten ist repräsentiert durch exogene Kristallbildner, einschließlich Quarz, Asbest und fibrillärem Amyloid-β {Dostert, 2008; Hornung, 2008; Halle, 2008}. Ferner ist bekannt, dass auch kleine Moleküle wie ATP das *Inflammasom* aktivieren können {Mariathasan, 2006}. Wie es möglich ist, dass diese enorme Vielzahl chemisch unterschiedlicher Stimuli durch einen Rezeptorkomplex erkannt werden können ist bis dato noch nicht geklärt.

RIG-I-like **Helikasen**

In einem anderen PRR-System wird virale RNA im Zytosol über die *RIG-I-like* Helikasen (RLH) erkannt, die RIG-I, MDA5 und LGP2 umfassen. Sowohl RIG-I als auch MDA5 besitzen eine zentrale Helikase-Domäne an die doppel-strängige RNA (dsRNA) bindet {Yoneyama, 2007}. Die physiologische Relevanz der RLH bei der Detektion von Virusinfektionen wurde eingehend in Mäusen untersucht, bei denen einzelne RLH ausgeschaltet wurden. Dabei zeigte sich, dass RIG-I für die Erkennung einiger Einzelstrang-RNA (ssRNA) Viren wie beispielsweise Influenza Virus und Newcastle Disease Virus essentiell ist, wohingegen MDA5 im Rahmen einer Infektion mit Picornaviren aktiviert wird {Kato, 2006}. Beide Helikasen interagieren auf eine Stimulation mit ihren entsprechenden Agonisten mit dem Adaptorprotein MAVS (auch Cardif, IPS-1, VISA), welches in der äußeren Membran von Mitochondrien lokalisiert ist {Kawai, 2005; Seth, 2005; Xu, 2005; Meylan, 2005}. Die Rekrutierung der zytosolischen Kinasen IKK und TBK1 führt schließlich über die Aktivierung von IRFs und NF-κB zur Induktion von Typ I Interferon. Es sei an dieser Stelle betont,

dass im Unterschied zu den oben aufgeführten PRRs RLH sowohl in Zellen des Immunsystems als auch in somatischen Zellen operieren. TLRs und NLRs sind hingegen vorwiegend in spezialisierten Immunzellen aktiv.

C-type lectins

C-type lectins umfassen eine äußerst heterogene Protein-Superfamilie, denen vielfältige immunologische Funktionen zugeschrieben werden können. Der Terminus „*C-type lectin"* wurde ursprünglich durch ihre Eigenschaft geprägt, Kohlenhydrate in einem Calciumionen-abhängigen Prozess zu binden. Diese Definition ist mittlerweile überholt, da *C-type lectins* oder *C-type lectin receptors* (CLRs) auch Mitglieder umfasst, die weder in der Lage sind Calcium zu binden noch eine Kohlenhydrat-Spezifität aufweisen. Das inzwischen übliche Klassifizierungsmerkmal basiert auf dem Vorkommen eines konservierten strukturellen Motivs, der so genannten *C-type lectin* Domäne {Drickamer, 1999}. Diese Domäne ist entscheidend für die Spezifität des Rezeptors hinsichtlich der Erkennung seiner entsprechenden Liganden. Eine aktuelle Klassifizierung unterscheidet innerhalb der CLRs 17 distinkte Gruppen {Zelensky, 2005}. Es sei an dieser Stelle betont, dass CLRs im Gegensatz zu der Familie der TLRs oder RLHs keine einheitliche funktionelle Rezeptor-Gruppe bilden, die darauf spezialisiert ist PAMPs zu detektieren. Trotz dieser Einschränkung ist unumstritten, dass manche CLRs PAMPs erkennen und eine Immunantwort induzieren. Beispielsweise bindet die Untergruppe der *Collectins* (CLR Gruppe III), die in Form löslicher Proteine im Serum vorkommen, Pathogene direkt und aktiviert das Komplementsystem. *Mannose-binding lectin*, der Prototyp der *Collectins*, erkennt Zuckerreste, die an der Oberfläche von Viren, Bakterien oder Pilzen exprimiert werden und verleiht dem Körper Schutz vor Infektionen mit Neisseria meningitidis, Staphylococcus aureus und Streptococcus pneumoniae {Takahashi, 2006}. Diese Gruppe der CLRs kann man zwar im weiteren Sinne zu PRRs zählen sie sind aber nicht direkt Zell-assoziiert und nehmen auch keinen Einfluss auf Regulation der Genexpression. Im Gegensatz hierzu aktivieren einige transmembranöse CLR spezifische Signaltransduktionskaskaden in Zellen des angeborenen Immunsystem worüber die Phagozytose von Pathogenen wie auch die Produktion pro-inflammatorischer Zytokine gesteuert wird. Dectin-1, ein β-Glucan-spezifischer CLR, ist zum Beispiel für die Phagozytose von Hefen oder deren Derivate verantwortlich {Herre, 2004}. Darüber hinaus steuert die Aktivierung von Dectin-1 durch das Hefederivat Zymosan auch die Induktion pro-inflammatorischer Zytokine durch Makrophagen und dendritische Zellen {Brown, 2006}. Ferner wurden CLRs beschrieben, die Signalwege anderer PRRs modulieren, per se aber keine Zytokinproduktion hervorrufen. Beispielsweise induziert die Aktivierung des CLR DC-Sign keine inflammatorische Zytokinantwort, verstärkt jedoch die TLR4 getriggerte IL-10 Produktion nach Stimulation mit Lipopolysaccharid {Caparros, 2006}. Der diesem Phänomen zugrunde liegende Mechanismus ist sehr komplex und im Einzelnen noch nicht verstanden.

Ob DC-Sign direkt mit TLRs kooperiert oder ob der Effekt eine synergistische Wirkung von Signaltransduktionskaskaden auf Trankskriptionsebene widerspiegelt bleibt noch zu klären.

2. Antivirale Immunität

Die Erkennung einer Virusinfektion durch die Mechanismen des angeborenen Immunsystems löst eine antivirale Immunantwort aus {Theofilopoulos, 2005}. Genomische Nukleinsäuren und RNA, die im Zuge des viralen Replikationszyklus in infizierten Zellen entsteht, stellen Virus-assoziierte Moleküle dar und werden von PRRs erkannt {McCartney, 2009}. Diese Erkennung leitet unter anderem die Produktion zahlreicher antiviraler Zytokine ein. Insbesondere Typ I Interferone, die sich aus IFN-β und einigen IFN-α Subtypen zusammensetzen, werden von einer Vielzahl von Zellen als Antwort auf eine Virusinfektion produziert und spielen bei der Infektionsabwehr von Viren eine essentielle Rolle {Theofilopoulos, 2005}. Darüber hinaus hängt eine erfolgreiche antivirale Immunantwort auch von der Produktion pro-inflammatorischer Zytokine ab. Hierbei spielen TNF-α und IL-1β eine zentrale Rolle.

Die Erkennung von Nukleinsäuren durch das angeborene Immunsystem

In Anbetracht der Tatsache, dass Nukleinsäuren über die Grenzen aller Spezies hinweg vorkommen, scheint es auf den ersten Blick verwunderlich, dass das Immunsystem basierend auf diesen universellen Makromolekülen eingedrungene Pathogene aufspüren kann. Mittlerweile ist aber klar, dass das immunstimulatorische Potential von Nukleinsäuren nicht ohne weiteres auf die gesamte Molekülklasse übertragen werden kann. Vielmehr existieren mehrere Faktoren, die je nach betrachtetem Zell- und Erkennungsmechanismus, die immunogene Aktivität von DNA und RNA in unterschiedlichem Maße beeinflussen und somit die Qualität und die Quantität der nachfolgenden Immunantwort determinieren.

Die bis heute am intensivsten charakterisierte Interaktion zwischen dem Immunsystem und stimulatorischen Nukleinsäurederivaten ist die Aktivierung von TLR9 durch bakterielle DNA. Die Selektivität dieser Reaktion wird auf das Vorkommen charakteristischer unmethylierter CpG-Motive zurückgeführt, die vor allem im Genom von Bakterien vorzufinden sind {Krieg, 1995}. Die Erkennung dieser CpG-Motive erfolgt im Endosom dendritischer Zellen und Makrophagen und kann zur Induktion einer starken Interferonantwort führen {Latz, 2004}. Darüber hinaus wird seit langem die Existenz eines zytosolischen DNA-Rezeptors postuliert, der den TLR9-abhängigen Signalweg

ergänzt. Grundlage für diese Annahme bildet die Beobachtung, dass im Zytosol vorhandene doppel-strängige DNA (dsDNA) zu einer Aktivierung von Typ I Interferon führt {Ishii, 2006; Stetson, 2006}. Physiologische Relevanz erfährt letzterer Mechanismus dadurch, dass intrazellulär replizierende Baktieren, wie z.B. Listeria monocytogenes und Legionella pneumophila, und auch eine Vielzahl von DNA-Viren wie z.B. Herpes Simplex Virus-1 und Adenoviren über diesen Weg erkannt werden. Im Jahre 2008 wurde mit DAI (*DNA-dependent activator of IFN-regulatory factors*) ein vermeintlicher Kandidat für den intrazellulärer DNA-Rezeptor identifiziert {Takaoka, 2007}. Weitere Studien zeigten jedoch, dass die Funktion von DAI redundant ist und folglich zusätzliche Wege der DNA-Erkennung parallel zu DAI existieren müssen {Wang, 2008; Ishii, 2008}. Im selben Jahr wurde erstmals ein weiterer TLR9-unabhängiger DNA-Erkennungsmechanismus beschrieben, der zur Aktivierung von Caspase-1 und zur Produktion von IL-1β führt {Muruve, 2008}. Es wurde gezeigt, dass dieser Signalweg für die Immunantwort gegenüber Herpesviren relevant ist und durch dsDNA aktiviert werden kann. Die Identifizierung des zugrunde liegenden Rezeptors war zu diesem Zeitpunkt noch nicht erfolgt.

Alternativ aktivieren „fremde“ Nukleinsäuren das Immunsystem auch über RNA-erkennende TLRs (TLR3, TLR7 und TLR8). Schon lange ist bekannt, dass TLR3 lange doppel-strängige RNA (dsRNA), unabhängig von der zugrunde liegenden Sequenz, detektieren kann {Alexopoulou, 2001}. Neuere Erkenntnisse offenbarten ferner die zentrale Bedeutung von TLR7 und TLR8 bei der Erkennung von RNA {Lund, 2004; Heil, 2004; Diebold, 2004}. Im Vorfeld war bereits etabliert, dass Imidazoquinoline das angeborene Immunsystem über einen TLR7- oder TLR8-abhängigen Mechanismus stimulieren können {Jurk, 2002}. Obwohl letztere Moleküle in ihrem chemischen Aufbau den Purinbasen Adenin und Guanosin ähneln, repräsentieren sie keinen in der Natur physiologisch vorkommenden Liganden. Mit einzel-strängiger RNA (ssRNA) sind mittlerweile auch die natürlichen Agonisten für TLR7 und TLR8 identifiziert worden {Heil, 2004; Diebold, 2004}. Diese Schlussfolgerungen beruhten zunächst auf Untersuchungen in denen ssRNA aus dem Genom von HIV-1 oder Influenza Virus isoliert wurde. Aber auch synthetische ssRNA erwies sich als wirkungsstarker Induktor von Typ I Interferonen und pro-inflammatorischen Zytokinen.

Die Beobachtung, dass eine ganze Reihe von RNA Viren über einen TLR-unabhängigen Mechanismus detektiert werden, suggerierte die Existenz weiterer RNA-Erkennungsproteine. 2004 charakterisierten Yoneyama und Mitarbeiter mit RIG-I und MDA5 eine neue Familie intrazellulärer RNA-Rezeptoren {Yoneyama, 2004}. Bereits anfangs war klar, dass die RLH für die Kontrolle von Virusinfektionen essentiell sind und in der Lage sind, dsRNA zu binden. DsRNA wird von einigen Viren im Zuge ihres Replikationszyklus generiert und kommt normalerweise nicht im Zytoplasma von Eukaryoten vor. Daher eignet sich dsRNA als molekulares Muster, das dem Wirt die Präsenz von Viren signalisieren kann. Jedoch bilden nicht alle Viren dsRNA während einer Infektion. 2006

ergänzten Hornung et al. die wesentlichen molekularen Voraussetzungen für eine Aktivierung von RIG-I in dem sie zeigen konnten, dass eine Triphosphatgruppe am 5`-Ende von dsRNA für eine Erkennung durch RIG-I erforderlich ist {Hornung, 2006}. Es ist bekannt, dass virale Polymerasen nach der Synthese Virus-spezifischer RNA eine charakteristische Triphosphatgruppe am 5´Ende des RNA-Transkripts hinterlassen. Zwar erhalten die Transkripte eukaryotischer RNA-Polymerasen während ihrer Synthese im Zellkern initial auch ein Triphosphatende, die meisten endogenen Transkripte unterliegen aber vielfältigen Modifikationen, die das 5´Ende entweder maskieren oder abspalten.

Erst kürzlich konnten wir und Chiu et al. die aktuelle Vorstellung der Erkennung von Nukleinsäuren durch das Immunsystem um einen neuen intrazellulären DNA-Erkennungsweg ergänzen {Ablasser, 2009; Chiu, 2009}. Der beschriebene Erkennungsweg erfolgt dabei indirekt über die Generierung eines stimulatorischen RNA-Zwischenprodukts. Durch die DNA-abhängige RNA-Polymerase III wird im Zytoplasma vorhanden dsDNA in dsRNA umgeschrieben, die am 5´Ende ein Triphosphatende enthält, und von RIG-I erkannt wird.

3. Zusammenfassung der vorliegenden Arbeiten

Um eine Infektion rasch wahrzunehmen verfügt das angeborene Immunsystem über zahlreiche Rezeptorfamilien, die unter anderem *Toll-like* Rezeptoren (TLR), *RIG-I-like* Helikasen (RLH) und *Nucelotide-binding oligomerziation domain-like* Rezeptoren (NLR) umfassen. Gemeinsam erkennen sie molekulare Strukturen, die entweder nur in der Welt der Pathogene vorkommen oder die im Wirt in bestimmten intrazellulären Kompartimenten sequestriert vorliegen und unter normalen Bedingungen keinen Zugang zu diesen Rezeptoren haben. TLRs binden unter anderem einzel- oder doppel-strängige RNA (ssRNA, dsRNA) und DNA, die CpG-Motive beinhaltet, RLHs werden über zytosolische RNA aktiviert und auch NLRs können zytoplasmatische RNA detektieren. Ferner ist schon seit langem bekannt, dass das Vorhandensein von dsDNA im Zytosol Apoptose induzieren kann. Der zugrundeliegende Rezeptor hierfür wurde aber bis vor kurzem noch nicht charakterisiert.

Die Existenz mehrerer komplementären Erkennungsstrategien für ein und dieselbe Molekülklasse veranschaulichen ihre Relevanz für die Funktionsweise des angeborenen Immunsystems. Obwohl alle diese Erkennungsstrategien die Eigenschaft aufweisen, Pathogene aufgrund ihrer Nukleinsäuren aufzuspüren, hatte sich gezeigt, dass sie sich in grundlegenden Charakteristika unterscheiden. Hierzu zählen unterschiedliche Ligandenspezifitäten, distinkte intrazelluläre Positionen und ein anderes zelluläres Expressionsmuster. Die evolutionäre Logik hinter einer spezifischen Kombination dieser

Parameter ist im Moment noch nicht abschließend geklärt und stellt eine der grundlegenden Fragestellungen im Feld der angeborenen Immunität dar.

Vor diesem Hintergrund war es ein Ziel der hier vorliegenden Arbeit die differentiellen Effekte zu untersuchen, die eine Stimulation mit RNA auslöst. Die Identifikation des synthetischen RIG-I Liganden Triphosphat-RNA eröffnete die Möglichkeit verschiedene Immunzellpopulationen, namentlich Monozyten und plasmazytoide dendritische Zellen (PDC) hinsichtlich ihrer Reaktivität auf diesen Stimulus zu analysieren. Im Weiteren richtete sich das Hauptaugenmerk auf den mechanistischen Hintergrund der RNA-Erkennung und hier insbesondere auf die Beteiligung von TLRs und RIG-I. Abschließend sollten immunstimulatorische Komponenten von RNA-Oligonukleotiden herausgearbeitet werden, die es ermöglichen spezifisch eine TLR- bzw. RIG-I-abhängige Immunantwort hervorzurufen.

Es stellte sich heraus, dass Monozyten ausschließlich über die zytoplasmatische Detektion von Triphosphat-RNA (3pRNA) durch RIG-I in der Lage sind, Interferon zu produzieren. Das TLR-System lieferte in Monozyten hingegen keinen Beitrag zur Synthese von Typ I Interferon. In PDC zeigte sich demgegenüber eine reziproke Erkennungsstrategie. Hier erfolgte die Erkennung von 3pRNA durch TLR7. RIG-I ist in PDC an der Erkennung von 3pRNA überraschenderweise nicht involviert. Um eine TLR-abhängige Stimulation von Monozyten hervorzurufen wurde ein alternatives Verfahren entwickelt, um RNA effektiv in Endosomen zu platzieren, dort wo TLRs in hoher Dichte exprimiert werden. Unter Verwendung polykationischer Peptide als Transfektionsreagens gelang es nun auch durch RNA eine TLR-abhängige Aktivierung von Monozyten zu induzieren. Überraschend war der Befund, dass es damit möglich erschien auch die Produktion großer Mengen des Th-1 induzierenden Zytokins IL-12p70 hervorzurufen, einem sonst sehr streng regulierten Zytokin. Parallel zur Induktion pro-inflammatorischer Zytokine fiel die Produktion von Typ I Interferon ab. Zusammenfassend legen diese Beobachtungen nahe, dass unabhängig von dem zugrunde liegenden Liganden die RNA-Erkennung in entschiedener Weise sowohl von dem betrachteten Zelltyp als auch von der intrazellulären Positionierung der RNA (Endosom versus Zytoplasma) determiniert wird.

Der zweite Teil der hier vorliegenden Arbeit beschäftigt sich mit der Aktivierung des *Inflammasoms* durch dsDNA. Um nach Rezeptoren zu suchen die als Kandidat für die Erkennung dsDNA in Frage kommen wurde auf die PFAM Datenbank zurückgegriffen. Diese Datenbank speichert Proteinsequenzen und kategorisiert sie anhand bestimmter funktioneller Regionen innerhalb der Proteinsequenz. Auf diese Weise ist es möglich, gezielt nach Proteinen mit bestimmten Domänen zu suchen. Eine Voraussetzung für potentielle Kandidaten des DNA-Rezeptors war das Vorkommen einer Pyrin-Domäne, da bereits für andere NLRs gezeigt wurde, dass diese Domnäne für die Interaktion mit dem Adaptorprotein ASC erforderlich ist. Die PFAM Datenbanksuche nach Proteinen

mit Pyrin-Domäne lieferte unter anderem Proteine der PYHIN Familie. Diese Familie war dabei insbesondere von Interesse, da sie zusätzlich zu einer Pyrin-Domäne auch eine HIN200-Domäne besitzt, die DNA-Bindungseigenschaften aufweist. Im Menschen gibt es vier Vertreter der PYHIN Proteinfamilie, die IFIX, IFI16, MNDA und AIM2 umfassen. Wie sich herausstellte, war nur AIM2 im Zytosol lokalisiert und nur die Überexpression von AIM2 führte zu einer Interaktion mit ASC und schließlich zur Aktivierung von Caspase-1. Ferner konnte gezeigt werden, dass AIM2 an dsDNA bindet und die Herunterregulation von AIM2 zu einer Reduktion der Caspase-1 Aktivierung nach Stimulation mit dsDNA führte. Die Erkennung von Vaccinia Virus über den AIM2-Inflammasome Signalweg unterstreicht die physiologische Relevanz von AIM2 bei der Detektion von Pathogenen.

Beitrag des Doktoranden zu der in Ko-autorenschaft publizierten Arbeit:
Veit Hornung konzipierte die Arbeit und führte die Experiment mit Andrea Ablasser, Marie Charrel-Dennis, Franz Bauernfeind und Gabor Horvath durch. Daniel R. Caffrey führte die Sequenzanalysen durch. Eicke Latz und Katherine A. Fitzgerald betreuten das gesamte Projekt.

4. Summary of the presented publications

To detect infection quickly, the immune system relies on several families of receptors including the TLR family, RLHs and NLRs. Together these receptor systems detect molecules that are either unique to pathogens or that the corresponding host molecules are sequestered in intracellular compartments distinct from those in which the receptors are located. TLRs recognize single-stranded (ss) or double-stranded (ds) RNA or DNA containing CpG motifs in endosomes, RLRs bind cytoplasmic ssRNA or dsRNA and one of the NLRs, NALP3 (*Nacht domain-, leucine-rich repeat-, and PYD-containing protein 3*), can be activated by cytoplasmic nucleic acids. Furthermore, it has been known for many years that cytosolic DNA can trigger apoptosis, but the underlying mechanism for this phenomenon has not been elucidated so far.

The first section of this work focuses on the differential mechanism of RNA recognition employed by monocytes or plasmacytoid dendritic cells. In monocytes only cytosolic detection of triphosphate RNA (3pRNA) induces type I interferon production, whereas activation of the TLR pathway did not contribute to this response. This was in contrast to the situation in PDCs, here RNA was mainly detected through endosomal recognition via TLR7 but not RIG-I. To obtain TLR-dependent activation of monocytes by RNA an alternative delivery strategy was developed. Using polycationic peptides instead of a polycation lipid formulation, robust TLR8 activation was observed. Surprisingly this

response was accompanied by massive production of IL-12p70, a tightly controlled cytokine that is regarded to be low expressed by monocytes. In addition, the increase of IL-12p70 production paralleled with a decline in type I interferon induction, when poly-cationic peptides were used for RNA delivery. Altogether, these observations show that independent of the underlying RNA structure, recognition is mainly influenced by both cell-type specificity and intracellular distribution of the stimulatory RNA molecule.

The second section deals with dsDNA-induced activation of the inflammasome. Based on a bioinformatics approach using the PFAM database candidate receptors for dsDNA recognition and subsequent Caspase-1 activation were searched. Given that NLRs interact with the adaptor protein ASC through their Pyrin domain, it was hypothesized that a potential candidate receptor should contain at least a Pyrin domain. Based on this assumption the PYHIN protein family was identified. In humans this family consists of four members including IFIX, IFI16, MNDA and AIM2. Importantly, in addition to the Pyrin domain PYHIN proteins contain a HIN domain, which is capable of DNA binding. Of all PYHIN proteins only AIM2 localized in the cytosol and only AIM2 could interact with ASC and lead to the activation of Caspase-1. Furthermore, downregulation of AIM2 abrogated Caspase-1 activation. In addition it was shown, that AIM2 is essential for Vaccinia Virus induced Caspase-1 activation and hence underlines the importance of AIM2 for the recognition of intracellular pathogens.

Doctoral candidate´s contribution to the co-authorship:

Veit Hornung conceived the research and conducted the experiments with Andrea Ablasser, Marie Charrel-Dennis, Franz Bauernfeind und Gabor Horvath. Daniel R. Caffrey performed sequence analysis. Eicke Latz und Katherine A. Fitzgerald oversaw the whole project.

5. Literatur

Ablasser A, Bauernfeind F, Hartmann G, Latz E, Fitzgerald KA, Hornung V. 2009. RIG-I-dependent sensing of poly(dA:dT) through the induction of an RNA polymerase III-transcribed RNA intermediate. *Nat Immunol* 10: 1065-72

Alexopoulou L, Holt AC, Medzhitov R, Flavell RA. 2001. Recognition of double-stranded RNA and activation of NF-kappaB by Toll-like receptor 3. *Nature* 413: 732-8

Arend WP, Palmer G, Gabay C. 2008. IL-1, IL-18, and IL-33 families of cytokines. *Immunol Rev* 223: 20-38

Boyden ED, Dietrich WF. 2006. Nalp1b controls mouse macrophage susceptibility to anthrax lethal toxin. *Nat Genet* 38: 240-4

Brown, GD. 2006. Dectin-1: a signalling non-TLR pattern recognition receptor. *Nat Rev Immunol* 6:33-43

Caparros E, Munoz P, Sierra-Filardi E, Serrano-Gomez D, Puig-Kroger A, Rodriguez-Fernandez JL, Mellado M, Sancho J, Zubiaur M, Corbi AL. 2006. DC-SIGN ligation on dendritic cells results in ERK and PI3K activation and modulates cytokine production. *Blood* 107: 3950-8

Chiu YH, Macmillan JB, Chen ZJ. 2009. RNA polymerase III detects cytosolic DNA and induces type I interferons through the RIG-I pathway. *Cell* 138: 576-91

Diebold SS, Kaisho T, Hemmi H, Akira S, Reis e Sousa C. 2004. Innate antiviral responses by means of TLR7-mediated recognition of single-stranded RNA. *Science* 303: 1529-31

Dostert C, Petrilli V, Van Bruggen R, Steele C, Mossman BT, Tschopp J. 2008. Innate immune activation through Nalp3 inflammasome sensing of asbestos and silica. *Science* 320: 674-7

Drickamer K. 1999. C-type lectin-like domains. *Curr Opin Struct Biol* 9: 585-90

Faustin B, Lartigue L, Bruey JM, Luciano F, Sergienko E, Bailly-Maitre B, Volkmann N, Hanein D, Rouiller I, Reed JC. 2007. Reconstituted NALP1 inflammasome reveals two-step mechanism of caspase-1 activation. *Mol Cell* 25: 713-24

Franchi L, Eigenbrod T, Munoz-Planillo R, Nunez G. 2009. The inflammasome: a caspase-1-activation platform that regulates immune responses and disease pathogenesis. *Nat Immunol* 10: 241-7

Halle A, Hornung V, Petzold GC, Stewart CR, Monks BG, Reinheckel T, Fitzgerald KA, Latz E, Moore KJ, Golenbock DT. 2008. The NALP3 inflammasome is involved in the innate immune response to amyloid-beta. *Nat Immunol* 9: 857-65

Heil F, Hemmi H, Hochrein H, Ampenberger F, Kirschning C, Akira S, Lipford G, Wagner H, Bauer S. 2004. Species-specific recognition of single-stranded RNA via toll-like receptor 7 and 8. *Science* 303: 1526-9

Herre J, Marshall AS, Caron E, Edwards AD, Williams DL, Schweighoffer E, Tybulewicz V, Reis e Sousa C, Gordon S, Brown GD. 2004. Dectin-1 uses novel mechanisms for yeast phagocytosis in macrophages. *Blood* 104: 4038-45

Hornung V, Ablasser A, Charrel-Dennis M, Bauernfeind F, Horvath G, Caffrey DR, Latz E, Fitzgerald KA. 2009. AIM2 recognizes cytosolic dsDNA and forms a caspase-1-activating inflammasome with ASC. *Nature* 458: 514-8

Hornung V, Bauernfeind F, Halle A, Samstad EO, Kono H, Rock KL, Fitzgerald KA, Latz E. 2008. Silica crystals and aluminum salts activate the NALP3 inflammasome through phagosomal destabilization. *Nat*

Immunol 9: 847-56

Hornung V, Ellegast J, Kim S, Brzozka K, Jung A, Kato H, Poeck H, Akira S, Conzelmann KK, Schlee M, Endres S, Hartmann G. 2006. 5'-Triphosphate RNA is the ligand for RIG-I. *Science* 314: 994-7

Huysamen C, Brown GD. 2009. The fungal pattern recognition receptor, Dectin-1, and the associated cluster of C-type lectin-like receptors. *FEMS Microbiol Lett* 290: 121-8

Ishii KJ, Coban C, Kato H, Takahashi K, Torii Y, Takeshita F, Ludwig H, Sutter G, Suzuki K, Hemmi H, Sato S, Yamamoto M, Uematsu S, Kawai T, Takeuchi O, Akira S. 2006. A Toll-like receptor-independent antiviral response induced by double-stranded B-form DNA. *Nat Immunol* 7: 40-8

Ishii KJ, Kawagoe T, Koyama S, Matsui K, Kumar H, Kawai T, Uematsu S, Takeuchi O, Takeshita F, Coban C, Akira S. 2008. TANK-binding kinase-1 delineates innate and adaptive immune responses to DNA vaccines. *Nature* 451: 725-9

Janeway CA, Jr., Medzhitov R. 2002. Innate immune recognition. *Annu Rev Immunol* 20: 197-216

Jurk M, Heil F, Vollmer J, Schetter C, Krieg AM, Wagner H, Lipford G, Bauer S. 2002. Human TLR7 or TLR8 independently confer responsiveness to the antiviral compound R-848. *Nat Immunol* 3: 499

Kato H, Takeuchi O, Sato S, Yoneyama M, Yamamoto M, Matsui K, Uematsu S, Jung A, Kawai T, Ishii KJ, Yamaguchi O, Otsu K, Tsujimura T, Koh CS, Reis e Sousa C, Matsuura Y, Fujita T, Akira S. 2006. Differential roles of MDA5 and RIG-I helicases in the recognition of RNA viruses. *Nature* 441: 101-5

Kawai T, Akira S. 2007. TLR signaling. *Semin Immunol* 19: 24-32

Kawai T, Takahashi K, Sato S, Coban C, Kumar H, Kato H, Ishii KJ, Takeuchi O, Akira S. 2005. IPS-1, an adaptor triggering RIG-I- and Mda5-mediated type I interferon induction. *Nat Immunol* 6: 981-8

Krieg AM, Yi AK, Matson S, Waldschmidt TJ, Bishop GA, Teasdale R, Koretzky GA, Klinman DM. 1995. CpG motifs in bacterial DNA trigger direct B-cell activation. *Nature* 374: 546-9

Lund JM, Alexopoulou L, Sato A, Karow M, Adams NC, Gale NW, Iwasaki A, Flavell RA. 2004. Recognition of single-stranded RNA viruses by Toll-like receptor 7. *Proc Natl Acad Sci U S A* 101: 5598-603

Mariathasan S, Monack DM. 2007. Inflammasome adaptors and sensors: intracellular regulators of infection and inflammation. *Nat Rev Immunol* 7: 31-40

Mariathasan S, Weiss DS, Newton K, McBride J, O'Rourke K, Roose-Girma M, Lee WP, Weinrauch Y, Monack DM, Dixit VM. 2006. Cryopyrin activates the inflammasome in response to toxins and ATP. *Nature* 440: 228-32

Martinon F, Burns K, Tschopp J. 2002. The inflammasome: a molecular platform triggering activation of inflammatory caspases and processing of proIL-beta. *Mol Cell* 10: 417-26

McCartney SA, Colonna M. 2009. Viral sensors: diversity in pathogen recognition. *Immunol Rev* 227: 87-94

Meylan E, Curran J, Hofmann K, Moradpour D, Binder M, Bartenschlager R, Tschopp J. 2005. Cardif is an adaptor protein in the RIG-I antiviral pathway and is targeted by hepatitis C virus. *Nature* 437: 1167-72

Muruve DA, Petrilli V, Zaiss AK, White LR, Clark SA, Ross PJ, Parks RJ, Tschopp J. 2008. The inflammasome recognizes cytosolic microbial and host DNA and triggers an innate immune response. *Nature* 452: 103-7

Seth RB, Sun L, Ea CK, Chen ZJ. 2005. Identification and characterization of MAVS, a mitochondrial antiviral signaling protein that activates NF-kappaB and IRF 3. *Cell* 122: 669-82

Shi Y, Evans JE, Rock KL. 2003. Molecular identification of a danger signal that alerts the immune system to dying cells. *Nature* 425: 516-21

Stetson DB, Medzhitov R. 2006. Recognition of cytosolic DNA activates an IRF3-dependent innate immune response. *Immunity* 24: 93-103

Takahashi K, Ip WE, Michelow IC, Ezekowitz RA. 2006. The mannose-binding lectin: a prototypic pattern recognition molecule. *Curr Opin Immunol* 18: 16-23

Takaoka A, Wang Z, Choi MK, Yanai H, Negishi H, Ban T, Lu Y, Miyagishi M, Kodama T, Honda K, Ohba Y, Taniguchi T. 2007. DAI (DLM-1/ZBP1) is a cytosolic DNA sensor and an activator of innate immune response. *Nature* 448: 501-5

Takeda K, Akira S. 2005. Toll-like receptors in innate immunity. *Int Immunol* 17: 1-14

Takeda K, Akira S. 2007. Toll-like receptors. *Curr Protoc Immunol* Chapter 14: Unit 14 2

Theofilopoulos AN, Baccala R, Beutler B, Kono DH. 2005. Type I interferons (alpha/beta) in immunity and autoimmunity. *Annu Rev Immunol* 23: 307-36

Ting JP, Kastner DL, Hoffman HM. 2006. CATERPILLERs, pyrin and hereditary immunological disorders. *Nat Rev Immunol* 6: 183-95

Wang Z, Choi MK, Ban T, Yanai H, Negishi H, Lu Y, Tamura T, Takaoka A, Nishikura K, Taniguchi T. 2008. Regulation of innate immune responses by DAI (DLM-1/ZBP1) and other DNA-sensing molecules. *Proc Natl Acad Sci U S A* 105: 5477-82

Xu LG, Wang YY, Han KJ, Li LY, Zhai Z, Shu HB. 2005. VISA is an adapter protein required for virus-triggered IFN-beta signaling. *Mol Cell* 19: 727-40

Yoneyama M, Fujita T. 2007. RIG-I family RNA helicases: cytoplasmic sensor for antiviral innate immunity. *Cytokine Growth Factor Rev* 18: 545-51

Yoneyama M, Kikuchi M, Natsukawa T, Shinobu N, Imaizumi T, Miyagishi M, Taira K, Akira S, Fujita T. 2004. The RNA helicase RIG-I has an essential function in double-stranded RNA-induced innate antiviral responses. *Nat Immunol* 5: 730-7

Zelensky AN, Gready JE. 2005. The C-type lectin-like domain superfamily. *FEBS J* 272: 6179-217

2. Ergebnisse

2. 1. Selection of molecular structure and delivery of RNA oligonucleotides to activate TLR7 versus TLR8 and to induce high amounts of IL-12p70 in primary human monocytes

Ablasser A, Poeck H, Anz D, Berger M, Schlee M, Kim S, Bourquin C, Goutagny N, Jiang Z, Fitzgerald KA, Rothenfusser S, Endres S, Hartmann und Hornung V.

J Immunol. 2009 Jun 1;182(11):6824-33.

Selection of molecular structure and delivery of RNA oligonucleotides to activate TLR7 versus TLR8 and to induce high amounts of IL-12p70 in primary human monocytes[1]

Andrea Ablasser [*,+], Hendrik Poeck [*,+], David Anz [+], Michael Berger [+], Martin Schlee [*], Sarah Kim [+], Carole Bourquin [+], Nadege Goutagny [§], Zhaozhao Jiang [§], Katherine A. Fitzgerald [§], Simon Rothenfusser [+,‡], Stefan Endres [+], Gunther Hartmann [2,*] and Veit Hornung [2,*]

[*] Institute of Clinical Chemistry and Pharmacology, University Hospital, University of Bonn, Germany

[+] Division of Clinical Pharmacology, Department of Internal Medicine, Ludwig-Maximilians-University of Munich, Germany

[‡] Section Gastroenterology and Endocrinology, Department of Internal Medicine, University of Munich, 80336 Munich, Germany

[§] Division of Infectious Diseases, Department of Medicine, University of Massachusetts, Worcester, MA, USA

[2] Contributed equally

[1] This study was supported by grants BMBF Biofuture 0311896, SFB 670, SFB 704, KFO115 and KFO 177 to G.H.

Corresponding author:
Gunther Hartmann, M.D.
Institute of Clinical Chemistry and Pharmacology
University Hospital, University of Bonn
Sigmund-Freud-Str. 25
53105 Bonn
Germany
Tel: +49-228-287-16080
Fax: +49-228-287-16094
Email: gunther.hartmann@uni-bonn.de

Running title: RIG-I versus TLR activation by RNA oligonucleotides

Keywords: TLR7, TLR8, RIG-I, MDA5, monocytes, IFN-α, IL-12

Abstract

Detection of non-self RNA by Toll-like receptors (TLRs) within endosomes and by RIG-I-like helicases (RLHs) in the cytosol is central to mammalian antiviral immunity. Here we used pathway-specific agonists and targeted delivery to address RNA immunorecognition in primary human immune cells. Within PBMC, plasmacytoid dendritic cells (PDC) and monocytes were found to be responsible for IFN-α production upon immunorecognition of RNA. The mechanisms of RNA recognition in PDC and monocytes were distinct: In PDC recognition of single-strand (ss) and double-strand (ds) RNA oligonucleotides was TLR7-dependent whereas a 5' triphosphate moiety (RIG-I ligand activity) had no major contribution to IFN-α production. In monocytes the response to RNA oligonucleotides was mediated either by TLR8 or RIG-I: TLR8 was responsible for IL-12 induction upon endosomal delivery of ssRNA oligonucleotides; RIG-I was responsible for IFN-α production upon delivery of 5' triphosphate RNA into the cytosol. In conclusion, the dissection of these pathways by selecting the appropriate structure and delivery of RNA reveals PDC as major producer of IFN-α upon TLR-mediated stimulation and monocytes as major producer of IFN-α upon RIG-I-mediated stimulation; furthermore our results uncover the potential of monocytes to function as major producers of IL-12p70, a key Th1 cytokine - classically ascribed to myeloid dendritic cells - that can not be induced by CpG oligonucleotides in the human system.

Introduction

The presence of viral nucleic acids represents a danger signal for the immune system that initiates an antiviral immune response to impede viral replication and to consecutively eliminate the invading pathogen (1). In order to detect foreign nucleic acids immune cells are equipped with a set of pattern recognition receptors (PRR) that act at the frontline of the recognition process and which can be categorized into two major classes. First, members of the family of Toll-like receptors (TLR) have been implicated in the detection of long double-strand (ds) RNA (TLR3) (2), single-strand (ss) RNA (TLR7 and 8) (3, 4), short dsRNA (TLR7) (5) and CpG DNA (TLR9) (6), respectively. These nucleic acids sensing TLRs operate mainly within immune cells by responding to viral nucleic acids that have been ingested by the cell and are incorporated into endosomal compartments (7). Recently, the discovery of the cytoplasmic RNA helicases retinoic-acid inducible gene-I (RIG-I), melanoma differentiation-associated gene 5 (MDA5) and laboratory of genetics and physiology 2 (LGP2) has expanded the repertoire of the cellular virus-sensing receptors and constitutes a second class of immunoreceptors for nucleic acids (8, 9). These helicases function collectively as PRRs to detect replicating viruses and their genetic RNA components. As opposed to TLRs, cytosolic helicases are expressed in a wide spectrum of cell types including immune cells and non-immune cells like fibroblasts or epithelial cells (10). Both receptor systems co-operate to optimize detection of viral RNA.

Given the abundance of host RNA present in the cytoplasm it is an intricate task to specifically and reliably sense virus-derived RNA. Maximal sensitivity along with a high degree of specificity for “non-self” characteristics is required. Two major concepts seem to be in place to distinguish non-self from self via a protein receptor-based recognition system: (1) Detection of a certain molecular pattern that is specific for the pathogen and does not occur in the host system and (2) recognition based on pathogen-specific compartimentalization. For detection of pathogen-derived nucleic acids both mechanisms apply. Structural signatures exist that allow immune receptors to determine the origin of RNA. Long dsRNA is indicative for non-self RNA and has been proposed to stimulate an IFN response via TLR3 (2), RIG-I (9) and MDA5 (11). The 5’ triphosphate moiety of viral RNA transcripts, a characteristic feature of de novo transcribing RNA polymerases, was identified to be the ligand for RIG-I (12) (13). While endogenous host RNA transcripts initially also contain a 5’ triphosphate end, several nuclear posttranscriptional modifications of the host RNA including 5’ capping,

endonucleolytic cleavage and base- and backbone modifications of the nascent RNA transcript lead to ignorance by RIG-I. In addition, blunt-end short dsRNA has also been postulated to stimulate RIG-I (14). A clearly defined molecular pattern has not been reported for the ssRNA sensing TLRs (TLR7 and TLR8). However, the fact that certain sequence motifs are preferred over others suggests that the composition of nucleotides, on top of endosomal localization, might represent another basis to discriminate between self and non-self RNA (3-5, 8, 9, 15, 16).

Notably, also host RNA can regain the ability to stimulate an IFN response under certain pathologic situations, indicating that there is more to the immune system's definition of "foreign" than the underlying molecular structure (17)(18)(19)(20)(21). In fact, the subcellular localization of RNA receptors constitutes an important aspect of RNA recognition. Whereas RIG-I and MDA5 are expressed within the cytoplasm, TLR7, TLR8 and in immune cells also TLR3 are positioned within endosomal compartments (22,23). The sequestration of TLRs within certain subcellular compartments is believed to minimize the chance to encounter host-derived RNA while simultaneously maximize the probability to sense virus-derived RNA, which has entered the cell via the endocytosis pathway.

In this context it is important to keep in mind that RNA due to its susceptibility to nuclease degradation usually requires a cargo vehicle for protection and cellular delivery. Viral genomic RNA or DNA is usually protected by a viral capsid, a heterogeneous membrane composed of lipids and proteins. A common strategy harnessed to deliver synthetic RNA is to use transfection reagents, mostly lipid-based formulations.

Detection of viral nucleic acids by the immune system results in the production of type I IFNs (IFN-α and IFN-β) and various other cytokines finally promoting innate and adaptive immunity (1). Within immune cells dendritic cells (DC) and monocytes express the broadest spectrum of nucleic acids sensing TLRs (24). Plasmacytoid dendritic cells (PDC) express both TLR7 and TLR9 and are known to represent the major source of IFN-α within peripheral blood. Myeloid dendritic cells (MDC) express TLR3, TLR7 and TLR8 and produce interleukin-12 (IL-12), the key cytokine to promote Th1 polarization (25-27). However, IL-12 induction within DC is tightly controlled (29, 30). IL-12 production in monocytes (TLR8) is regarded to be weak.

The use of defined RIG-I ligand triphosphate RNA (3pRNA) allowed us to uncover the relationship between TLR7 in PDC and RIG-I and TLR8 in monocytes, respectively. Here we identify PDC as the major source of IFN-α in response to endosomal ssRNA and dsRNA, monocytes as the major source of IFN-α in response to cytoplasmic 3pRNA and monocytes as the major source of IL-12p70 in response to endosomal ssRNA. The results presented here provide a rationale for developing immunostimulatory oligoribonucleotides as adjuvants for cancer or as antiviral compounds.

Material and Methods

Media and reagents

RPMI 1640 (Biochrom, Berlin, Germany) supplemented with 10% (v/v) heat-inactivated FCS (Invitrogen, Karlsruhe, Germany), 1.5 or 3 mM L-glutamine, 100 U/ml penicillin and 100 µg/ml streptomycin (all from Sigma-Aldrich, Munich, Germany) was used. Recombinant human IFN-β and IL-3 were purchased from R&D Systems GmbH (Wiesbaden-Nordenstadt, Germany). CpG ODN was purchased from Coley Pharmaceutical Group (Wellesley, MA, US) and was used at a final concentration of 3 µg/ml (underlined letters, phosphorothioate linkage at the 3` end of the base; bold letters, CpG dinucleotides): ODN 2216: 5`-GGGGGA**CG**AT**CG**TC**G**GGGGG-3`. The TLR7/8 agonist R848 was purchased from Invivogen (San Diego, CA, US), Polyinosinic:polycytidylic acid (poly(I:C)) was purchased from Sigma-Aldrich.

Mice

TLR7-deficient mice were kindly provided by S. Akira (3). Female C57BL/6 mice were purchased from Harlan-Winkelmann (Borchen, Germany). Mice were 6-12 weeks of age at the onset of experiments. Animal studies were approved by the local regulatory agency (Regierung von Oberbayern, Munich, Germany).

Cell culture

PDC from Flt3-ligand-induced (Flt3-L) bone marrow cultures were sorted with B220 microbeads (Miltenyi Biotec, Bergisch-Gladbach, Germany). Murine primary cells were cultivated in VLE RPMI 1640 (Biochrom) supplemented with 10% FCS, 100 µg/mL streptomycin, 100 U/mL penicillin, 3 mM L-glutamine and 10 mM β-mercaptoethanol. Human PBMC were isolated from whole human blood of healthy, voluntary donors by Ficoll-Hypaque density gradient centrifugation (Biochrom). PDC were positively depleted using magnetically labelled anti-CD304 antibody (Miltenyi Biotec). PDC isolation was always performed prior to the following purification steps to exclude IFN-production by contaminating PDC. Untouched monocytes were obtained by negative depletion from PBMC after isolation of PDC according to the manufacturer's instructions (Human Monocyte Isolation Kit II, Miltenyi Biotec). MDC were purified from PBMC by immunomagnetic sorting with anti-CD1c beads (CD1c (BDCA-1)+ Dendritic Cell Isolation Kit, human, Miltenyi Biotec). Viability of all cells was above 95 %, as determined by trypan blue

exclusion. If not indicated otherwise, cells were cultured in 96-well plates for stimulation experiments. MDC (0,5 Mio/ ml) were kept in RPMI 1640 containing 10% FCS, 1.5mM L-glutamine, 100 U/ml penicillin and streptomycin 100 µg/ml. PDC (0,25 Mio /ml) were cultured in complete medium as described above supplemented with 10 ng/ml IL-3 (R&D Systems GmbH). PBMC (2 Mio/ml) and Monocytes (0,5 Mio/ml) were resuspended in RPMI medium with 2% AB serum (BioWhittaker, Heidelberg, Germany), 1.5mM L-glutamine, 100 U/ml penicillin and streptomycin (100 µg/ml). All compounds were tested for endotoxin contamination prior to use.

***In vitro* cell stimulation and transfection**

CpG ODN was used at a final concentration of 3 µg/ml. Stimulation with the TLR7/8 agonist R848 was performed at a concentration of 5 µg/ml. Exogenous stimulation with poly(I:C) without transfection was performed at doses of 10 µg/ml. RNAs were transfected with Lipofectamine 2000 (Invitrogen) according to the manufacturer's protocol. Cells were transfected with 200ng of nucleic acid with 0,5µl of Lipofectamine 2000. As a control we used Lipofectamine 2000 diluted in OPTIMEM (Invitrogen) without nucleic acids. For transfection with the polycationic polypeptide Poly-L-Arginine (pLa) (P7762 from Sigma), 239ng nucleic acids diluted in 15 µl PBS (PAA Laboratories GmBH, Germany) were mixed with 280ng pLa and incubated for 20min prior to stimulation. The particle size (600 – 700 nm) and ζ potential (10±5 mV) were determined by dynamic light scattering and potentials were measured electrophoretically (Zetasizer 3000HS; Malvern Instruments, Herrenberg, Germany). Pre-treatment with recombinant human IFN-β (Peprotech, Hamburg, Germany) was performed at a concentration of 500 U/ml for 3h prior to stimulation. In some experiments cells were pre-treated with chloroquine (Sigma) for 30min prior to stimulation. For cytokine assays cells were cultured for 20h to 24h, supernatants were collected and assayed for secreted amounts of cytokines.

RNAs

Chemically synthesized RNA oligonucleotides were purchased from Eurogentec (Leiden, Belgium) or MWG-BIOTECH AG (Ebersberg, Germany). For a detailed list of all chemically synthesized RNA oligonucleotides see Table I. In vitro transcribed RNAs were synthesized according to the manufacturers instructions using the megashort script kit (Ambion, Huntingdon, UK). For a detailed list of all in vitro transcription templates see Table II. The templates contained a T7 RNA Polymerase consensus promoter followed by the sequence of

interest to be transcribed. An extra guanosine was added at the 5´end to both the sense and the antisense strands in order to transcribe with T7 RNA polymerase. The DNA template was digested using DNAse-I (Ambion) and RNAs were purified by phenol:chloroform extraction and alcohol precipitation. Excess salts and NTPs were removed by passing the RNAs through a Mini Quick SpinTM Oligo Column (Roche, Mannheim, Germany). Integrity of RNAs was checked via gel electrophoresis.

Detection of cytokines by ELISA

The amount of IFN-α production was determined using the IFN-α module set from Bender MedSystems (Vienna, Austria). Quantification of IL-12p70, IL-12p40, TNF-α, IFN-γ, IL-6, IL-8, IL-1β, IL-10 and IP-10 was performed using the respective ELISA kit from OPTEIA (BD PharMingen, Heidelberg, Germany). Quantification of human RANTES was performed using the human RANTES construction Kit (Antigenix America, New York). ELISA assays were performed according to the manufacturer's protocol. The concentration of cytokines was determined by the standard curve obtained using known amounts of recombinant cytokines. For some experiments, murine IFN-α was measured according to the following protocol: monoclonal rat anti-mouse IFN-α (clone RMMA-1) was used as capture antibody and polyclonal rabbit anti-mouse IFN-α serum was used for detection (both PBL Biomedical Laboratories, Piscataway, NJ, US) together with HRP-conjugated donkey anti-rabbit IgG as secondary reagent (Jackson ImmunoResearch Laboratories, Baltimore, PA, US). Mouse rIFN-α (PBL Biomedical Laboratories) was used as standard (IFN-α concentration in IU/ml).

Flow cytometry

Cell purity was assessed by FACS analysis of cell surface antigens using a FACSCalibur (BD Biosciences, Heidelberg, Germany). Human monocytes were stained with antibody against CD14-FITC or CD14-APC and cell purity was between 83% and 99%. Human PDC were positively labelled with antibody against CD123-PE, HLA-DR-PerCp and negatively for CD11c-APC and a cocktail to lineage markers (FITC). Cells were routinely between 81% and 98% pure. For identification of human MDC we used antibody for CD11c-APC, HLA-DR-PerCP for positive staining and CD123-PE and a cocktail to lineage markers for negative staining (cell purity: 90% and 92%). Antibodies were purchased from BD PharMingen. Intracellular staining of cytokines was performed with human PBMC (2Mio/ml) transfected with 3pRNA or synthetic RNA 9.2 sense and cultured for 7 h. Lipofectamine alone or no stimulus served as controls. After 3 h brefeldin-A (10µg/ml) (Sigma) was added to PBMC

and cells were cultured for another 4 h. Cells were washed and diluted in PBS supplemented with 1% FCS and cell-surface staining was performed with APC-conjugated antibody against CD14 (BD Pharmingen). After fixation cells were permeabilized with 1% Saponin in PBS/1% FCS and labelled with FITC-conjugated antibody against human IFN-α (PBL Interferon Source, USA). Data analysis was performed on viable cells using CellQuest software (BD Biosciences).

Fluorescence microscopy

Freshly isolated human monocytes (0,5 Mio/ml) were stimulated with 200ng FITC-labelled 9.2 sense RNA complexed to Poly-L-Arginine (280ng) or Lipofectamine 2000 (0,5µl in 50µl OPTIMEM) for the indicated durations and consequently adhered to poly-l-lysine coated microscope slides. Cells were then fixed in 100% acetone for 10min and incubated with antibodies directed against EEA-1 (BD Biosciences). Biotinylated rat-anti-mouse F(ab)2 fragment and rhodamine-red-X conjugated streptavidin (both Jackson Immunoresearch) were used as secondary reagents. Topro-3 (Invitrogen) was used for nuclear counterstaining. Stained cells were visualized using a Zeiss fluorescence microscope and Adobe Photoshop was used for adjustment of contrast and size.

siRNA electroporation

For siRNA experiments primary human monocytes were differentiated into monocyte-derived DCs in the presence of 800 U/ml IL-4 and GM-CSF (both ImmunoTools GmbH, Friesoythe, Germany). On day 6 cells were harvested, washed and diluted in OPTIMEM (Invitrogen). For siRNA transfection siRNA duplexes (7.5 µg) targeting human RIG-I, human TLR8 or luciferase were transferred into a 4 mm-cuvette (Thermo Fisher Scientific, Bonn, Germany), filled with 100 µl cell suspension containing 400,000 cells and pulsed in a GenePulser Xcell (Bio-Rad, Munich, Germany) (Instrument settings: Square Wave, 1000 V, 2 pulses, 0.5 ms). After electroporation cells were transferred into pre-warmed RPMI Medium (200,000 cells/ 200 µl) for another 2 days. Cells were transfected with RNA or stimulated with R848 as indicated. 24 h later supernatants were collected and subjected to ELISA for quantification of cytokines. SiRNA sequences for knock-down experiments are shown in Table III and were all purchased from Eurogentec S.A., Belgium.

Quantitative real-time PCR

RNA from human monocytes and PDC was extracted using the RNeasy kit (Qiagen, Hilden, Germany). cDNA was synthesized with the SuperScript VILO cDNA Synthesis Kit (Invitrogen). Quantitative RT-PCR was performed on a Lightcycler 480 (Roche) using the Maxima SYBR Green qPCR Master Mix (Fermentas, St. Leon-Rot, Germany). The specifity of amplification was assessed for each sample by melting curve analysis. Relative quantification was performed using standard curve analysis. The quantification data are presented as a ratio to the hypoxanthine phosphoribosyltransferase 1 (HPRT-1) level. The following primer for detection of IFN-β and HPRT-1 mRNAs were used: hsHPRT-1, 5`-TGA CCT TGA TTT ATT TTG CAT ACC-3`(forward) and 5´-CGA GCA AGA CGT TCA GTC CT-3`(reverse); hsIFN-β, 5´-AAA CTC ATG AGC AGT CTG CA-3` (forward) and 5´-AGG AGA TCT TCA GTT TCG GAG G-3´(reverse); hsRIG-I, 5`-AGC TCA GCT TGA TGA GGG ACA-3`(forward) and 5´-GTC TGG CAT CTG GAA CAC CA-3`(reverse); hsMDA, 5`-AGA GTG GCT GTT TAC ATT GCC-3`(forward), 5`-GCT GTT CAA CTA GCA GTA CTT T-3`(reverse); hsTLR9, 5`-CGT CTT GAA GGC CTG GTG TTG A-3`(forward), 5`-CTG GAA GGC CTT GGT TTT AGT GA-3`(reverse).

Results

3pRNA induces IFN-α in monocytes, MDC and PDC

Unlike the TLR system which is confined to certain immune cell subsets, RIG-I is expressed in a broad spectrum of cell types. Here we studied the sensitivity of primary immune cell subsets to the RIG-I ligand 3pRNA. 3pRNA was transfected using the cationic lipid Lipofectamine and IFN-α production was analyzed. As controls poly(I:C) (TLR3/ MDA5), R848 (TLR7/ TLR8) and CpG-A (TLR9) were used. Poly(I:C) was used with and without transfection. To increase the sensitivity towards stimulation cells were pretreated with IFN-β for 3 h (white bars). In monocytes 3pRNA, but not R848, CpG or poly(I:C) (with or without transfection) induced IFN-α. No increase was seen when monocytes were primed with IFN-β (Fig. 1A). Although monocytes do not produce IFN-α upon lipofectamine-mediated transfection of poly(I:C), monocytes do respond to poly(I:C) by upregulating IFN-β mRNA within 4 hours suggesting that MDA-5 is functional in monocytes (data not shown). In MDC 3pRNA induced low but considerable amounts of IFN-α (Fig. 1B). Poly(I:C) with and without transfection only induced substantial amounts of IFN-α in MDC primed with IFN-β. In PDC, 3pRNA induced much less IFN-α than CpG and R848, and no significant increase was seen when PDC were primed with IFN-β (Fig. 1C). No IFN-α production in response to 3pRNA was observed in primed or unprimed B cells, T cells or NK cells (data not shown). While these experiments showed that transfected 3pRNA was able to induce IFN-α in monocytes, MDC or PDC, depletion of monocytes from PBMC substantially diminished 3pRNA-triggered IFN-α production (Fig. 1D). The finding that monocytes were the main source of 3pRNA-mediated IFN-α induction was further supported by the analysis of IFN-α production at the single cell level using intracellular staining (Fig. 1E).

Distinct recognition pathways exist for 3pRNA in monocytes and PDC

PDC, MDC and monocytes were reported to detect RNA via TLR7 and TLR8. Therefore, 3pRNA may activate these cells via a TLR-dependent pathway. Previous studies have shown that TLR7 mediates the recognition of RNA in a sequence-dependent manner and that the minimal structural requirement for TLR7-mediated recognition of RNA is the presence of uracil (15, 5). To study the impact of the RNA sequence on the activity of the 3pRNA

molecule we established two different versions of 3pRNA: 3pRNA GFPs contains a TLR7/8 stimulatory RNA motif; 3pRNA GA contains no uracil and lacks TLR7 activity (Table I). We examined stimulation of monocytes and PDC with 3pRNA GFPs in the presence of chloroquine, a potent inhibitor of TLR7-, TLR8- or TLR9- mediated nucleic acid recognition. No inhibitory effect of chloroquine on IFN-α production was seen in monocytes transfected with 3pRNA GFPs (TLR7/8 activity) or with 3pRNA GA (Fig. 2A). In contrast, in PDC the presence of chloroquine strongly impaired IFN-α induction upon stimulation with 3pRNA GFPs, while 3pRNA GA-induced IFN-α was much lower but not sensitive to chloroquine. Similar data were obtained using bafilomycin A, another inhibitor of lysosomal acidification (data not shown). To directly address the role of TLR7 in the recognition of 3pRNA in PDC, we examined IFN-α induction in cultured PDC from TLR7 -/- mice upon transfection with both synthetic ssRNA 2.2s (no triphosphate) and 3pRNA 2.2s in comparison to the response observed with PDC from wild-type mice. As shown in Fig. 2B, wild-type PDC produced IFN-α after transfection of synthetic ssRNA 2.2s and 3pRNA 2.2s. In contrast PDC from TLR7 -/- showed a strongly reduced IFN-α production upon stimulation with 3pRNA and no IFN-α upon stimulation with ssRNA 2.2s. This demonstrates that in PDC TLR7 is required for recognition of synthetic ssRNA and is responsible for most of the IFN-α induction by 3pRNA. siRNA experiments conducted in human monocyte-derived dendritic cells showed that knocking down RIG-I expression specifically reduced 3pRNA triggered IFN-α expression while R848-mediated IL-12 production was not reduced (Fig 2C). These findings are consistent with the observation that RIG-I expression in PDC was marginal (Fig. 2D). Further, MDA5 expression in PDC was low. Altogether, these results indicated that monocytes and PDC display distinct mechanisms for the recognition of 3pRNA. The observation that in PDC TLR7 overrules RIG-I for IFN-α induction is in accordance with data obtained within whole viruses in the murine system. In this regard, Kato and colleagues have shown that Newcastle Disease Virus (NDV) is recognized via TLR7 whereas IFN-production in myeloid dendritic cells and non-immune cells is RIG-I dependent (10).

3pRNA but not synthetic blunt-end double-strand RNA oligonucleotides drives TLR-independent IFN-α production

Previous studies have proposed that the presence of 2 nucleotide (nt) overhangs at the 3' end acts as an inhibitory feature of dsRNA oligonucleotides and prevents activation of RIG-I,

whereas blunt-end dsRNA oligonucleotides induces immunostimulation (14). In a previous work we have shown that the presence of a 2 nt overhang did not change the IFN-α inducing activity of a triphosphate dsRNA oligonucleotide. To further characterize the effect of the terminal conformation of short dsRNA for IFN-α induction we studied PDC activation by blunt-end and overhang dsRNA. The respective ssRNAs were used as controls. In this respect, we found that both types of synthetic dsRNA were equally active in PDC regardless of whether a 2 nt overhang was present or not (Fig. 3A). In contrast, when we transfected monocytes with blunt-end and overhang dsRNA, but no triphosphate, no IFN-α response was detected (Fig. 3B). Instead, IFN-α production in monocytes strictly required the presence of a triphosphate at the 5' end. This was also the case when IFN-β production was assessed at the transcriptional level (Fig. 3C). Together, these results indicated that activation of the TLR system in PDC rather than RIG-I is responsible for IFN-α production upon stimulation with blunt-end dsRNA (no triphosphate 5' end) in primary immune cells.

The type of RNA delivery determines cell-type specific cytokine responses

The findings above showed that chemically synthesized RNA with no triphosphate end failed to stimulate monocytes to produce IFN-α. However, studies by other groups using different methods of delivery suggested that synthetic ssRNA activates monocytes in a TLR-dependent manner (3, 4, 16, 30). This prompted us to investigate whether the use of transfection reagents influenced the stimulatory potential of RNA. Therefore an alternative method to effectively complex RNA based on the polycationic peptide poly-L-arginine (pLa) was established. PBMC (containing both PDC and monocytes) were stimulated with increasing doses of RNA 9.2sense or 3pRNA using distinct modes of delivery (Lipofectamine vs. pLa). While all RNA complexes tested induced IFN-α to some extent, 3pRNA transfected with Lipofectamine was by far the most potent stimulus (Fig. 4A left panel). The effect of Lipofectamine-complexed 3pRNA was not inhibited by chloroquine (Fig. 4A left panel, white bars); however chloroquine inhibited IFN-α induced by both RNA 9.2sense and 3pRNA complexed with pLa (Fig. 4A left panel, white bars). In purified monocytes only Lipofectamine-transfected 3pRNA but not pLa-delivered 3pRNA induced IFN-α (Fig. 4A, right panel). However the analysis of pro-inflammatory cytokines in the supernatants of transfected monocytes showed an opposite picture with strong induction of IL-12p70 by pLa and 3pRNA but no IL-12p70 induction by Lipofectamine (Fig. 4B). Of note, pLa RNA triggered IL-12p70 production in

PBMC was highly dependent on the presence of monocytes (Fig. 4C). Next to IL-12p70 production, several key pro-inflammatory cytokines were almost exclusively seen for pLa mediated delivery of RNA (Fig. 5). Among those were TNF-α, IL-6, IL-12p40 and IL-1β, which were only observed when RNA was delivered using pLa, but not Lipofectamine. A similar cytokine profile to pLa complexed RNA was seen for the TLR7/8 ligand R848 (data not shown). Altogether, these data suggested that the type of delivery impacts on the subsequent cytokine response.

pLa-mediated transfection results in prolonged endosomal signalling, which is required for efficient TLR8-dependent IL-12 production

Given the striking differences in the cytokine response observed for pLa and Lipofectamine, we next sought to study if the mode of delivery influences the intracellular distribution of RNA oligonucleotides. To follow the uptake process of ssRNA complexes in monocytes we performed microscopy studies in monocytes using fluorescein-tagged ssRNA (FITC-RNA). Monocytes were incubated with FITC-RNA in complex with Lipofectamine or pLa for 120 minutes and 180 minutes, and co-localization with the endosomal marker EEA-1 was analyzed. We observed co-localization of EEA-1 with FITC-RNA after both 120 min and 180 min of incubation when pLa was used for transfection (Fig. 6). In contrast, no co-localization was seen after transfection with Lipofectamine. Instead, transfection with Lipofectamine resulted in a predominant translocation of FITC-RNA into the cytoplasm. These results indicated that pLa but not Lipofectamine complexes are retained in endosomal compartments and that only Lipofectamine delivers RNA into the cytosol. The fact that pLa results in a prolonged endosomal retention of RNA prompted us to investigate whether a TLR-mediated mechanism would be involved in the recognition of RNA. To address this question we pretreated PBMC with chloroquine to inhibit endosomal maturation. Indeed we found, that the IL-12p70 response was highly sensitive to the inhibition with chloroquine, whereas IFN-α production induced by 3pRNA complexed with Lipofectamine was not inhibited (Fig. 7A). Given its high and predominant expression in monocytes, TLR8 was the most likely candidate receptor for the recognition of pLa complexed RNA. To address this question, we performed siRNA knock down experiments in human monocyte-derived dendritic cells. Notably, the induction of IL-12 by pLa complexed ssRNA was markedly reduced after pretreatment with anti-TLR8 siRNA (Fig 7B left panel). At the same time IFN-α levels induced by

Lipofectamine mediated transfection of 3pRNA remained unaffected by siRNA targeting TLR8 (Fig 7B right panel). The superiority of pLa over Lipofectamine for the activation of TLR8 by RNA was in line with the predominant localization of pLa RNA complexes in the endolysosomal compartment. Accordingly we found that also in PDC, where RNA recognition is based on TLR7, delivery of 3pRNA with pLa was more potent in type I IFN induction than Lipofectamine (Fig. 7C). Collectively, these experiments showed that the method of delivery of RNA per se critically determines the initial recognition pathway in monocytes.

Single-strand conformation is required for maximal IL-12 production by RNA in monocytes

Based on the observation that pLa exclusively targets RNA to the endosome but not the cytosol, we further characterized the structural requirements for TLR-mediated recognition of RNA. Previous studies demonstrated that in immune cells TLR7 and TLR8 contribute to RNA recognition. In PDC (exclusively expressing TLR7) both ssRNA and dsRNA oligonucleotides (siRNA, sense and antisense strand) induce IFN-α in a sequence dependent manner (5). Based on these earlier observations we compared the activity of different short dsRNA and the respective sense and antisense strands complexed with pLa to induce IL-12p70 in monocytes. While the sense and the antisense ssRNA oligonucleotides were active at inducing IL-12p70, the corresponding dsRNA oligonucleotides did not induce IL-12p70 (Fig. 8A). To further clarify conformation requirements, partial dsRNA oligonucleotides were generated by annealing short derivatives of the 9.2sense strand to the respective complete 9.2antisense strand and used for stimulation of PBMC. Partial 12mer duplexes, partial 16mer duplexes and a complete 21mer duplex and the corresponding ssRNAs were analyzed (Fig. 8B). A short portion of dsRNA conformation was sufficient to reduce IL-12 induction of a potent ssRNA oligonucleotide (Fig. 8B, for example compare 9.2 as to Ads or Bds). On the other hand, high stimulation of IFN-α was seen with a partial (Fig. 8B, for example Ads, Bds) or full RNA duplex (Fig. 8B, 9.2 ds). A 12mer ssRNA was not sufficient to induce IL-12p70 and IFN-α, but limited activity was seen with 16mer ssRNA (Fig. 8B). To further address the role of RNA structure in TLR-dependent activation of monocytes we designed a fully self-complementary ssRNA oligonucleotide that forms a dsRNA under physiological conditions. We found that this self-complementary ssRNA was active in inducing IFN-α in PBMC,

however lacked the ability to induce IL-12p70 (Fig. 8C). We next asked what degree of "single-strandedness" within this self-complementary RNA was required to restore IL-12 induction. Therefore we gradually increased the number of mismatches within the complementary regions. Testing this panel of RNA oligonucleotides revealed that an increasing number of mismatches was associated with a higher level of IL-12 induction, while decreasing IFN-α induction (Fig. 8D). Notably, an introduction of three mismatches was sufficient to markedly reduce IFN-α production, while markedly enhancing IL-12 production. The non-linear increase of IL-12 induction with increasing numbers of mismatches may be due to changes in the TLR8 sequence motif activity. Together, these data suggested that single-strand but not double-strand RNA is required for optimal TLR-dependent stimulation in monocytes (IL-12).

Discussion

The vertebrate immune system has established versatile ways to sense invading viruses based on certain molecular patterns of viral nucleic acids. Several receptors participate in a non-redundant system to master the recognition of foreign RNA (1). Ligand specificity, distinct expression profiles, subcellular localization and distinct downstream signalling pathways explain the ability of these receptor systems to elicit appropriate immune responses. In this study we aimed at dissecting these different components in order to identify optimal compositions of immunologically active oligoribonucleotide complexes.

Our results demonstrate that in addition to the sequence, both the structure and the type of delivery determine the stimulatory potential of RNA oligonucleoides. By comparing different transfection techniques we made the observation that the mode of delivery dramatically directs the subsequent cytokine responses by determining the access of the RNA to the respective receptors. While cytosolic delivery by Lipofectamine was required to activate RIG-I in monocytes, endosomal delivery through pLa allowed the activation of the TLR7 and the TLR8 pathway in PDC and monocytes, respectively. Activation of RIG-I by RNA oligonucleotides required a triphosphate at the 5' end and activation of TLR8 in monocytes required single-strand conformation.

Given the strong type I interferon response upon transfection of 5' triphosphate RNA in PBMC, we sought to identify the immune cell subsets that were responsible for this activity. Using mice genetically deficient in TLR7, siRNA targeting TLR8 and a 3pRNA molecule lacking TLR7/8 activity (3pRNA GA), blocking endolysosomal nucleic acid recognition and specifically targeting nucleic acid complexes to distinct cellular compartments, we now conclude that 3pRNA is sensed in a clearly cell-type specific manner: cytosolic detection of 3pRNA by RIG-I leads to a robust IFN-α response in monocytes and MDC, but not in PDC. Blocking endolysosomal nucleic acid recognition (chloroquine) or using a 3pRNA molecule with no TLR7/8 activity (3pRNA GA) did not diminish the type I IFN response in monocytes. Consequently, positioning 3pRNA exclusively in endosomal compartments of monocytes (polycationic peptides) does not lead to an interferon response. Finally siRNA experiments substantiate that in myeloid cells IFN-α induction is exclusively due to RIG-I and not to TLR7/8. An opposite picture is seen for PDC: 3pRNA also readily induces IFN-α, but this is due to sensing by TLR7 and occurs independently of its 5' triphosphate end. RNA without a

5` triphosphate is equally potent to induce IFN-α in PDC and chloroquine reduces this response. Moreover, delivery of 3pRNA containing TLR7 ligand activity more efficiently to the endosomal compartment of PDC by pLa was even more potent than transfection with cationic lipids. In line with these observations we found that RIG-I is only marginally expressed in PDC when compared to monocytes. Supporting this concept of cell-type specific involvement of RIG-I for RNA detection, PDC from RIG-I deficient mice challenged with the RNA virus NDV were reported to show normal production of IFN-α, while no IFN-α could be induced in RIG-I deficient MDCs and MEFs (10). Of note, Kato and colleagues proposed a residual activity of RIG-I in PDC, a concept that is supported by our findings. Thus being responsible for the early type I IFN response in viral infection, PDC seem to mostly but not exclusively rely on TLR dependent recognition of RNA viruses.

Using polycationic peptides to directly deliver RNA oligonucleotides into endosomal compartments lead to the notable observation that large quantities of bioactive IL-12p70 can be induced in monocytes by one single TLR agonist: pLa complexed ssRNA. So far DC are thought to represent the major source of IL-12p70. However IL-12p70 production within DC is known to be tightly controlled usually requiring multiple stimuli to synergize in order to induce its expression (28). In fact we identified monocytes as the major source of IL-12p70 upon ssRNA stimulation within PBMC. The exclusive expression of TLR8 in monocytes (24, 28), sensitivity towards inhibition by chloroquine and siRNA-mediated knock-down experiments support the concept of TLR8-dependent recognition of RNA-pLa complexes to be responsible for massive IL-12p70 induction. This previously unappreciated capability of monocytes to produce large amounts of IFN-α and IL-12p70 can be employed to establish and maintain potent Th1 immune responses.

Interestingly, TLR8-mediated recognition of RNA oligonucleotides strictly requires single-strand conformation of RNA in monocytes. Any structural alteration in the RNA leading to even partial double-strand conformations abolishes the activity of RNA in monocytes. It is tempting to speculate that the receptor molecules - TLR7 and TLR8 - themselves are responsible for the ability to detect different RNA conformations. Besides TLR7 and TLR8, PDC- and monocyte-specific co-factors may contribute to differential TLR response to ssRNA and dsRNA.

In conclusion, our data demonstrate that introducing or avoiding certain molecular patterns (5’ triphosphate group; TLR7/8 motif; ssRNA or dsRNA conformation) combined with specific types of delivery (cytoplasmic; endosomal) and sequence motifs allows the modular design of immunostimulatory RNA oligonucleotides that trigger specific receptor systems provoking distinct downstream immune responses including potent IL-12 and IFN-α induction in monocytes. This information will facilitate the rational design of RNA-based drugs.

Acknowledgements

This work is part of the dissertation of A. Ablasser at the Ludwig-Maximilians-University, Munich, Germany. We thank Julia Vorac from the Divsion of Clinical Pharmacology of the University of Munich for technical assistance.

References

1. Kawai, T., and S. Akira. 2006. Innate immune recognition of viral infection. *Nat Immunol* 7:131-137.
2. Alexopoulou, L., A. C. Holt, R. Medzhitov, and R. A. Flavell. 2001. Recognition of double-stranded RNA and activation of NF-kappaB by Toll-like receptor 3. *Nature* 413:732-738.
3. Diebold, S. S., T. Kaisho, H. Hemmi, S. Akira, and C. Reis e Sousa. 2004. Innate antiviral responses by means of TLR7-mediated recognition of single-stranded RNA. *Science* 303:1529-1531.
4. Heil, F., H. Hemmi, H. Hochrein, F. Ampenberger, C. Kirschning, S. Akira, G. Lipford, H. Wagner, and S. Bauer. 2004. Species-specific recognition of single-stranded RNA via toll-like receptor 7 and 8. *Science* 303:1526-1529.
5. Hornung, V., M. Guenthner-Biller, C. Bourquin, A. Ablasser, M. Schlee, S. Uematsu, A. Noronha, M. Manoharan, S. Akira, A. de Fougerolles, S. Endres, and G. Hartmann. 2005. Sequence-specific potent induction of IFN-alpha by short interfering RNA in plasmacytoid dendritic cells through TLR7. *Nat Med* 11:263-270.
6. Hemmi, H., O. Takeuchi, T. Kawai, T. Kaisho, S. Sato, H. Sanjo, M. Matsumoto, K. Hoshino, H. Wagner, K. Takeda, and S. Akira. 2000. A Toll-like receptor recognizes bacterial DNA. *Nature* 408:740-745.
7. Latz, E., A. Schoenemeyer, A. Visintin, K. A. Fitzgerald, B. G. Monks, C. F. Knetter, E. Lien, N. J. Nilsen, T. Espevik, and D. T. Golenbock. 2004. TLR9 signals after translocating from the ER to CpG DNA in the lysosome. *Nat Immunol* 5:190-198.
8. Kato, H., O. Takeuchi, S. Sato, M. Yoneyama, M. Yamamoto, K. Matsui, S. Uematsu, A. Jung, T. Kawai, K. J. Ishii, O. Yamaguchi, K. Otsu, T. Tsujimura, C. S. Koh, C. Reis e Sousa, Y. Matsuura, T. Fujita, and S. Akira. 2006. Differential roles of MDA5 and RIG-I helicases in the recognition of RNA viruses. *Nature* 441:101-105.
9. Yoneyama, M., M. Kikuchi, T. Natsukawa, N. Shinobu, T. Imaizumi, M. Miyagishi, K. Taira, S. Akira, and T. Fujita. 2004. The RNA helicase RIG-I has an essential function in double-stranded RNA-induced innate antiviral responses. *Nat Immunol* 5:730-737.
10. Kato, H., S. Sato, M. Yoneyama, M. Yamamoto, S. Uematsu, K. Matsui, T. Tsujimura, K. Takeda, T. Fujita, O. Takeuchi, and S. Akira. 2005. Cell type-specific involvement of RIG-I in antiviral response. *Immunity* 23:19-28.
11. Gitlin, L., W. Barchet, S. Gilfillan, M. Cella, B. Beutler, R. A. Flavell, M. S. Diamond, and M. Colonna. 2006. Essential role of mda-5 in type I IFN responses to

polyriboinosinic:polyribocytidylic acid and encephalomyocarditis picornavirus. *Proc Natl Acad Sci U S A* 103:8459-8464.

12. Hornung, V., J. Ellegast, S. Kim, K. Brzozka, A. Jung, H. Kato, H. Poeck, S. Akira, K. K. Conzelmann, M. Schlee, S. Endres, and G. Hartmann. 2006. 5'-Triphosphate RNA is the ligand for RIG-I. *Science* 314:994-997.
13. Pichlmair, A., O. Schulz, C. P. Tan, T. I. Naslund, P. Liljestrom, F. Weber, C. and Reis e Sousa. 2006. RIG-I-mediated antiviral responses to single-stranded RNA bearing 5'-phosphates. *Science* 314: 997-1001.
14. Marques, J. T., T. Devosse, D. Wang, M. Zamanian-Daryoush, P. Serbinowski, R. Hartmann, T. Fujita, M. A. Behlke, and B. R. Williams. 2006. A structural basis for discriminating between self and nonself double-stranded RNAs in mammalian cells. *Nat Biotechnol* 24:559-565.
15. Judge, A. D., V. Sood, J. R. Shaw, D. Fang, K. McClintock, and I. MacLachlan. 2005. Sequence-dependent stimulation of the mammalian innate immune response by synthetic siRNA. *Nat Biotechnol* 23:457-462.
16. Sioud, M. 2006. Single-stranded small interfering RNA are more immunostimulatory than their double-stranded counterparts: a central role for 2'-hydroxyl uridines in immune responses. *Eur J Immunol* 36:1222-1230.
17. Lau, C. M., C. Broughton, A. S. Tabor, S. Akira, R. A. Flavell, M. J. Mamula, S. R. Christensen, M. J. Shlomchik, G. A. Viglianti, I. R. Rifkin, and A. Marshak-Rothstein. 2005. RNA-associated autoantigens activate B cells by combined B cell antigen receptor/Toll-like receptor 7 engagement. *J Exp Med* 202:1171-1177.
18. Vollmer, J., S. Tluk, C. Schmitz, S. Hamm, M. Jurk, A. Forsbach, S. Akira, K. M. Kelly, W. H. Reeves, S. Bauer and A. M. Krieg. 2005. Immune stimulation mediated by autoantigen binding sites within small nuclear RNAs involves Toll-like receptors 7 and 8. *J Exp Med* 202:1575-1585.
19. Barrat, F. J., T. Meeker, J. Gregorio, J. H. Chan, S. Uematsu, S. Akira, B. Chang, O. Duramad and R. L. Coffman. 2005. Nucleic acids of mammalian origin can act as endogenous ligands for Toll-like receptors and may promote systemic lupus erythematosus. *J Exp Med* 202:1131-1139.
20. Lovgren, T., M. L. Eloranta, B. Kastner, M. Wahren-Herlenius, G. V. Alm and L. Ronnblom. 2006. Induction of interferon-alpha by immune complexes or liposomes containing systemic lupus erythematosus autoantigen- and Sjogren's syndrome autoantigen-associated RNA. *Arthritis Rheum* 54:1917-1927.

21 Savarese, E.. O. W. Chae, S. Trowitzsch, G. Weber, B. Kastner, S. Akira, H. Wagner, R. M. Schmid, S. Bauer and A. Krug. 2006. U1 small nuclear ribonucleoprotein immune complexes induce type I interferon in plasmacytoid dendritic cells through TLR7. *Blood.* 107:3229-3234.

22. Matsumoto, M., K. Funami, M. Tanabe, H. Oshiumi, M. Shingai, Y. Seto, A. Yamamoto, and T. Seya. 2003. Subcellular localization of Toll-like receptor 3 in human dendritic cells. *J Immunol* 171:3154-3162.

23. Nishiya, T., and A. L. DeFranco. 2004. Ligand-regulated chimeric receptor approach reveals distinctive subcellular localization and signaling properties of the Toll-like receptors. *J Biol Chem* 279:19008-19017.

24. Hornung, V., S. Rothenfusser, S. Britsch, A. Krug, B. Jahrsdorfer, T. Giese, S. Endres, and G. Hartmann. 2002. Quantitative expression of toll-like receptor 1-10 mRNA in cellular subsets of human peripheral blood mononuclear cells and sensitivity to CpG oligodeoxynucleotides. *J Immunol* 168:4531-4537.

25. Ito, T., R. Amakawa, T. Kaisho, H. Hemmi, K. Tajima, K. Uehira, Y. Ozaki, H. Tomizawa, S. Akira, and S. Fukuhara. 2002. Interferon-alpha and interleukin-12 are induced differentially by Toll-like receptor 7 ligands in human blood dendritic cell subsets. *J Exp Med* 195:1507-1512.

26. Krug, A., A. Towarowski, S. Britsch, S. Rothenfusser, V. Hornung, R. Bals, T. Giese, H. Engelmann, S. Endres, A. M. Krieg, and G. Hartmann. 2001. Toll-like receptor expression reveals CpG DNA as a unique microbial stimulus for plasmacytoid dendritic cells which synergizes with CD40 ligand to induce high amounts of IL-12. *Eur J Immunol* 31:3026-3037.

27. Trinchieri, G. 2003. Interleukin-12 and the regulation of innate resistance and adaptive immunity. *Nat Rev Immunol* 3:133-146.

28. Bekeredjian-Ding, I., S. I. Roth, S. Gilles, T. Giese, A. Ablasser, V. Hornung, S. Endres, and G. Hartmann. 2006. T cell-independent, TLR-induced IL-12p70 production in primary human monocytes. *J Immunol* 176:7438-7446.

29. Napolitani, G., A. Rinaldi, F. Bertoni, F. Sallusto, and A. Lanzavecchia. 2005. Selected Toll-like receptor agonist combinations synergistically trigger a T helper type 1-polarizing program in dendritic cells. *Nat Immunol* 6:769-776.

30. Sugiyama, T., M. Gursel, F. Takeshita, C. Coban, J. Conover, T. Kaisho, S. Akira, D. M. Klinman, and K. J. Ishii. 2005. CpG RNA: identification of novel single-stranded RNA that stimulates human CD14+CD11c+ monocytes. *J Immunol* 174:2273-2279.

Figure legends

Figure 1 IFN-α is induced in monocytes, MDC and PDC upon stimulation with 3pRNA

(A-C) Monocytes, MDC and PDC were isolated from human PBMC, primed with IFN-β (500U/ml) (white bars) for 3h or left untreated (black bars). Cells were stimulated with CpG ODN 2216 (3 μg/ml), R848 (5 μg/ml), poly(I:C) (10 μg/ml), Lipofectamine alone, 3pRNA (200ng) and poly(I:C) (200ng) complexed with Lipofectamine or left untreated. After 20h of incubation supernatants were collected and assayed for IFN-α production by ELISA. Data are expressed as the mean ± SEM of four (monocytes, MDC) and six (PDC) independent experiments. (D) PBMC with or without CD14+ monocytes were transfected with Lipofectamine alone or 3pRNA complexed with Lipofectamine. No stimulus served as a control. Supernatants were collected 24 h after stimulation and IFN-α was measured by ELISA. Mean and SEM of two independent experiments is shown. (E) Intracellular staining of IFN-α is shown and plotted against CD14 surface staining. PBMC were transfected with Lipofectamine alone or with Lipofectamine complexed with RNA 9.2sense or 3pRNA and IFN-α production was assessed by flow cytometry after 7 h. Untreated PBMC served as a control. Numbers represent IFN-α-positive cells out of the CD14-positive cell population. One representative experiment out of two is depicted.

Figure 2 Recognition of 3pRNA occurs through differential pathways in monocytes and PDC

(A) Monocytes and PDC were pre-incubated with 1000 ng/ml chloroquine (white bars) or left untreated (black bars). After 30min cells were stimulated with 3pRNA GA or 3pRNA GFPs complexed with Lipofectamine or control (no stimulus). Supernatants were collected 20 h post stimulation and IFN-α production was determined by ELISA. Mean and SEM of two independent experiments is shown. **(**B**)** Sorted PDC from Flt3-L induced bone marrow cultures of wild-type (WT; black bars) and TLR7-deficient mice ($TLR7^{-/-}$; white bars) were transfected with synthetic ssRNA 2.2 sense (ssRNA 2.2s), 3pRNA 2.2 sense (3pRNA 2.2s) or CpG 2216 (3 μg/ml). After 24 h supernatants were collected and IFN-α production was quantified by ELISA. Data are expressed as the mean ± SEM of two independent experiments. (C) Monocyte-derived dendritic cells were electroporated with siRNA directed against RIG-I or control siRNA. 48 h after electroporation cells were transfected with 3pRNA

complexed to Lipofectamine. No stimulus, Lipofectamine alone and R848 (5 µg/ml) served as control. Supernatants were collected 24 h after transfection and cytokines were quantified by ELISA. Mean and SEM of two independent experiments is depicted. (D) PDC and monocytes were isolated from human PBMC and relative expression of RIG-I, MDA5 and TLR9 was determined by quantitative RT-PCR. Mean and SEM of two independent experiments is depicted.

Figure 3 Blunt-end dsRNA is a poor inducer of type I IFN in monocytes

(A, B) Synthetic ssRNA (27+0 s, 27+0 a, 27+2 s, 27+2 a) and dsRNA with (27+2 ds) or without (27+0 ds) 2 nt overhangs were transfected into PDC and monocytes in complex with Lipofectamine. ODN 2216 (3 µg/ml) or 3pRNA (200 ng) were used as a control stimulus for IFN-α or RIG-I, respectively. The levels of IFN-α production were analyzed by ELISA 24 h after stimulation and are depicted as mean ± SEM out of two independent experiments. (C) Human monocytes were transfected with 3pRNA or synthetic dsRNA with (27+2 ds) or without (27+0 ds) 2 nt overhangs using Lipofectamine as a transfection reagent. Lipofectamine alone was used as control. After 4 h relative expression of IFN-β mRNA was determined by quantitative RT-PCR. Mean and SEM of four independent experiments is shown.

Figure 4 The mode of delivery differentially regulates subsequent cytokines responses in monocytes

(A) PBMC or monocytes were stimulated with increasing doses (100 ng, 200 ng, 400ng) of 3pRNA and RNA 9.2sense complexed with Lipofectamine or pLa alone (black bars) or in the presence of 1000 ng/ml chloroquine (white bars only PBMC). After 20h IFN-α production was measured by ELISA. Mean ± SEM of two independent experiments is shown. (B) pLa and Lipofectamine were incubated with 3pRNA and tested for stimulatory activity in human monocytes. Supernatants were collected after 24h to measure IL-12p70 and IFN-α production by ELISA (mean ± SEM, n=2). (C) PBMC with or without CD14+ monocytes (left panel) and PBMC with or without PDC, MDC or both (right panel) were transfected with RNA 9.2sense complexed with pLa and IL-12p70 was measured 24 h after stimulation. Mean and SEM of two independent experiments is shown.

Figure 5 Cytokine profile of 3pRNA versus synthetic ssRNA in human PBMC

PBMC were transfected with RNA 9.2sense complexed with pLa or 3pRNA complexed with Lipofectamine or left untreated. Supernatants were collected 24 h after stimulation and cytokines were detected by ELISA. Mean and SEM of three independent experiments is shown.

Figure 6 ssRNA in complex with Lipofectamine rapidly translocates into the cytoplasm whereas pLa complexed ssRNA is retained in endosomal compartments

Fluorescent images of monocytes transfected with FITC-labelled ssRNA 9.2 sense (FITC-RNA) complexed to pLa or Lipofectamine and incubated for the indicated durations. Fixed cells were stained with EEA-1 (rhodamine-red-X) to mark endosomes and nuclear counterstaining was performed using TOPRO-3.

Figure 7 Directed endolysosomal delivery activates TLR8 in monocytes

(A) PBMC were pre-incubated with chloroquine for 30 min and subsequently stimulated with RNA 9.1sense in complex with pLa or 3pRNA complexed with Lipofectamine, respectively, or left untreated. IL-12p70 or IFN-α production was analyzed by ELISA 24 h after stimulation (mean ± SEM, n=2). (B) Monocyte-derived DCs were electroporated with siRNA against TLR8 or control siRNA. Cells were transfected with RNA 9.2sense complexed with pLa, pLa alone, Lipofectamine alone and 3pRNA complexed with Lipofectamine. Supernatants were collected 24h after transfection and cytokines were quantified by ELISA. Mean and SEM of two experiments is shown. (C) PDC were stimulated with 3pRNA complexed with Lipofectamine or pLa. After 20 h IFN-α production was measured by ELISA. Mean and SEM of two independent experiments is shown.

Figure 8 Selection of structure and sequence for the induction of IL-12 or IFN-α

(A) Monocytes were transfected with different versions of ssRNA and dsRNA using pLa as indicated. 24 h after transfection supernatants were collected and subjected to ELISA for determination of IL-12p70 production. Mean and SEM of three independent experiments is shown. (B) Different versions of RNA 9.2sense were annealed with 9.2antisense to form partial or complete RNA duplexes and subsequently transfected into PBMC using pLa. The respective single stranded RNA molecules served as controls, whereas the sense strand was used for normalization. After 24 h supernatants were analyzed for IL-12p70 and IFN-α production (mean ± SEM, n=2). (C, D) PBMC were transfected using pLa with a self-

complementary ssRNA (P20) and a panel of its derivatives containing an increasing number of mismatches within the complementary regions (P20-3M, P20-5M, P20-6M, P20-20M). CpG A 2216 (3 μg/ml) and R848 (5 μg/ml) served as controls. Supernatants were analyzed for IL-12p70 and IFN-α production 24 h post stimulation (mean ± SEM, n=2).

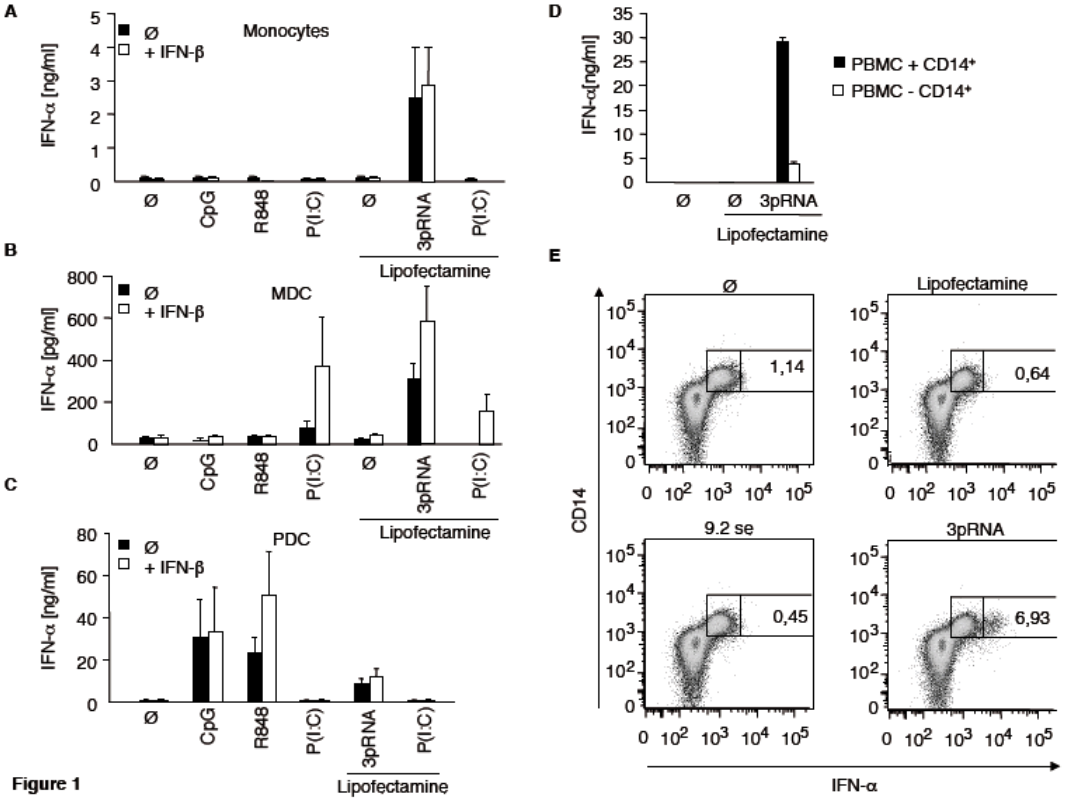
A
IFN-α [ng/ml]
Ø
+ IFN-β
Monocytes
Ø
CpG
R848
P(I:C)
Ø
3pRNA
P(I:C)
Lipofectamine
B
IFN-α [pg/ml]
MDC
C
IFN-α [ng/ml]
PDC
D
IFN-α[ng/ml]
PBMC + CD14+
PBMC - CD14+
3pRNA
E
CD14
IFN-α
1,14
0,64
9.2 se
0,45
6,93

Figure 1

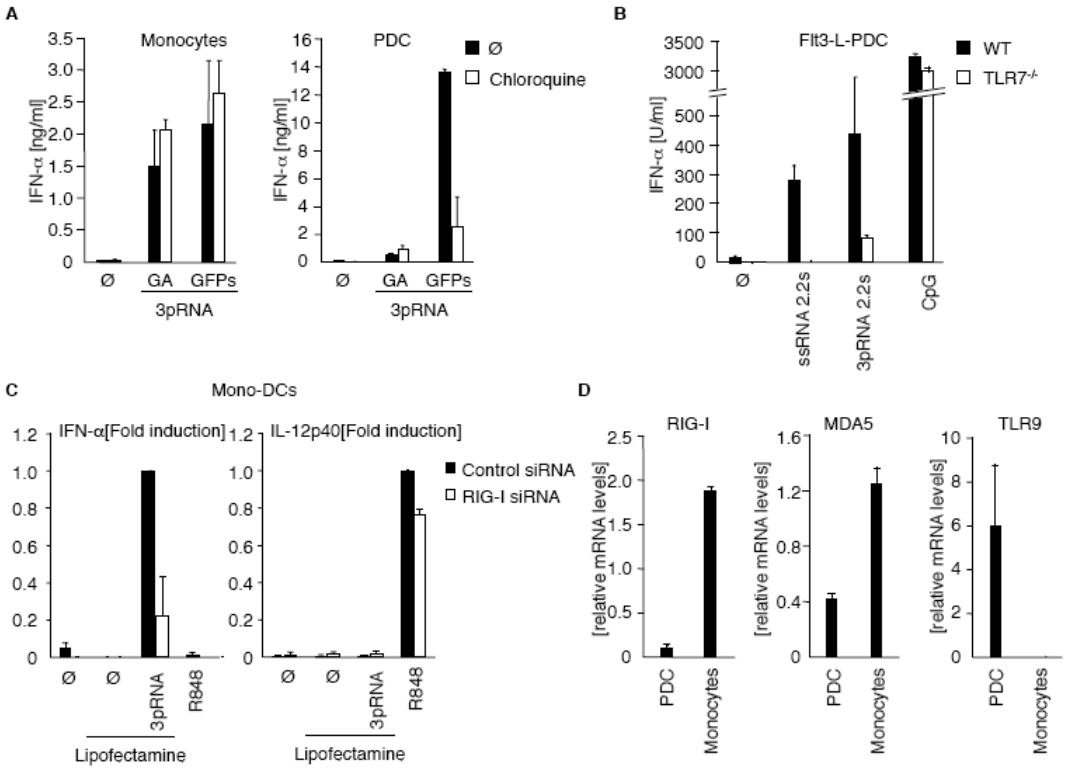
A
Monocytes
PDC
IFN-α [ng/ml]
Ø
Chloroquine
Ø
GA
GFPs
3pRNA
B
Flt3-L-PDC
IFN-α [U/ml]
WT
TLR7-/-
Ø
ssRNA 2.2s
3pRNA 2.2s
CpG
C
Mono-DCs
IFN-α[Fold induction]
IL-12p40[Fold induction]
Control siRNA
RIG-I siRNA
Ø
3pRNA
R848
Lipofectamine
D
RIG-I
MDA5
TLR9
[relative mRNA levels]
PDC
Monocytes

Figure 2

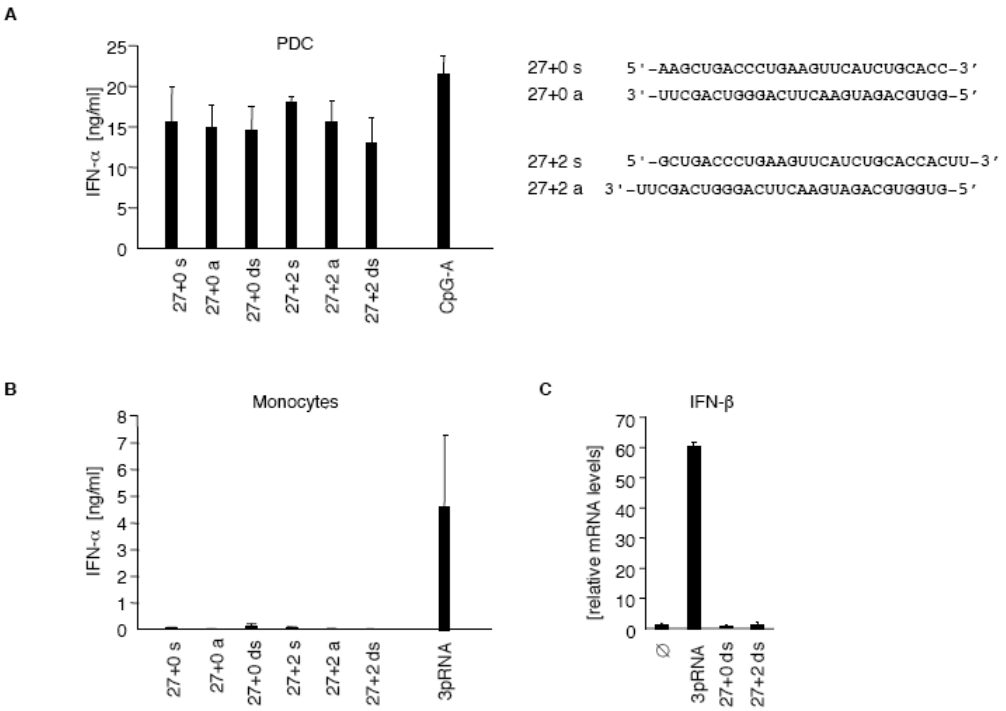
A
PDC
IFN-α [ng/ml]
25
20
15
10
5
0
27+0 s
27+0 a
27+0 ds
27+2 s
27+2 a
27+2 ds
CpG-A
27+0 s 5'-AAGCUGACCCUGAAGUUCAUCUGCACC-3'
27+0 a 3'-UUCGACUGGGACUUCAAGUAGACGUGG-5'
27+2 s 5'-GCUGACCCUGAAGUUCAUCUGCACCACUU-3'
27+2 a 3'-UUCGACUGGGACUUCAAGUAGACGUGGUG-5'
B
Monocytes
IFN-α [ng/ml]
8
7
6
5
4
3
2
1
0
27+0 s
27+0 a
27+0 ds
27+2 s
27+2 a
27+2 ds
3pRNA
C
IFN-β
[relative mRNA levels]
70
60
50
40
30
20
10
0
∅
3pRNA
27+0 ds
27+2 ds

Figure 3

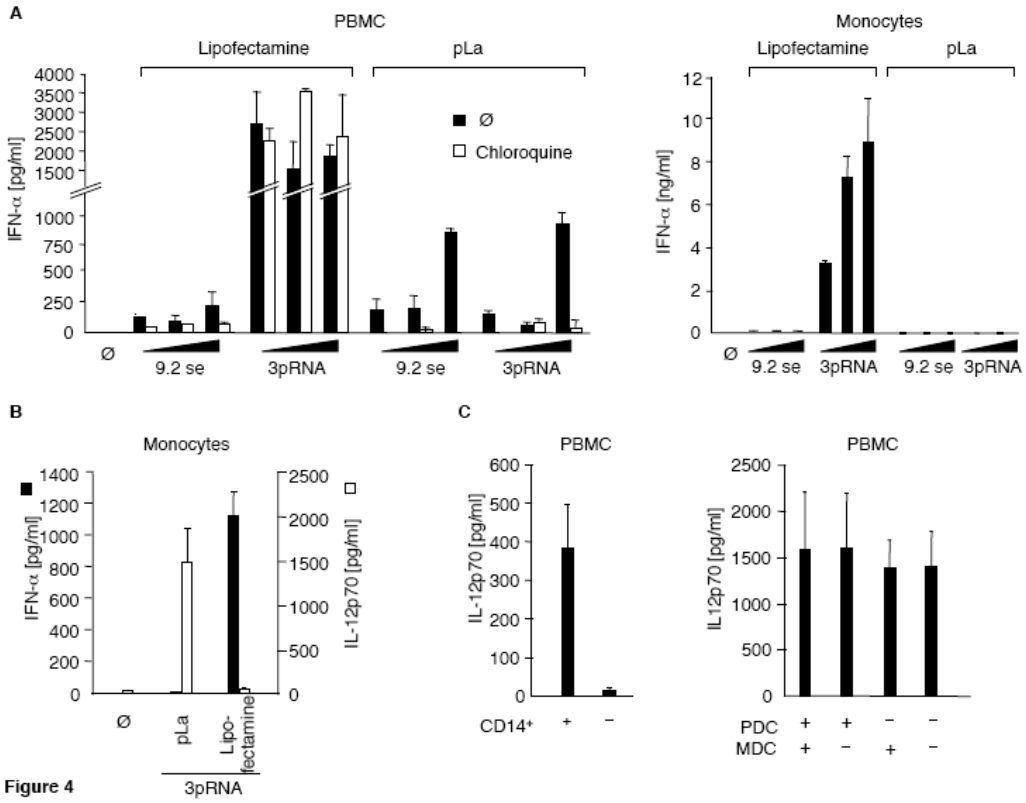
A
PBMC
Lipofectamine
pLa
IFN-α [pg/ml]
4000
3500
3000
2500
2000
1500
1000
750
500
250
0
Ø
Chloroquine
Ø
9.2 se
3pRNA
9.2 se
3pRNA
Monocytes
Lipofectamine
pLa
IFN-α [ng/ml]
12
10
8
6
4
2
0
Ø
9.2 se
3pRNA
9.2 se
3pRNA
B
Monocytes
IFN-α [pg/ml]
1400
1200
1000
800
600
400
200
0
IL-12p70 [pg/ml]
2500
2000
1500
1000
500
0
Ø
pLa
Lipo-fectamine
3pRNA
C
PBMC
IL-12p70 [pg/ml]
600
500
400
300
200
100
0
CD14+
+
–
PBMC
IL12p70 [pg/ml]
2500
2000
1500
1000
500
0
PDC
MDC
+
+
–
–
+
–
+
–

Figure 4

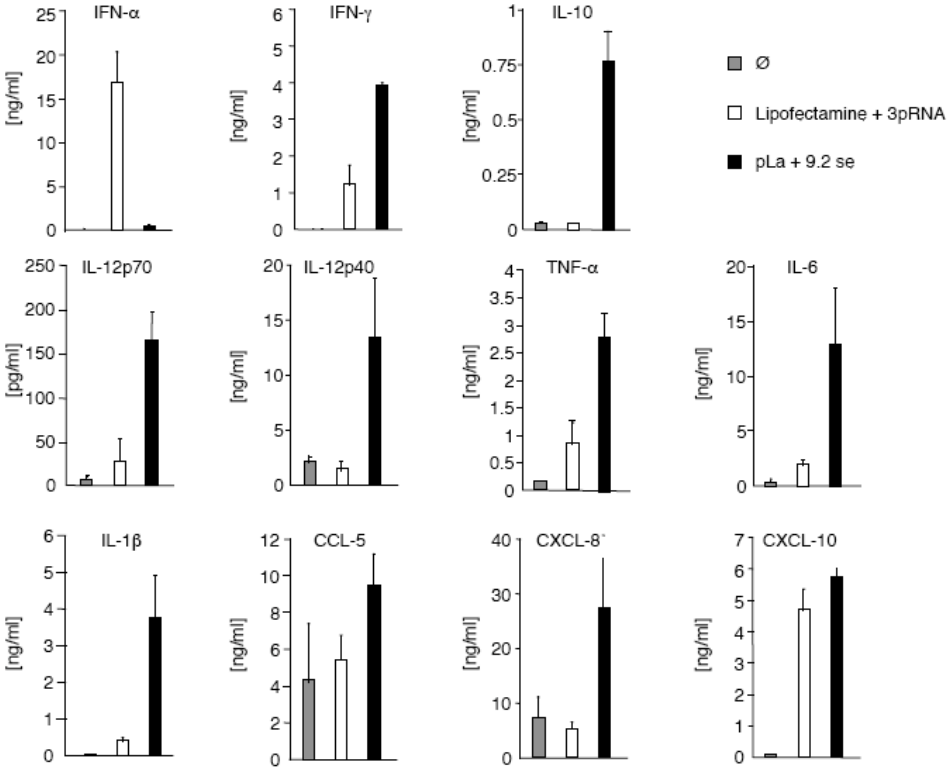
IFN-α
IFN-γ
IL-10
Ø
Lipofectamine + 3pRNA
pLa + 9.2 se
IL-12p70
IL-12p40
TNF-α
IL-6
IL-1β
CCL-5
CXCL-8
CXCL-10
[ng/ml]
[pg/ml]

Figure 5

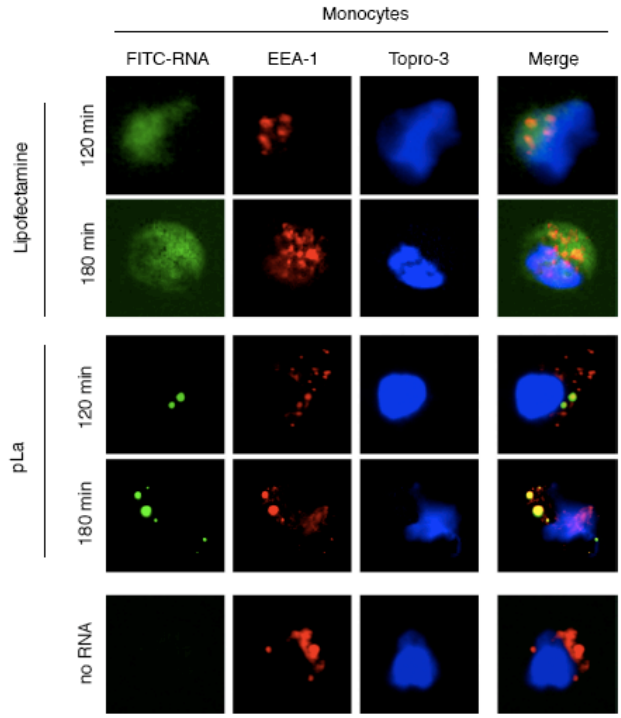
Monocytes
FITC-RNA
EEA-1
Topro-3
Merge
Lipofectamine
120 min
180 min
pLa
120 min
180 min
no RNA

Figure 6

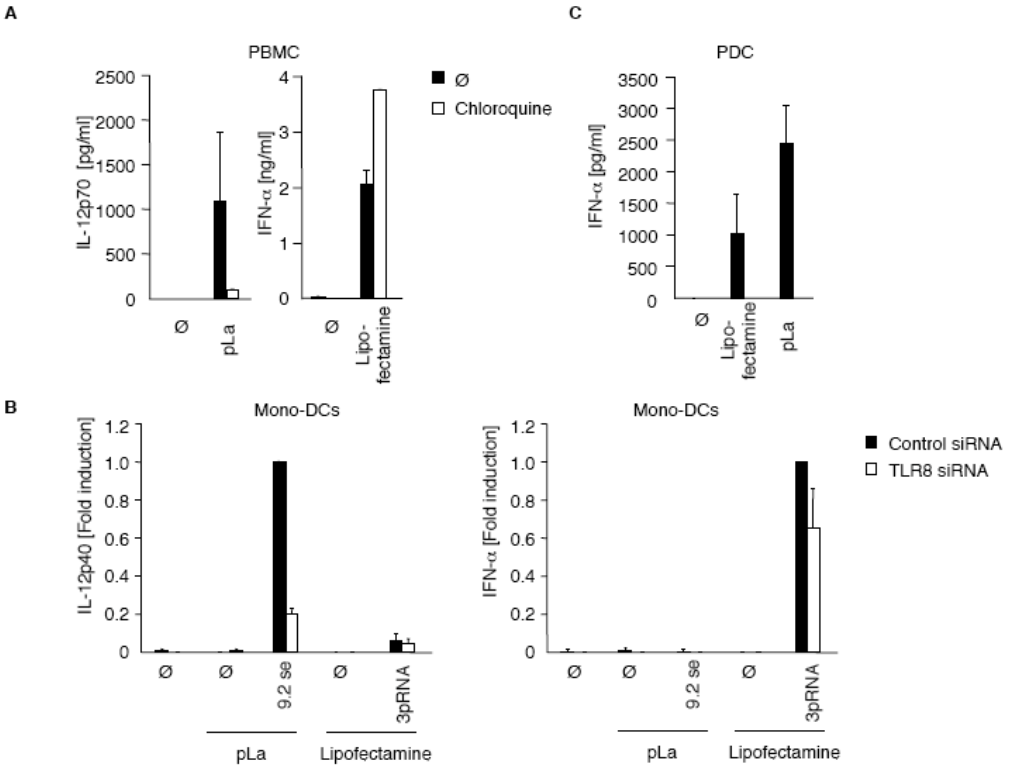
A
PBMC
IL-12p70 [pg/ml]
IFN-α [ng/ml]
Ø
Chloroquine
Ø
pLa
Ø
Lipo-fectamine
C
PDC
IFN-α [pg/ml]
Ø
Lipo-fectamine
pLa
B
Mono-DCs
IL-12p40 [Fold induction]
Ø
Ø
9.2 se
Ø
3pRNA
pLa
Lipofectamine
Mono-DCs
IFN-α [Fold induction]
Ø
Ø
9.2 se
Ø
3pRNA
pLa
Lipofectamine
Control siRNA
TLR8 siRNA

Figure 7

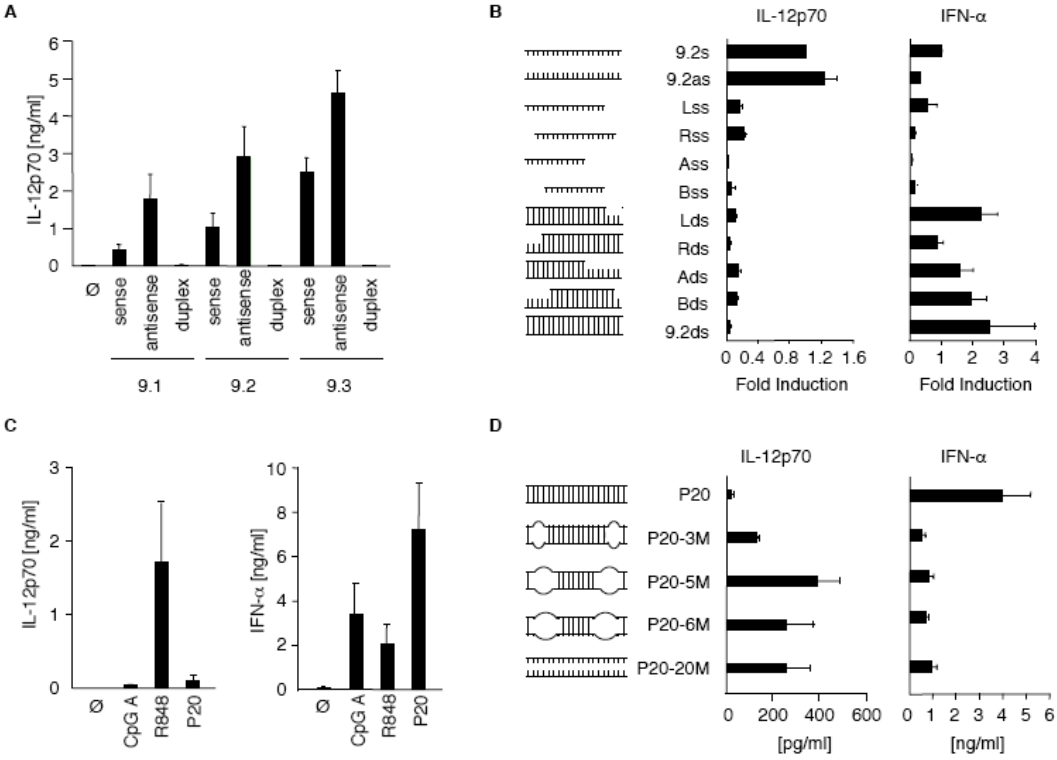
A
IL-12p70 [ng/ml]
Ø
sense
antisense
duplex
9.1
9.2
9.3
B
IL-12p70
IFN-α
9.2s
9.2as
Lss
Rss
Ass
Bss
Lds
Rds
Ads
Bds
9.2ds
Fold Induction
C
IL-12p70 [ng/ml]
IFN-α [ng/ml]
CpG A
R848
P20
D
P20
P20-3M
P20-5M
P20-6M
P20-20M
[pg/ml]
[ng/ml]

Figure 8

Table I. RNA Sequences

Name	Sequence 5´→ 3´
2.2 sense*	GCAUGCGACCUCUGUUUGA
9.1 sense	UGGACGGCAACUGUUAUUA
9.1 antisense	UAAUAACAGUUGCCGUCCA
9.2 sense	AGCUUAACCUGUCCUUCAA
9.2 antisense	UUGAsAGGACAGGUUAAGCU
9.3 sense	ACCUGUCCUUCAAUUACCA
9.3 antisense	UGGUAAUUGAAGGACAGGU
Ass	AGCUUAACCUGU
Bss	AACCUGUCCUUC
Lss	AGCUUAACCUGUCCUU
Rss	UUAACCUGUCCUUCAA
P20	**UUGAAGGACAUGUCCUUCAA**
P20 – 3M	**U**GUC**AGGACAUGUCCU**UCA**A**
P20 – 5M	**U**GUCCU**GACAUGUC**CUUCA**A**
P20 – 6M	**U**GUCCUU**ACAUGU**CCUUCA**A**
P20 - 20M	**U**GUCCUUCA**AU**GUCCUUCA**A**
27+2 sense	GCUGACCCUGAAGUUCAUCUGCACCACUU
27+2 antisense	GUGGUGCAGAUGAACUUCAGGGUCAGCUU
27+0 sense	AAGCUGACCCUGAAGUUCAUCUGCACC
27+0 antisense	GGUGCAGAUGAACUUCAGGGUCAGCUU
GFPs*	**ppp**GGGGCUGACCCUGA**AGUUCA**UCUU
GA*	**ppp**GGGGGGGGGGAAAAAAAAAAA

* These RNA oligonucleotides were generated by *in vitro* transcription.
(For GFPs a TLR7/8 motif is depicted in bold letters underlined)

Table II. DNA-Oligonucleotides (Templates) for *in vitro* transcription

Name	Sequence 5´→ 3´
2.2 sense	TCAAACAGAGGTCGCATGCCTATAGTGAGTCG
2.2 antisense	GCATGCGACCTCTGTTTGACTATAGTGAGTCG
GA	TTTTTTTTTTTTCCCCCCCCCCCCTATAGTGAGTCG
GFPs	AAGATGAACTTCAGGGTCAGCCCTATAGTGAGTCG
GFPas	AAGCTGACCCTGAAGTTCATCCCTATAGTGAGTCG

Table III. siRNA sequences

Name	Sequence 5´→ 3´
Luc sense	CUUACGCUGAGUACUUCGAdTdT
Luc antisense	UCGAAGUACUCAGCGUAAGdTdT
RIG-I sense	AAGGCUGGUUCCGUGGCUUUUdTdT
RIG-I antisense	AAAAGCCACGGAACCAGCCUUdTdT
TLR8 sense	GGGAGUUACUGCUUGAAGAdTdT
TLR8 antisense	UCUUCAAGCAGUAACUCCCdTdT

2. 2. AIM2 recognizes cytosolic dsDNA and forms a caspase-1 activating inflammasome with ASC

Hornung V, Ablasser A, Charrel-Dennis M, Bauernfeind F, Horvath G, Caffrey D. R, Latz E und Fitzgerald K.A.

Nature. 2009 Mar 26;458(7237):514-8.

AIM2 recognizes cytosolic dsDNA and forms a caspase-1 activating inflammasome with ASC

Veit Hornung[1,2], Andrea Ablasser[1,2], Marie Charrel-Dennis[1], Franz Bauernfeind[1,2], Gabor Horvath[1], Daniel. R. Caffrey[3], Eicke Latz[1,*] and Katherine A. Fitzgerald[1,*]

[*]Equal contributors

[1]Division of Infectious Diseases and Immunology, Department of Medicine, University of Massachusetts Medical School, Worcester, MA, 01605, USA.
[2]Institute of Clinical Chemistry and Pharmacology, Universitätsklinikum Bonn, Germany.
[3]Pfizer, 620 Memorial Drive, Cambridge, MA 02139, USA.

The innate immune system senses nucleic acids via germ-line encoded pattern recognition receptors. RNA is sensed via Toll-like receptor (TLR)-3, -7 and -8 or by the cytoplasmic RNA helicases RIG-I and MDA-5[1]. Little is known about sensors for cytoplasmic DNA, which when delivered to the cytoplasm trigger type I IFN gene transcription and caspase-1-mediated processing of IL-1β[2-6]. Here we identify the IFI20X/IFI16 (PYHIN) family member[7], absent in melanoma 2 (AIM2), which is uniquely localized to the cytosol, as a receptor for cytosolic DNA. The HIN200 domain of AIM2 binds to DNA, while the PYD domain (but not that of the other PYHIN family members) associates with the adapter molecule ASC to activate NF-κB and caspase-1. Knockdown of AIM2 abrogates caspase-1 activation in response to cytoplasmic dsDNA and the dsDNA virus, vaccinia. Collectively, these observations identify AIM2 as a novel receptor for cytoplasmic DNA, which forms an inflammasome with the ligand and ASC to activate caspase-1.

While pathways of cytoplasmic viral RNA recognition have been studied extensively [reviewed in[1]], little is known about mechanisms sensing cytoplasmic DNA. Recent evidence indicates that in addition to TLR9, cells express one or more cytosolic DNA sensors, which trigger potent antiviral and/or inflammatory responses[2-6]. The best characterized of these responses involves activation of the TANK-binding kinase (TBK1)-Interferon Regulatory Factor (IRF)-3 signaling axis to trigger transcriptional induction of IFNα/β genes[6,8]. A second, less well-defined pathway leads to the activation of an 'inflammasome', which via caspase-1, controls the catalytic cleavage of the pro-forms of the cytokines IL-1β and IL-18[4,9]. Recently, a candidate receptor called DAI (DNA-dependent Activator of IFN-regulatory factors) was identified as an upstream component of the DNA induced IFN pathway[5]. More recent studies in cells lacking DAI however, suggest that additional receptors for cytoplasmic dsDNA induced IFN responses exist[3]. NLRP3, (also called Nalp3, Cryopyrin) has recently been shown to activate the caspase-1 pathway in response to internalized adenoviral DNA[4]. Correspondingly, NLRP3- and ASC-deficient mice display reduced innate inflammatory responses to adenoviral particles. However, caspase-1 activation in response to transfected bacterial, viral, mammalian or synthetic DNA does not appear to involve NLRP3, although the adapter molecule ASC is required for this response[4,9]. Collectively, these data indicate that additional cytosolic DNA sensors exist to regulate the type I IFN response and/or the ASC dependent inflammasome pathway. Here, we sought to identify upstream components of the dsDNA activated ASC inflammasome pathway. We hypothesized that an upstream activator of this pathway would contain a pyrin domain (PYD) for homotypic interaction with ASC and at least one additional domain, for direct binding of the dsDNA ligand itself or for the interaction with another further upstream receptor. We used the synthetic dsDNA, poly(dA-dT) • poly(dA-dT) [hereafter referred to as poly(dA-dT)])[10], eukaryotic and prokaryotic dsDNA, as well as a dsDNA virus (vaccinia virus) to study DNA signalling. In addition to NLRP3[11], the related proteins NLRP6[12] and NLRP12[13] have previously been shown to associate with and function upstream of ASC. We therefore first tested the role of these NLRs in dsDNA-mediated inflammasome activation using bone marrow derived macrophages from mice lacking these NLRs. While ASC-deficient macrophages failed to activate caspase-1 and trigger IL-1β release in response to poly(dA-dT), macrophages lacking NLRP3, -6 and -12 responded normally (Fig. 1a). Surprisingly, when we monitored cytokine production, we found that macrophages lacking ASC had a greatly enhanced poly(dA-dT)-induced cytokine response (IFNβ and IL-6), which was not observed in cells lacking NLRP3, the IL1R or to a lesser extent caspase-1. In agreement with previous reports showing that inflammasome

activation was associated with cell death, we observed that poly(dA-dT) induced cell death occurred in an ASC-dependent manner (Supplementary Fig. 1). We speculate that the increased cytokine production observed in ASC-deficient cells relates to their resistance to poly(dA-dT) induced cell death. In addition to poly(dA-dT), dsDNA from natural sources could also activate this response (Supplementary Fig. 2a-b). In contrast, a small immunostimulatory oligonucleotide (ISD)[6] or long ssDNA (poly(dI)) failed to trigger caspase-1 cleavage. Moreover, the ssRNA virus Sendai virus or transfected dsRNA also failed to induce caspase-1 cleavage in NLRP3-deficient macrophages (Supplementary Fig. 2c). We next searched the PFAM database[14] and identified several PYD-domain containing proteins, which also contained HIN200 domains. The HIN200 domain has previously been shown to function as a DNA binding domain[15]. In humans, the HIN200 protein family consists of four members[16]; IFIX[17], IFI16[18], MNDA[19] and AIM2[20], all of which are encoded on the same locus on chromosome 1[7]. A multiple sequence alignment of PYD domains from the PYHIN family with selected PYD domains from the NLRs is shown (Fig. 1b). Sequence analysis of IFIX, IFI16 and MNDA predicted that these proteins would localize to the nucleus. In contrast, AIM2 was predicted to reside in the cytosolic compartment (Fig. 1c, lower panel). We examined the subcellular localization of these proteins directly using fluorescent protein chimeras by confocal microscopy. Consistent with the predicted localizations, IFIX, IFI16 and MNDA predominantly localized to the nucleus, while AIM2 was almost exclusively cytoplasmic (Fig. 1d). To study the possibility that these PYHIN proteins associated with ASC in the cytosol, we generated C-terminally tagged CFP PYD-domain fusions. Of note, the putative nuclear localization sequences were predicted to be absent in these fusion proteins thereby preventing their nuclear retention. Consistent with these predictions, all of the PYD CFP fusion proteins were localized in the cytoplasm (Supplementary Fig. 3), enabling us to study homotypic molecular interactions between overexpressed PYD domains of the PYHIN family proteins and ASC. To test whether induced clustering of PYD-CFP fusion proteins leads to association with ASC-YFP via homotypic pyrin-pyrin interactions, we utilized a HEK293 cell line that stably expressed ASC-YFP in the cytosol. This cell line expressed ASC-YFP at low enough levels to be polydispersed throughout the cytoplasm without visible aggregates (Fig. 2a, Mock) allowing an analysis of proteins, which would induce ASC complex formation. Indeed, overexpression of the ASC-interacting NLRP3-CFP-tagged PYD domain led to the formation of large cytosolic aggregates, which co-aggregated ASC-YFP (Fig. 2a). Notably, in most transfected cells extensive intracellular co-localization with ASC YFP was observed with a complete loss of cytoplasmic distribution of ASC-YFP. This

observation is indicative of complete recruitment of ASC into the NLRP3-PYD complex[11,12,21]. Of all the PYHIN-PYD proteins tested, only AIM2-PYD led to complex formation with ASC (Fig. 2a, b and Supplementary Fig. 4). Even though the overexpression of IFIX-PYD, IFI16-PYD and MNDA-PYD led to self-aggregation, no change in the expression pattern of ASC YFP was observed. Expression of full-length AIM2-CFP similarly led to pronounced co aggregation of ASC-YFP, while full-length IFIX, IFI16 and MNDA were localized to the nucleus and did not change the aggregation status of ASC-YFP (Fig. 2a, b and Supplementary Fig. 5a, b). In agreement with these results, only AIM2-PYD and NLRP3-PYD were found to bind ASC in co-immunoprecipitation studies from cells overexpressing the respective CFP-tagged PYD proteins together with HA-tagged ASC (Fig. 2c). Indeed, when we immunopreciptated endogenous ASC from primed THP-1 cells, we copreciptated endogenous AIM2, but not IFI16 (Fig. 2d). Alltogether, these data indicated that AIM2 but not IFIX, IFI16 and MNDA can physically interact with ASC and induce ASC pyroptosome formation. It is known that overexpression of ASC-interacting proteins can lead to the activation of both NF-κB and caspase-1[11,22]. To examine the functional relevance of AIM2-ASC complex formation, we first studied activation of an NF-κB reporter gene in cells overexpressing the PYD-PYHIN proteins in the presence of increasing amounts of ASC. Consistent with the imaging and co-immunoprecipitation studies, only NLRP3-PYD and AIM2-PYD led to potent NF-κB activation with increasing concentrations of ASC (Fig. 2e). The effect of full length AIM2 in this assay was even more dramatic, showing up to 60-fold increases in NF-κB activation in the presence of ASC (Fig. 2e, bottom panel). The full-length versions of IFIX, IFI16 and MNDA failed to activate NF-κB (Supplementary Fig. 5c). ASC was absolutely required for NF-κB activation, since no significant NF-κB reporter activity was observed in 293T cells not transfected with ASC. We further examined IFNβ gene induction in these assays and in contrast to what we observed with NF-κB signaling, no significant activation of the IFNβ promoter reporter gene was observed with any of the PYHIN family members (Supplementary Fig. 6). Altogether, these results indicated that AIM2 is unique amongst the PYHIN family by being localized to the cytosol, interacting with ASC leading to cytosolic pyroptosome complex formation and subsequent NF-κB activation. We next examined whether the AIM2-ASC complex could lead to the formation of a functional inflammasome complex and caspase-1-dependent maturation of pro-IL-1β. To this effect, we employed a transient transfection assay overexpressing the respective proteins of interest in the presence of ASC, caspase-1 and a flag-tagged version of pro-IL-1β in 293T cells. In this experimental setup the cleavage of pro-IL-1β into IL-1β can be assessed in cell

lysates by immunoblot analysis. Among the PYD proteins tested, only that of NLRP3-PYD and AIM2-PYD induced maturation of pro-IL-1β, when ASC and caspase-1 were co-expressed (Fig. 3a). Expression of full-length AIM2 induced a more potent cleavage of pro-IL-1β When compared to AIM2-PYD (Fig. 3a, lower panel). Only a very low level expression of full-length AIM2 was required to induce cleavage of pro-IL-1β in the presence of ASC and caspase-1, while the PYD domain or full-length versions of IFIX, IFI16 or MNDA failed to induce IL-1β cleavage (Supplementary Fig. 7). To study the role of AIM2 in cells with a functional poly(dA-dT)-triggered or dsDNA virus induced inflammasome complex, we used lentiviruses encoding shRNAs to knock down expression of AIM2 in a murine macrophage cell line generated by immortalizing bone marrow derived macrophages from C57BL/6 mice (B6 MCLs) or NLRP3-deficient mice (N3-KO-MCLs)[9]. AIM2 was expressed constitutively in both primary murine macrophages and in B6-MCLs and was inducible upon stimulation with poly(dA-dT) or with the paramyxovirus, Sendai virus (Supplementary Fig. 8). Three different shRNAs were used to knock down AIM2, of which two (shRNA AIM2 #2 and AIM2 #3) resulted in a strong reduction of AIM2 expression as determined by real time PCR (Fig. 3b). Knocking down AIM2 expression, but not an unrelated control gene, resulted in a strong attenuation of poly(dA-dT)-mediated IL-1β release (Fig. 3c) and caspase-1 cleavage (Fig. 3d). Targeting AIM2 in THP1 cells using siRNA corroborated these findings (Supplementary Fig. 8d and e). Moreover and consistent with what we had seen in ASC-deficient macrophages (Supplementary Fig. 1), knocking down AIM2 expression resulted in a marked enhancement of poly(dA-dT)-mediated type I IFN induction (Supplementary Fig. 8b). This effect was specific to poly(dA-dT) activation since the IFNβ response to Sendai virus was unaffected when AIM2 levels were knocked down by shRNA (Supplementary Fig. 8c). In addition, and in agreement with the results obtained in ASCdeficient macrophages, macrophages that were targeted with AIM2 targeting shRNAs were stronlgy resistant to poly(dA-dT) triggered cell death (Fig. 3e). We next sought to determine the effect of AIM2 on the recognition of a dsDNA virus. We infected mouse macrophages from wild-type, NLRP3- and ASC-deficient mice with vaccinia virus and monitored caspase-1 cleavage. Similarly to what we had observed with sensing of transfected poly(dA-dT), vaccinia virus-induced caspase-1 cleavage occurred in an NLRP3-independent, yet ASC-dependent fashion (Fig. 3f). This effect was dependent on AIM2, since shRNA-mediated knock down of AIM2 greatly impaired caspase-1 cleavage in response to vaccinia virus but not in response to an AIM2-independent stimulus. Moreover, knock down of a control protein did not alter caspase-1 cleavage after vaccinia virus infection (Fig. 3g). Vaccinia virus-triggered cell death

was also strongly reduced in AIM2 shRNA targeted macrophages, but not in control shRNA targeted macrophages (Fig. 3h). Altogether, these results indicated that AIM2 was required for poly(dA-dT) and vaccinia virus-mediated inflammasome activation and that AIM2 positively regulated dsDNA and vaccinia virus-triggered cell death. The fact that AIM2 harbors a C-terminal HIN200 domain previously shown to bind dsDNA prompted us to examine if AIM2 could be involved in the recognition of dsDNA directly. To address this question, we generated fluorescein-labeled poly(dA-dT), (FITCdsDNA) and co-transfected FITC-DNA together with CFP-tagged versions of full-length AIM2, AIM2-HIN domain, AIM2-PYD domain or full-length NLRP3. While cells expressing NLRP3 or AIM2-PYD showed no co-localization of the respective proteins with FITC-dsDNA, full-length AIM2 and AIM2-HIN domain showed extensive co-localization with FITC-dsDNA and led to the formation of DNA/protein aggregates in the cytosol (Fig. 4a). To quantitate these DNA/protein interactions we analyzed the interaction of AIM2 with FITC-dsDNA by fluorescence resonance energy transfer (FRET) measurements using flow cytometry (Fig. 4b). We found dose dependent increases in FRET between the full-length AIM2 protein and FITC-dsDNA, while the AIM2-PYD domain protein did not lead to measurable FRET. Other proteins such as NLRP3 or IFI16 did not show any FRET even at the highest concentration of FITC-dsDNA (data not shown). Additionally, binding studies using purified AIM2, AIM2-HIN domain and AIM2-PYD domain proteins with biotinylated poly(dA-dT) (biotin-dsDNA) demonstrated that AIM2 directly interacts with poly(dA-dT) with high affinity; only full-length AIM2 or the AIM2-HIN domain were able to bind biotin DNA, whereas no binding was observed for the AIM2-PYD domain (Fig. 4c). Binding of poly(dA-dT) to AIM2 was specific, since AIM2 did not bind biotin-LPS, which bound to soluble CD14 under similar assay conditions (Fig. 4c).

Collectively, these data identify AIM2 as a receptor for cytosolic dsDNA, which forms a novel inflammasome complex with ASC to activate caspase-1-mediated processing of IL-1β. Thus, in addition to viral and bacterial components or danger signals in general, the identification of AIM2 reveals that inflammasomes also sense cytoplasmic DNA, strengthening their central role in innate immunity. Our data suggest that the activation of the AIM2 inflammasome is likely to be important in host-defense against dsDNA viruses or potentially bacterial pathogens known to trigger cytosolic signaling pathways such as Francisella tularensis[23] or Listeria monocytogenes[6]. In addition, accumulation of aberrant host DNA and exaggerated responses to DNA have been associated with autoimmune diseases

[reviewed in[10]], suggesting a potential role for AIM2 in pathological autoimmunity. Elevated levels of IL-1β have been found in patients with systemic lupus erythematosis, consistent with this possibility[24]. Indeed, AIM2 and related HIN200 family members have already been linked to SLE[25], although whether this relates to inflammasome activation and IL-1 processing is unknown. Further characterization of the AIM2 inflammasome as a sensor of microbial, as well as host DNA therefore may enable the rational design of new therapies and treatments for infectious as well as autoimmune diseases.

Methods Summary

Reagents. All cDNAs were cloned by PCR from cDNA into pEFBOS-C-term-CFP and subcloned into pEFBOS-C-term-FLAG/HIS as indicated. Biotinylated and FITC-labeled poly(dA-dT) were made by adding Biotin-dUTP or FITC-dUTP (Fermentas) in a molar ratio of 1:8 to dTTP in the enzymatic synthesis of poly(dA-dT) as described[26]. Vaccinia virus (Western Reserve strain) was kindly provided by Drs. Lianjun Shen and Kenneth Rock (University of Massachusetts Medical School, Worcester, MA).

Mice. NLRP3, NLRP6, NLRP12 and ASC-deficient mice were from Millennium Pharmaceuticals (Cambridge, MA), Caspase-1-deficient mice were from R. Flavell (Yale University, New Haven, CT) and IL-1R-deficient (*Il1r1*–/–) were purchased from Jackson Laboratories (Bar Harbor, ME).

Cell culture and stimulation. Bone marrow derived macrophages were stimulated as indicated (see supplementary methods for more details). Poly(dA-dT) DNA and all other DNAs were transfected using Lipofectamine 2000 at a concentration of 1 μg/ml according to the manufacturer's instructions.

ELISA. Cell culture supernatants were assayed for IL-1β using ELISA kits from BD Biosciences (Franklin Lakes, NJ).

Confocal microscopy. Confocal microscopy was performed on a Leica SP2 AOBS confocal laser scanning microscope. Separation of CFP and YFP was performed using sequential scanning and 405 and 514 nm excitation.

Flow cytometry Fluorescence Resonance Energy Transfer (FRET). FRET efficiencies were calculated on a cell-by-cell basis[27] and then calculated FRET efficiency histograms were plotted with GraphPad Prism 5.01 (GraphPad Software).

Immunoblot analysis. For caspase-1 immunoblotting, supernatants were precipitated as previously described[9] and examined by immunoblotting (see supplemental methods for more details).

Quantitative real-time PCR. RNA from murine macrophages was extracted, cDNA was synthesized and quantitative RT-PCR analysis performed on a DNA engine Opticon 2 cycler (MJ Research, Watertown MA) with the iQ SYBR Green Supermix (Biorad, Hercules, CA) as outlined in supplemental methods.

shRNA mediated silencing. Lentiviral shRNAs targeting AIM2 were obtained from OpenBiosystems and shRNA silencing carried out as described (http://www.broad.mit.edu/genome_bio/trc/publicProtocols.html).

AlphaScreen Assay. The AlphaScreen (amplified luminescent-proximity homogeneous assay) was set up as an association assay as outlined in supplemental methods and read with the Envision HT microplate reader (Perkin Elmer).

Reporter assays. Reporter assays for NF-κB or IFNβ luciferase reporters were carried out as described[28].

References

[1] E. Meylan, J. Tschopp, and M. Karin, *Nature* **442** (7098), 39 (2006).

[2] K. J. Ishii, C. Coban, H. Kato et al., *Nat Immunol* **7** (1), 40 (2006).

[3] K. J. Ishii, T. Kawagoe, S. Koyama et al., *Nature* **451** (7179), 725 (2008).

[4] D. A. Muruve, V. Petrilli, A. K. Zaiss et al., *Nature* **452** (7183), 103 (2008).

[5] A. Takaoka, Z. Wang, M. K. Choi et al., *Nature* **448** (7152), 501 (2007).

[6] D. B. Stetson and R. Medzhitov, *Immunity* **24** (1), 93 (2006).

[7] L. E. Ludlow, R. W. Johnstone, and C. J. Clarke, *Experimental cell research* **308** (1), 1 (2005).

[8] S. Sharma, B. R. tenOever, N. Grandvaux et al., *Science* **300** (5622), 1148 (2003); K. A. Fitzgerald, S. M. McWhirter, K. L. Faia et al., *Nat Immunol* **4** (5), 491 (2003).

[9] V. Hornung, F. Bauernfeind, A. Halle et al., *Nat Immunol* **9** (8), 847 (2008).

[10] Ken J. Ishii and Shizuo Akira, *Trends in Immunology* **27** (11), 525 (2006).

[11] G. A. Manji, L. Wang, B. J. Geddes et al., *The Journal of biological chemistry* **277** (13), 11570 (2002).

[12] J. M. Grenier, L. Wang, G. A. Manji et al., *FEBS Lett* **530** (1-3), 73 (2002).

[13] L. Wang, G. A. Manji, J. M. Grenier et al., *The Journal of biological chemistry* **277** (33), 29874 (2002).

[14] R. Finn, S. Griffiths-Jones, and A. Bateman, *Current protocols in bioinformatics / editoral board, Andreas D. Baxevanis ... [et al* **Chapter 2**, Unit 2 5 (2003).

[15] M. Albrecht, D. Choubey, and T. Lengauer, *Biochemical and biophysical research communications* **327** (3), 679 (2005).

[16] S. Landolfo, M. Gariglio, G. Gribaudo et al., *Biochimie* **80** (8-9), 721 (1998).

[17] Y. Ding, L. Wang, L. K. Su et al., *Oncogene* **23** (26), 4556 (2004).

[18] J. A. Trapani, K. A. Browne, M. J. Dawson et al., *Immunogenetics* **36** (6), 369 (1992).

[19] G. R. Burrus, J. A. Briggs, and R. C. Briggs, *Journal of cellular biochemistry* **48** (2), 190 (1992).

[20] K. L. DeYoung, M. E. Ray, Y. A. Su et al., *Oncogene* **15** (4), 453 (1997).

[21] J. W. Yu, J. Wu, Z. Zhang et al., *Cell death and differentiation* **13** (2), 236 (2006).

[22] S. M. Srinivasula, J. L. Poyet, M. Razmara et al., *The Journal of biological chemistry* **277** (24), 21119 (2002).

[23] T. Henry, A. Brotcke, D. S. Weiss et al., *The Journal of experimental medicine* **204** (5), 987 (2007).

[24] K. H. Sun, C. L. Yu, S. J. Tang et al., *Immunology* **99** (3), 352 (2000).

[25] D. Choubey and R. Panchanathan, *Immunology letters* **119** (1-2), 32 (2008).

[26] H. K. Schachman, J. Adler, C. M. Radding et al., *The Journal of biological chemistry* **235**, 3242 (1960).

[27] G. Szentesi, G. Horvath, I. Bori et al., *Computer methods and programs in biomedicine* **75** (3), 201 (2004).

[28] M. Severa, E. M. Coccia, and K. A. Fitzgerald, *The Journal of biological chemistry* (2006).

[29] R. C. Edgar, *Nucleic acids research* **32** (5), 1792 (2004).

Acknowledgements

The authors would like to thank Anna Cerny for animal husbandry and genotyping. V.H. is supported by a fellowship from the DFG (Ho2783/2-1), E.L. and K.A.F. are supported by grants from the NIH (AI-065483 (to E.L.) and AI-067497 (to K.A.F.).

Author Contributions

V.H conceived the research and conducted the experiments with A.A., M.C.D., F.B, G.H, and D.R.C conducted the bioinformatics analysis. E.L and K.A.F oversaw the whole project.

Author Information:

Reprints and permissions information is available at npg.nature.com/reprintsandpermissions. Correspondence and requests for materials should be addressed to K.A.F, E.L or V.H.; kate.fitzgerald@umassmed.edu, eicke.latz@umassmed.edu or veit.hornung@ukb.uni-bonn.de

Figure legends:

Figure 1 | poly(dA-dT)-mediated inflammasome activation involves ASC, but is independent of NLRP3, NLRP6 and NLRP12. a, Macrophages from either wild type, ASC -/-, NLRP3 -/-, NLRP6 -/- or NLRP12 -/- mice were LPS-primed and then stimulated with ATP or transfected with poly(dA-dT). After 6h, supernatants were assessed for IL-1β by ELISA and for cleaved caspase-1 by immunoblot. **b,** A multiple sequence alignment of human PYHIN and select NLR PYD domains was generated using MUSCLE[29] **c,** The domain structures of the four human PYHIN proteins are depicted, with predicted monopartite or bipartite nuclear localization signals indicated. The predicted subcellular localization was calculated for the four human PYHIN proteins and for murine and rat AIM2 and is shown in the lower panel. **d,** 293T cells overexpressing CFP-tagged IFIX, IFI16, MNDA, AIM2 or NLRP3 (green) were analyzed by confocal microscopy. Membranes were stained with fluorescent choleratoxin (blue) and nuclei with DRAQ5 dye (red). Data from one representative experiment out of three are shown (a, d).

Figure 2 | The PYD domain of AIM2 interacts with ASC. **a,** Stable HEK293-ASC-YFP (green) cells were transiently transfected with CFP-tagged PYD domains of NLRP3, IFIX, IFI16, MNDA or AIM2 or with CFP-tagged full-length AIM2 (all in red), the membrane was stained with choleratoxin (blue) and cells were then imaged by confocal microscopy. Fluorescence intensities of the green (YFP-ASC) and red (PYD-CFP) channels were quantified along selected lines (white lines) and the percentage of ASC-YFP speckles per transfected cells assessed **(b)**. **c,** 293T cells were transfected with expression plasmids encoding HAtagged ASC and CFP-tagged constructs as in **(a)**. The protein levels of the CFP tagged PYD proteins in cell lysates were assessed by immunoblot analysis (INPUT, upper panels). Cell extracts were immunoprecipitated (IP) with anti-HA antibodies and immunoblotted (WB) with anti-HA antibody and anti-CFP antibody (lower panel). **d,** ASC was immunoprecipitated from THP-1 cell lysates primed with Sendai virus, whereas beads without anti-ASC antibody served as a negative control. The presence of ASC, IFI16 and AIM2 was assessed by immunoblot analysis in the cell lysate and the ASC immunoprecipitaion. The band above the AIM2 band in the ASC immunoprecipitation corresponds to the heavy chain of the anti-ASC antibody that is also detected by the secondary antibody. **e,** 293T cells were transfected with a multimerized NF-κB luciferase reporter construct together with fixed amounts of constructs as in **(a)** alone or together with

increasing amounts of ASC. Cellular NF-κB activation was quantified in cell lysates 24 hours after transfection. Data of one representative experiment out of three (a, b, c and d) or two (e) are depicted.

Figure 3 | AIM2 is required for poly(dA-dT) triggered inflammasome activation. a, 293T cells were transfected with caspase-1 (12.5 or 25 ng), ASC (3.1, 6.2 or 12.5 ng), pro-IL-1β (100ng) and NLRP3-PYD, IFIX, IFI16 and MNDA-PYD, AIM2-PYD or AIM2 full length (50ng). Cell lysates were immunoblotted for the C-terminally tagged IL-1β, recognizing both pro-IL-1β (>) and cleaved IL-1β (-) 24h after transfection. **b,** Murine macrophage cells (B6 MCLs) were transduced with lentiviral vectors encoding shRNAs targeting AIM2 (AIM2#1, AIM2#2, AIM2#3) or an irrelevant control gene (Ctrl.). AIM2/HPRT1 expression was determined in shRNA expressing cells. **c,** Cells as in (b) were primed with LPS and then stimulated with poly(dA-dT) or ATP. After 6h supernatants were assessed for IL-1β by ELISA. The poly(dA-dT) triggered IL-1β release was normalized to the respective ATP induced IL-1β release. The absolute values for the ATP-triggered IL-1β release were 1790, 2078, 2676 and 1119 pg/ml (AIM2#1, AIM2#2, AIM2#3 and Control) respectively (b). **d,** In addition, murine macrophages as in (b) were transfected with poly(dA-dT) or stimulated with LPS/ATP and assessed for cleavage of caspase-1 after 6h. **e**, Murine macrophages transduced with shRNA targeting AIM2 (AIM#3) or an irrelevant control gene (Ctrl.) were transfected with 200ng poly(dA-dT) or 100 ng poly(dAdT) and cell counts were assessed 24h after transfection. **f,** Macrophages from either wild type, ASC -/- or NLRP3 -/- were infected with vaccinia virus, transfected with poly(dA-dT) or stimulated with LPS/ATP and assessed for cleavage of caspase-1 after 6h. **g,** NLRP3-deficient shRNA expressing murine macrophages as in (b) were infected with vaccinia virus or stimulated with Anthrax lethal toxin and assessed for cleavage of caspase-1 after 6h. **h,** Cells as in (b) were infected with ascending doses of vaccinia virus (MOI 0.625 - 5) and cell survival was determined by calcein AM staining 24 h after infection. One representative experiment out of three (a, d, e, f, g and h) four (c) or five (b) is depicted.

Figure 4 | AIM2 binds dsDNA via its HIN domain. a, 293T cells were transfected with expression plasmids encoding CFP-tagged AIM2-full length, AIM2-HIN, AIM2-PYD, and NLRP3 (red) together with fluorescein labeled poly(dA-dT) (FITC-DNA, green). Cells were analyzed by confocal microscopy 24h after transfection. Fluorescence intensities of the green

(FITC-DNA) and red (CFP fusion protein) channels were quantified along selected lines (white lines). **b,** 293T cells were transfected with either CFP-tagged AIM2 full-length or AIM2-PYD and FITC-DNA or unlabeled DNA. Cells were analyzed by flow cytometry after 24 h and CFP and FITC positive cells were gated (left panel) and analyzed for FRET efficiency on a cell-bycell basis. Calculated FRET efficiency histograms are shown (right panel). **c,** AlphaScreen (homogenous ligand-binding assay) assessment of AIM2 full length, AIM2-HIN domain or AIM2-PYD domain binding to poly(dA-dT)/Biotin-dUTP (Biotin-DNA) (upper panel) AlphaScreen assay of AIM2 or sCD14 binding to Biotin-DNA or biotin LPS (lower panel). Representative data from 2 (d) or three (a, b, c) independent experiments are shown.

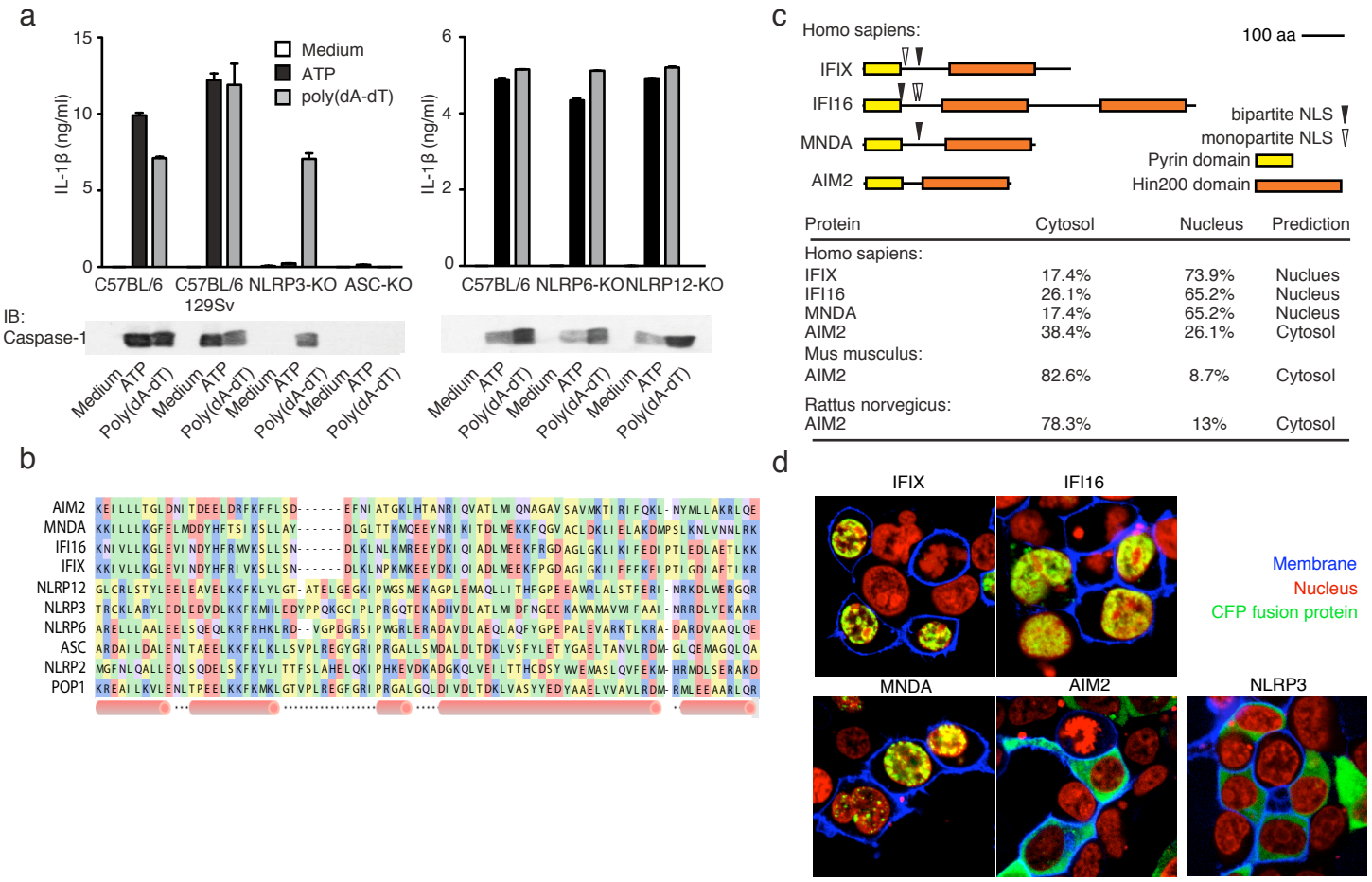

Protein	Cytosol	Nucleus	Prediction
Homo sapiens:			
IFIX	17.4%	73.9%	Nuclues
IFI16	26.1%	65.2%	Nucleus
MNDA	17.4%	65.2%	Nucleus
AIM2	38.4%	26.1%	Cytosol
Mus musculus:			
AIM2	82.6%	8.7%	Cytosol
Rattus norvegicus:			
AIM2	78.3%	13%	Cytosol

Figure 1

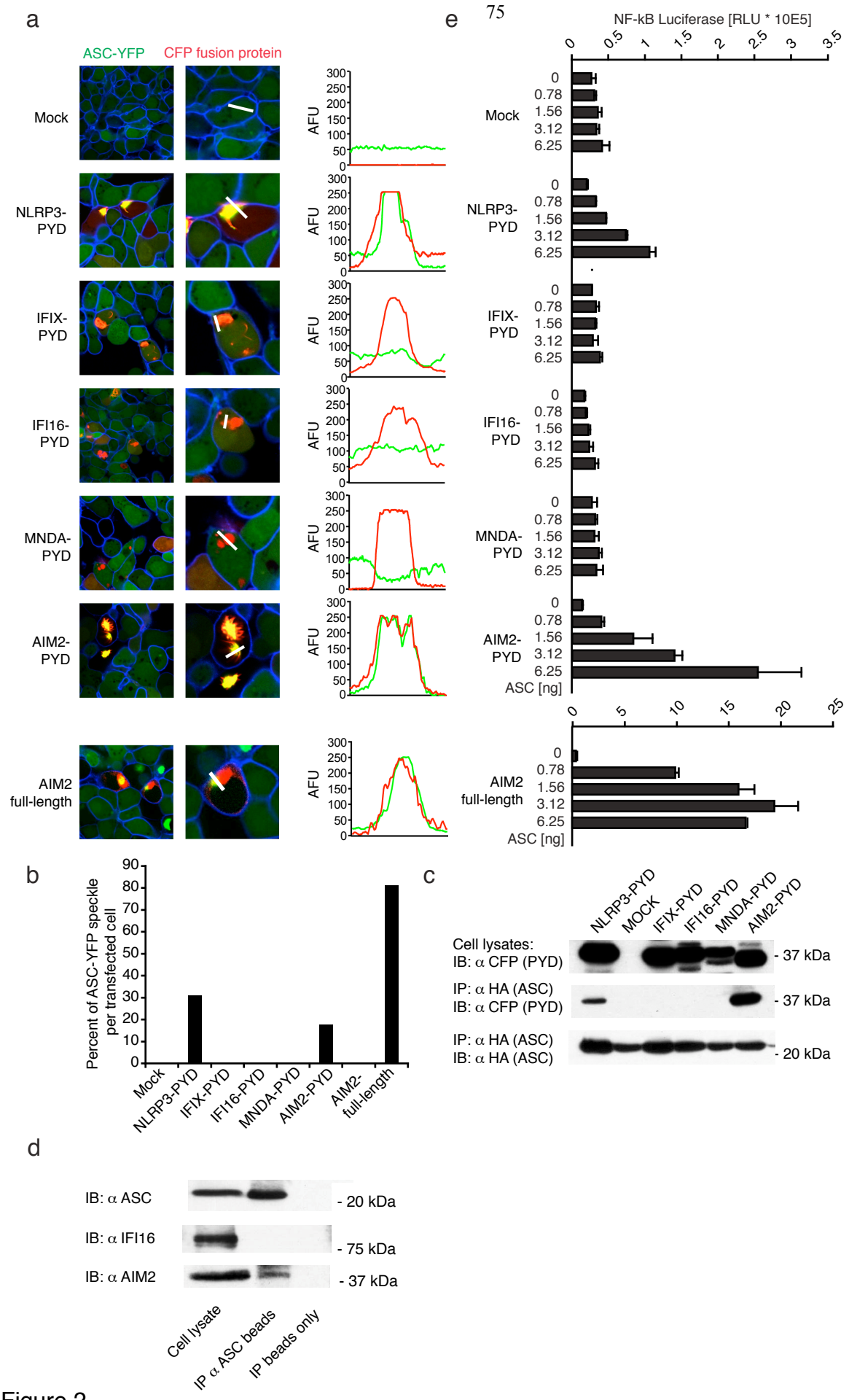
a
ASC-YFP
CFP fusion protein
Mock
NLRP3-PYD
IFIX-PYD
IFI16-PYD
MNDA-PYD
AIM2-PYD
AIM2 full-length
AFU
e
NF-kB Luciferase [RLU * 10E5]
ASC [ng]
b
Percent of ASC-YFP speckle per transfected cell
Mock
NLRP3-PYD
IFIX-PYD
IFI16-PYD
MNDA-PYD
AIM2-PYD
AIM2-full-length
c
Cell lysates:
IB: α CFP (PYD)
IP: α HA (ASC)
IB: α CFP (PYD)
IP: α HA (ASC)
IB: α HA (ASC)
- 37 kDa
- 37 kDa
- 20 kDa
d
IB: α ASC
IB: α IFI16
IB: α AIM2
- 20 kDa
- 75 kDa
- 37 kDa
Cell lysate
IP α ASC beads
IP beads only

Figure 2

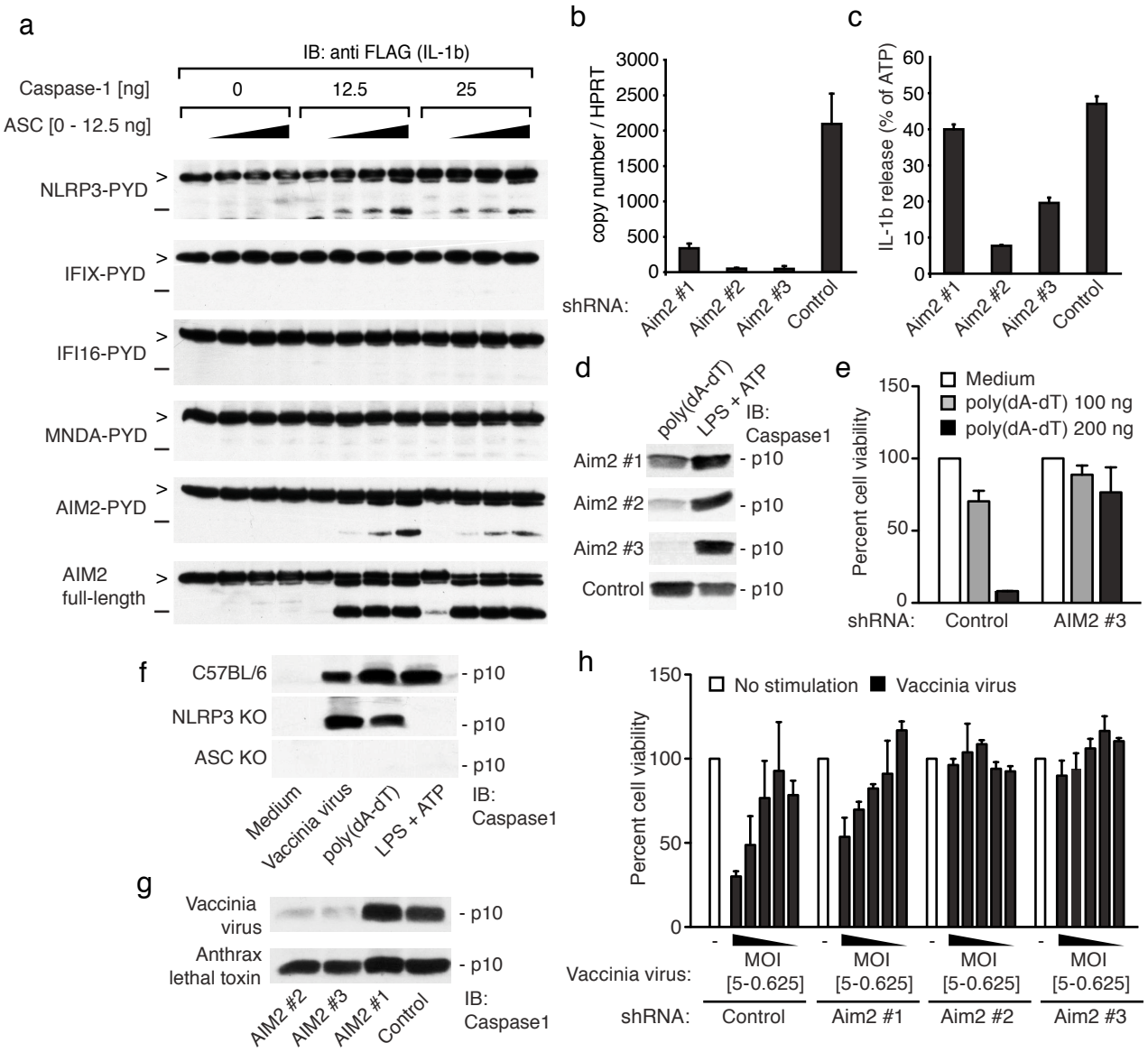
a
IB: anti FLAG (IL-1b)
Caspase-1 [ng]
0
12.5
25
ASC [0 - 12.5 ng]
NLRP3-PYD
IFIX-PYD
IFI16-PYD
MNDA-PYD
AIM2-PYD
AIM2 full-length
b
copy number / HPRT
shRNA:
Aim2 #1
Aim2 #2
Aim2 #3
Control
c
IL-1b release (% of ATP)
d
poly(dA-dT)
LPS + ATP
IB: Caspase1
Aim2 #1 - p10
Aim2 #2 - p10
Aim2 #3 - p10
Control - p10
e
Medium
poly(dA-dT) 100 ng
poly(dA-dT) 200 ng
Percent cell viability
shRNA:
Control
AIM2 #3
f
C57BL/6 - p10
NLRP3 KO - p10
ASC KO - p10
Medium
Vaccinia virus
poly(dA-dT)
LPS + ATP
IB: Caspase1
g
Vaccinia virus - p10
Anthrax lethal toxin - p10
AIM2 #2
AIM2 #3
AIM2 #1
Control
IB: Caspase1
h
No stimulation
Vaccinia virus
Percent cell viability
MOI [5-0.625]
Vaccinia virus:
shRNA:
Control
Aim2 #1
Aim2 #2
Aim2 #3

Figure 3

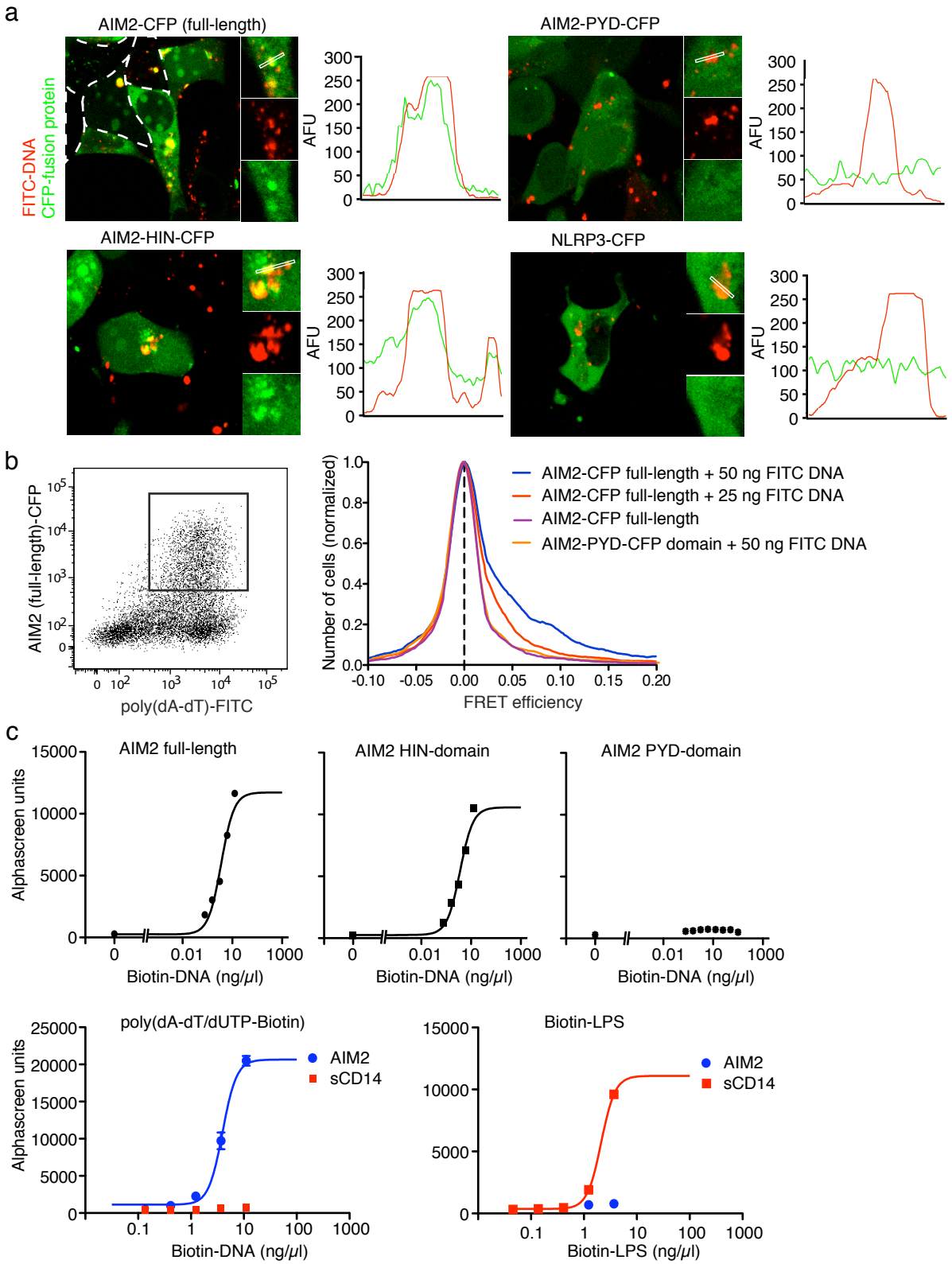
a
AIM2-CFP (full-length)
AIM2-PYD-CFP
AIM2-HIN-CFP
NLRP3-CFP
FITC-DNA
CFP-fusion protein
AFU
b
AIM2 (full-length)-CFP
poly(dA-dT)-FITC
Number of cells (normalized)
FRET efficiency
AIM2-CFP full-length + 50 ng FITC DNA
AIM2-CFP full-length + 25 ng FITC DNA
AIM2-CFP full-length
AIM2-PYD-CFP domain + 50 ng FITC DNA
c
AIM2 full-length
AIM2 HIN-domain
AIM2 PYD-domain
Alphascreen units
Biotin-DNA (ng/μl)
poly(dA-dT/dUTP-Biotin)
Biotin-LPS
AIM2
sCD14
Biotin-LPS (ng/μl)

Figure 4

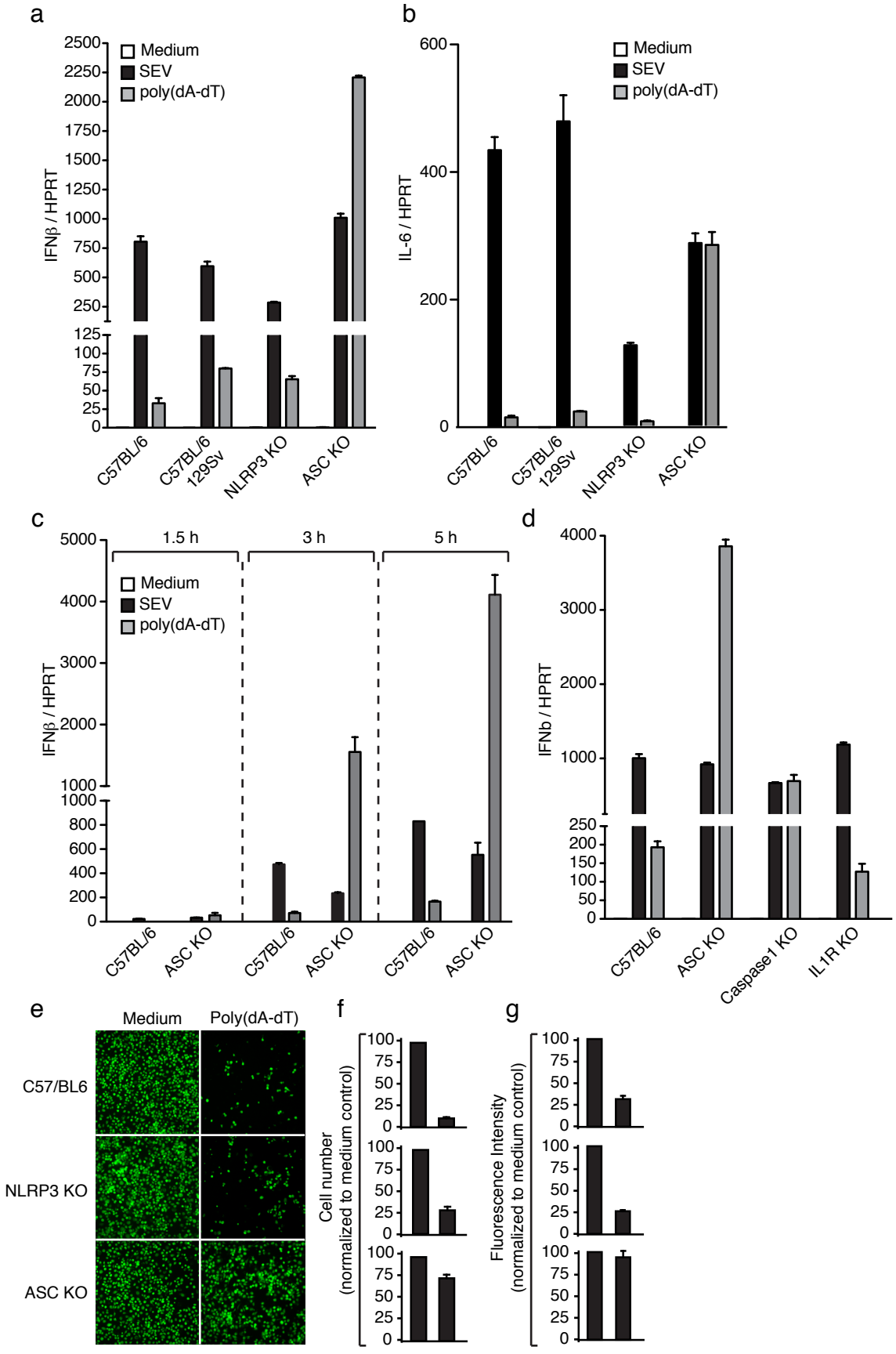

Supplementary Figure 1

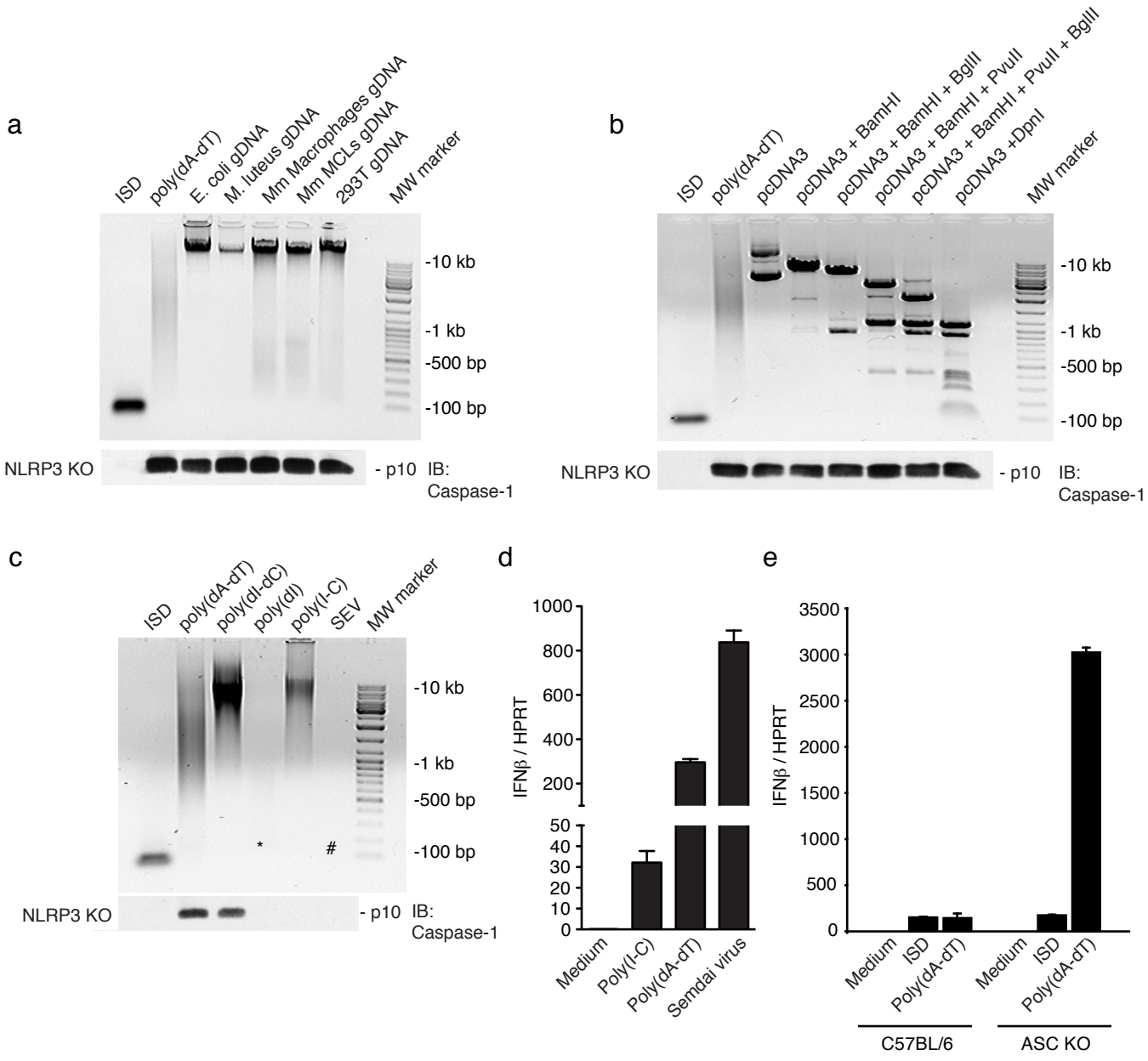

Supplementary Figure 2

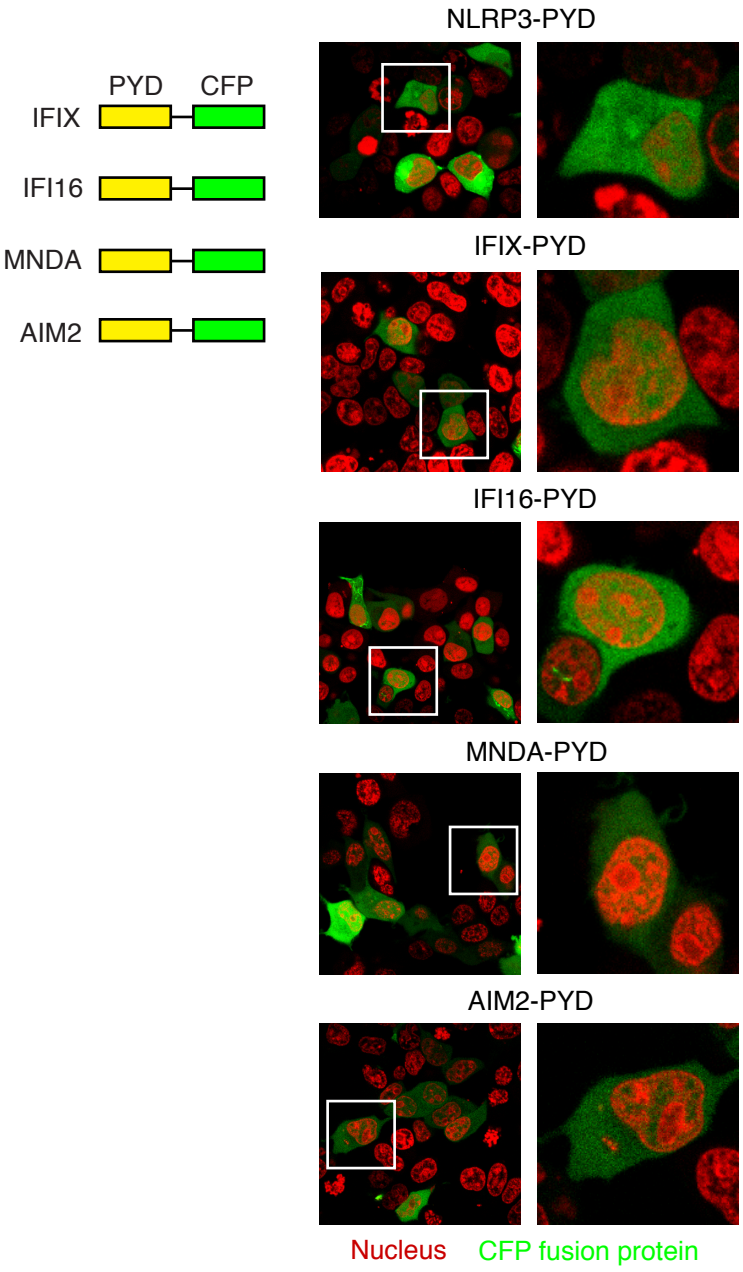

Supplementary Figure 3

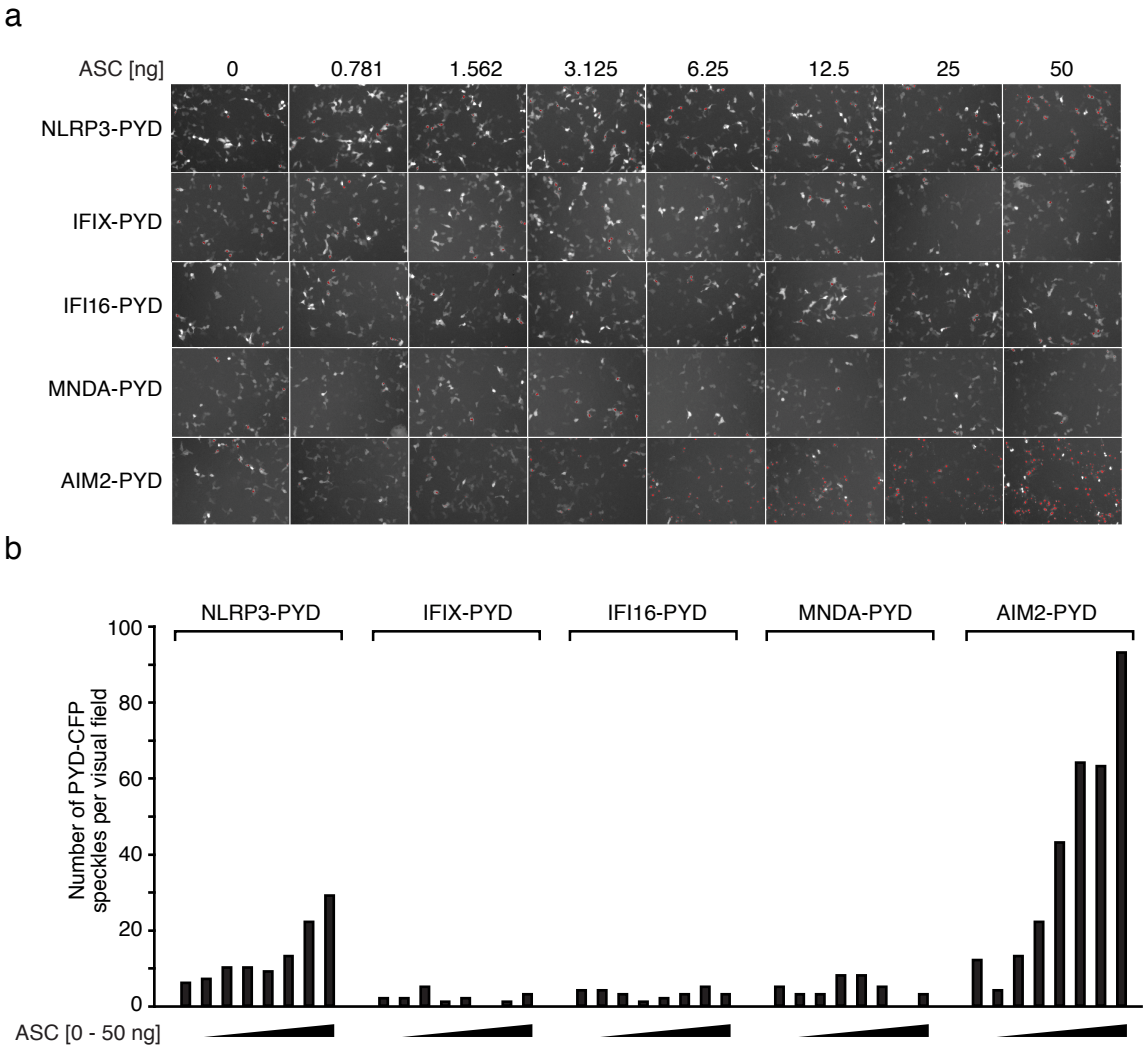

Supplementary Figure 4

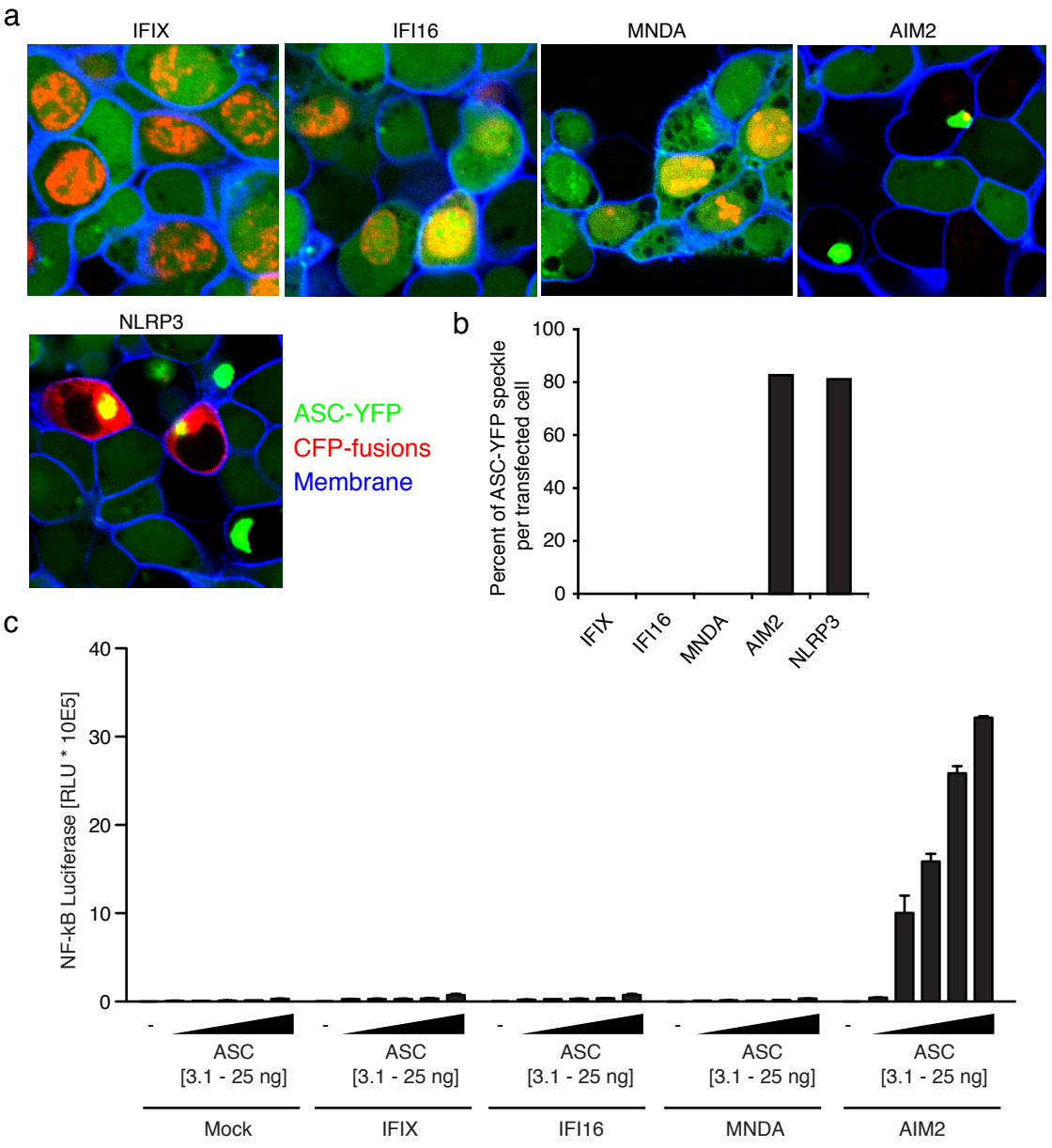

Supplementary Figure 5

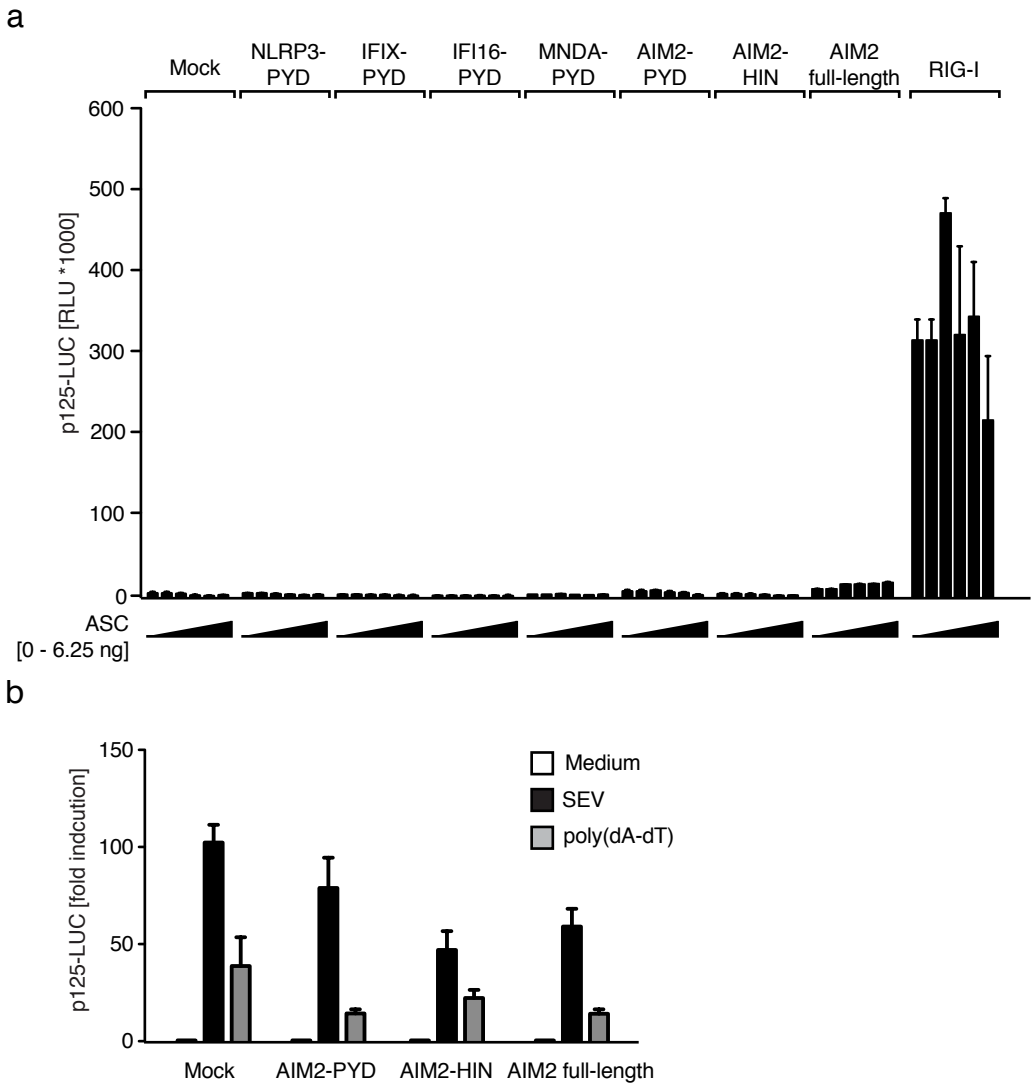

Supplementary Figure 6

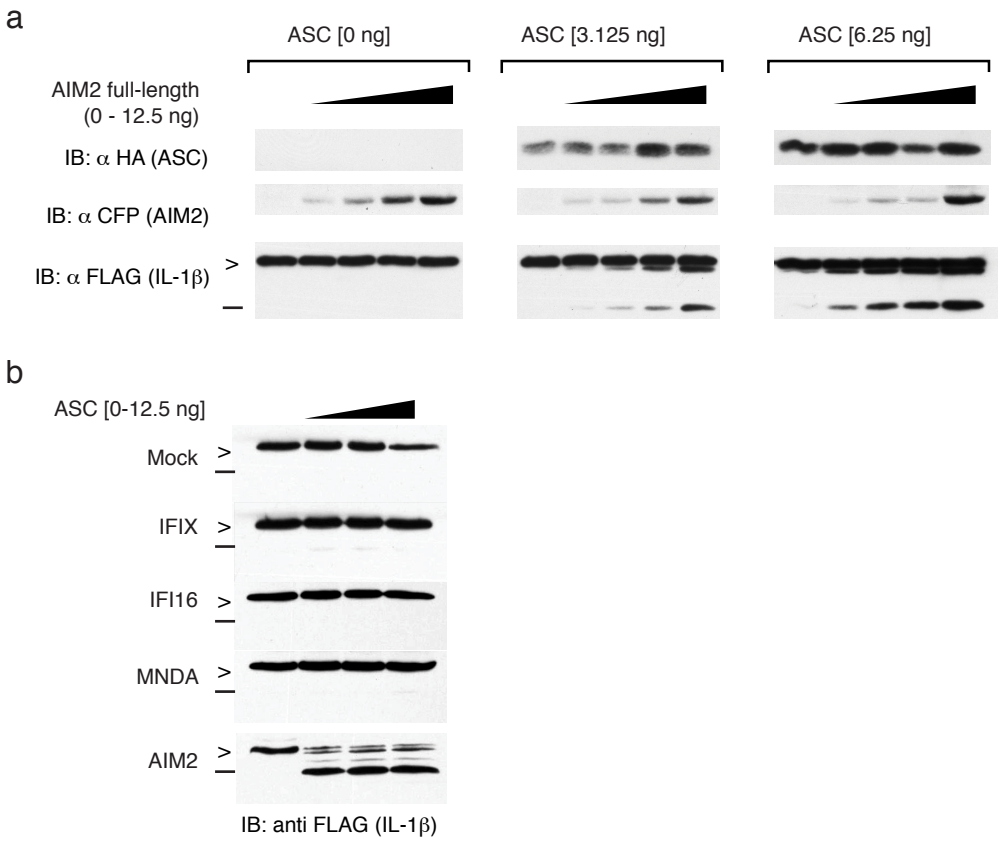

Supplementary Figure 7

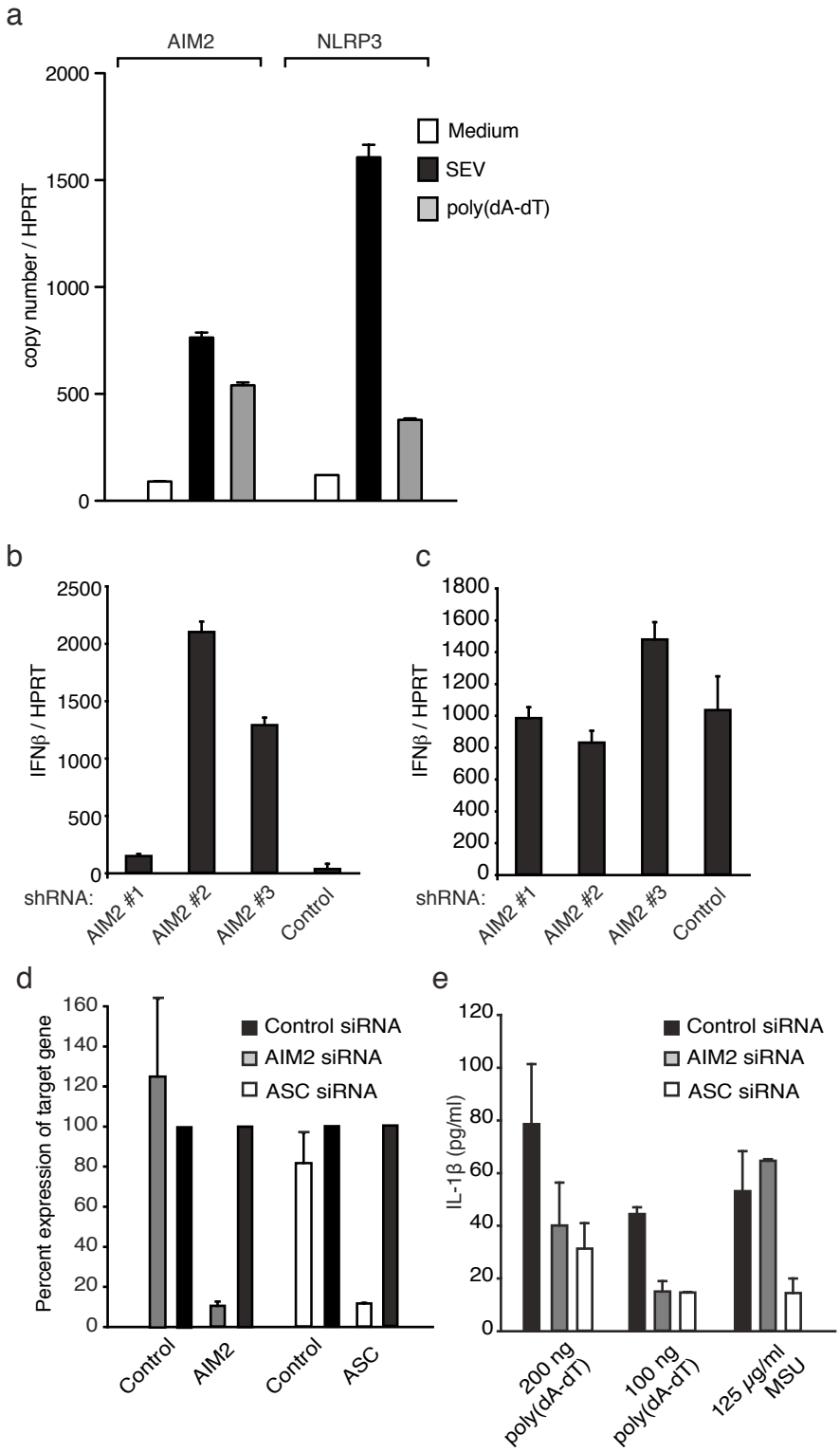

Supplementary Figure 8

METHODS

Plasmid constructs. Full length human AIM2 (AS 1-356; based on BC010940.1), AIM2 PYD (1-83), AIM2-HIN (148-356), IFIX (1-461; based on NM_198929), IFIX-PYD (1-84), IFI16 (1- 729; based on NM_005531), IFI16-PYD (1-84), MNDA (1-407), MNDA-PYD (1 84; based on NM_002432) and NLRP3-PYD (1-87; based on NM_004895.3) were cloned by PCR from cDNA into pEFBOS-C-term-CFP by using PCR-generated XhoI and BamHI or BglII restriction sites. AIM2 full length, AIM2-PYD and AIM2-HIN were subcloned into pEFBOS-C-term- FLAG/HIS using XhoI and BamHI. Murine pro-IL-1β (1-269) was obtained by PCR from cDNA and fused into pEFBOS-C-term-GLuc/FLAG using XhoI and BglII/BamHI. Primer sequences are available upon request. All constructs obtained by PCR-cloning were confirmed by sequencing. Expression plasmids (pCI) encoding human Caspase 1 and ASC-HA were from Millenium Pharmaceuticals (Cambridge, MA).

Reagents. ATP, LPS, poly(deoxyadenylic-thymidylic) acid sodium salt poly(dA-dT), were purchased from Sigma-Aldrich. A555-conjugated choleratoxin B was obtained from Molecular Probes, Invitrogen. DRAQ5 was purchased from Biostatus. Biotinylated and FITC labeled poly(dA-dT) were made by adding Biotin-dUTP or FITC-dUTP (Fermentas) in a molar ratio of 1:8 to dTTP in the enzymatic synthesis of poly(dA-dT) as described[1]. Anthrax lethal toxin was from List Biologicals (5 μg/ml PA and 5 μg/ml LF).

Mice. NLRP3 and ASC-deficient mice (*NLRP3*–/– and *Pycard*–/– respectively) were as previously described[2]. Both strains, as well as NLRP6–/– and NLRP12–/– mice were kindly 84 provided by Millennium Pharmaceuticals (Cambridge, MA). Caspase-1-deficient mice were from R. Flavell (Yale University, New Haven, CT). C57BL/6 mice, 129/Sv mice, C57/Bl6 # 129 F1 mice, IL-1R-deficient (*Il1r1*–/–) were purchased from Jackson Laboratories (Bar Harbor, ME). Seven to nine week-old animals were used in all experiments. All mouse strains were bred and maintained under specific pathogen-free conditions in the animal facilities at the University of Massachusetts Medical School.

Bioinformatics. Pyrin domain containing sequences were retrieved from UniProt after identifying them in SMART. A multiple sequence alignment of selected pyrin domains was generated using MUSCLE[3]. Secondary structure elements from the POP1 crystal structure ([4]; PDB code: 2HM2) were mapped to the multiple sequence alignment in PFAAT[5]. Prediction of nuclear targeting sequences and subcellular localization was done using PSORTII (http://psort.ims.u-tokyo.ac.jp/).

Cell culture and stimulation. Bone marrow derived macrophages were generated as described[6]. Macrophages were stimulated at a cell density of 2 Mio cells/ml. All primary cells and cell lines except THP1 cells were cultured in DMEM supplemented with L-Glutamine, Ciprofloxacin (all Cellgro, Manassas, VA) and 10% fetal calf serum (Hyclone, Logan, UT). THP1 cells were cultured in RPMI supplemented with 10% fetal calf serum (Cellgro), L-Glutamine, sodium pyruvate (Cellgro), and Ciprofloxacin. One day prior to stimulation, THP1 cells were differentiated using 0.5 μM PMA for three hours, washed three times and plated for stimulation. All experiments that were performed for caspase-1 immunoblot analysis were carried out in serum free DMEM medium. ATP stimulations were carried out at 5 mM one hour prior to harvesting supernatants. Poly(dA-dT) DNA and all other DNAs were transfected using Lipofectamine 2000 at a concentration of 1 μg/ml according to the manufacturer's instructions. Expression plasmids were transfected into 293T cells using GeneJuice (Novagen) according to the manufacturer's instructions. Vaccinia virus (WR strain) was used for infection at an MOI of 5 if not indicated otherwise.

ELISA. Cell culture supernatants were assayed for IL-1β using ELISA kits from BD Biosciences (Franklin Lakes, NJ) according to the manufacturer's instructions. To measure intracellular IL-1β, cells were washed and subjected to three freeze thaw cycles in assay diluent.

Confocal microscopy. Confocal microscopy was performed on a Leica SP2 AOBS confocal laser scanning microscope. Separation of CFP and YFP was performed using sequential scanning and 405 and 514 nm excitation.

Flow cytometry Fluorescence Resonance Energy Transfer (FRET). FRET is a dipole-dipole interaction where an excited donor fluorophore transfers its energy to an acceptor fluorophore in close proximity (1-10 nm). Shortly, three fluorescent intensities were measured: I1 – direct excitation and emission of donor, I2 – indirect excitation and direct emission of acceptor (also called sensitized emission), and I3 – direct excitation and emission of acceptor. After full correction for spectral bleed-through and cross excitation, FRET efficiency is calculated on a cell-by-cell basis[7] and then calculated FRET efficiency histograms were plotted with GraphPad Prism 5.01 (GraphPad Software).

Immunoblot analysis. For immunoblotting, cells were lysed in lysis buffer (150 mM NaCl, 10 mM Tris HCl pH 7.4, 1% CHAPS, protease inhibitor cocktail (Roche Applied Science)) and separated on sodium dodecyl sulphate-polyacrylamide gels and then transferred to nitrocellulose membranes (Amersham). For caspase-1 immunoblotting, supernatants were precipitated as previously described[8]. Membranes were blocked with 5% milk proteins in PBS and 0.05% Tween-20 and then incubated with the following antibodies: Anti murine caspase-1 p10 (sc-514, Santa Cruz Biotechnology), anti FLAG (M2, Sigma), anti HA (Roche Applied Science), anti CFP (Santa Cruz Biotechnology), anti ASC (Alexis, AL177), anti IFI16 (sc-8023, Santa Cruz Biotechnology), anti AIM2 (3B10 mouse IgG1[9]). Species-specific HRP-conjugated secondary antibodies were used and proteins detected using ECL reagent (GE Healthcare).

Co-immunoprecipitation assays. 293T cells in 24 wells were transfected with 1550 ng of the PYD-CFP expression plasmid of interest and 50 ng of ASC-HA. 24h after transfection, cells were lysed with lysis buffer. Lysates were cleared by centrifugation at 20.000 g for 30 min and subsequently incubated with anti-HA agarose beads for 2h at 4°C. Beads were washed 5 times and then boiled with Laemmli buffer for immunoblot analysis. THP1 cells were differentiated with PMA and primed with sendai virus (300 HAU/ml) overnight and subsequently lysed in high salt lysis buffer (250 mM NaCl, 10 mM Tris HCl pH 7.4, 1% CHAPS, protease inhibitor cocktail). Lysates were cleared by centrifugation at 20.000 g for 30 min, the salt concentration was adjusted to 125 mM NaCl and ASC was immunopreciptated using polyclonal rabbit anti-ASC (Alexis, AL177) bound to protein G

sepharose overnight. After 6 washes, beads were boiled with Laemmli buffer for immunoblot analysis.

Quantitative real-time PCR. RNA from murine macrophages was extracted with the RNeasy kit (Qiagen Inc., Valencia, CA). cDNA was synthesized with the iScript cDNA synthesis kit (Biorad, Hercules, CA), and quantitative RT-PCR analysis was performed on a DNA engine Opticon 2 cycler (MJ Research, Watertown MA) with the iQ SYBR Green Supermix (Biorad, Hercules, CA). The specificity of amplification was assessed for each sample by melting curve analysis. Relative quantification was performed using standard curve analysis. The murine quantification data are presented as a ratio to the hypoxanthine phosphoribosyltransferase 1 (HPRT1) level. The following primers for detection of *IFNβ*, *HPRT1* mRNAs were used. mmHPRT1, 5'-CTGGTGAAAAGGACCTCTCG-3' (forward) and 5'- TGAAGTACTCATTATAGTCAAGGGCA-3' (reverse), mmIFN*β*, 5'-ATAAGCAGCTCCAGCTCCAA-3' (forward) and 5'-CTGTCTGCTGGTGGAGTTCA-3' (reverse), mmAIM2 5'- GGCCGCATAGTCATCCTTTA-3' (forward) and mmAIM2 5'-CAACAGCATTTCCCGGTACT-3' (reverse) and mmNLRP3 5'-ATGCTGCTTCGACATCTCCT- 3' (forward) and mmNLRP3 5'-AACCAATGCGAGATCCTGAC-3' (reverse).

shRNA mediated silencing. The lentiviral shRNA expression plasmids were purchased from OpenBiosystems (Huntsville, AL). The shRNAs targeting AIM2 are TRCN0000096104 (#1), TRCN0000096105 (#2), TRCN0000096106 (#3). The control shRNA is directed against murine IFIH1 (TRCN0000103648) and was confirmed not to have impact on NLRP3 expression and AIM2 expression. The production of viral particles and transduction of target cells were conducted according to the following protocols (http://www.broad.mit.edu/genome_bio/trc/publicProtocols.html).

AlphaScreen Assay. The AlphaScreen (amplified luminescent-proximity homogeneous assay) was set up as an association assay. The protein of interest was transiently expressed in 293T cells and purified using FLAG beads (Sigma) binding to the C-terminal FLAG/HIS tag. The protein of interest was incubated at a concentration of 100 nM with biotinylated ligand at the indicated concentration in PBS, 0.1% BSA, and 0.01% Tween 20 for 60 min.

Subsequently, Nickel chelate acceptor beads (binding to the HIS tag) and streptavidin-coated donor beads (Alphascreen beads, Perkin Elmer) were added from 5x stock concentrations. After 30 min incubation at 25°C in the dark, samples in white 384-well plates (Proxiplate, Perkin Elmer) were read with the Envision HT microplate reader (Perkin Elmer). Data were analyzed by GraphPad Prism.

Reporter assays. For reporter assays, 293T cells (2 x 10E4 cells/100 µl/well in 96-well plates) were transfected with 50 ng of the indicated luciferase reporter gene. The thymidine kinase *Renilla*-luciferase reporter gene (Promega) (50 ng/well) was co transfected in order that the data could be normalized for transfection efficiency. In all cases, cell lysates were prepared and reporter gene activity was measured using the Dual Luciferase Assay System (Promega). Data are expressed as the mean relative stimulation + S.D. All of the experiments described were performed a minimum of three occasions and gave similar results.

siRNA transfection. THP1 cells were differentiated for 3h using 0.5µM PMA. Subsequently cells were plated at 2.5 x 10E4 cells/100 µl/well in 96-well plates and transfected with siRNA targeting human AIM2 (sense strand: 5'-CCCGAAGATCAACACGCTTCA-3'), human ASC (sense strand: 5'-CGGGAAGGTCCTGACGGATGA-3') or human TLR8 (5'-GGGAGUUACUGCUUGAAG A-3') using 275 ng siRNA and 0.75 µl Lipofectamine 2000. 48h after transfection cells were stimulated as indicated.

Cell viability assay. To quantify cell viability, macrophages (1 x 10E5 cells/100 µl/well in 96- well plates) were treated as described and subsequently incubated for 24h. After 24h, cells were washed with PBS and incubated in PBS with 5 µM calcein AM (Invitrogen) for 30 min at 37°C. The number of viable cells was assessed by counting fluorescent cells in two independent visual fields (20x) using ImageJ or by determining the overall fluorescence intensity using an Envision HT microplate reader.

Supplementary Figures

Supplementary Figure 1 | ASC-deficient macrophages are resistant to dsDNA-triggered cell death and show increased cytokine production in response to cytosolic dsDNA. A and b, Macrophages from either wild type, ASC- or NLRP3-deficient mice were transfected with poly(dA-dT) or stimulated with Sendai virus (300 HAU/ml). After 5h, IFN-β, IL-6 and HPRT1 mRNA expression was determined by real time PCR, whereas IFN-β (a) or IL-6 (b) expression levels were normalized to HPRT1 expression. **c,** Macrophages from wild type or ASC-deficient mice were treated as in (a) and IFN-β/HPRT1 expression was determined 1.5, 3 and 5h after stimulation. **d,** Macrophages from either wild type, ASC- caspase-1- or IL1Rdeficient mice were treated as in (a) and IFN-β/HPRT1 expression was determined 5h after stimulation. **e**, Macrophages were transfected with poly(dA-dT) or left untreated. 24h after transfection viable cells were labeled using calcein AM and subsequently visualized using fluorescent microscopy. Viable cells were counted in two independent visual fields of a 20X objective using ImageJ (**f**). In addition, overall fluorescent intensity was assessed (**g**). One representative experiment out of two independent experiments (a, b, c, d, e and f) is depicted as mean values ± s.d.

Supplementary Figure 2 | dsDNA from prokaryotic and eukaryotic sources activates caspase-1 independent of NLRP3. a, NLRP3-deficient macrophages were transfected with the dsDNA oligonucleotide immune stimulatory DNA (ISD), poly(dA-dT), genomic DNA from Escherichia coli (gram negative bacteria), genomic DNA from Micrococcus luteus (gram positive bacteria), genomic DNA from primary macrophages, genomic DNA from immortalized macrophages or genomic DNA from 293T cells. 6h after stimulation caspase-1 cleavage was assessed by immunoblot (lower panel). **b,** NLRP3-deficient macrophages were transfected with ISD, poly(dA-dT) or pcDNA3 undigested or digested to yield a maximal dsDNA product of either 5446 bp (BamHI), 4551 bp (BamHI and BglII), 2899 bp (BamHI and PvuII), 2004 bp (BamHI, PvuII and BglII) or 1108 bp (DpnI). 6h after stimulation caspase-1 cleavage was assessed by immunoblot (lower panel). **c,** NLRP3-deficient macrophages were transfected with ISD, poly(dA-dT), poly(dI-dC), poly(dI), poly(I-C) or infected with Sendai virus. 6h after stimulation caspase-1 cleavage was assessed by immunoblot. All nucleic acids (a, b, and c) were separated on a 1% agarose gel and stained

with ethidium bromide (upper panels). Of note, the single stranded homopolymer poly(dI) (*) could not be visualized using this technique given that ethidium bromide only intercalates in double stranded nucleic acids. **d**, wild type macrophages were transfected with poly(I-C), poly(dA-dT) or infected with Sendai virus. In addition, wild type macrophages or NLRP3 deficient macrophages were transfected with ISD or poly(dA-dT) (**e**). After 5h, IFN-β and HPRT1 mRNA expression was determined by real time PCR, whereas IFN-β expression levels were normalized to HPRT1 expression. Data from one representative experiment (a, b, c, d and e) out of two are shown.

Supplementary Figure 3 | PYD-CFP fusion constructs of the PYHIN family are located in the cytosol. 293T cells overexpressing CFP-tagged NLRP3-PYD, IFIX-PYD, IFI16-PYD, MNDA-PYD or AIM2-PYD (green) were analyzed by confocal microscopy and nuclei were stained with DRAQ5 dye (red). Data from on representative experiments out of three are shown.

Supplementary Figure 4 | Over expression of ASC induces complex formation of AIM2-PYD. 293T cells grown in 96-well were transfected with fixed amounts of PYD-CFP fusion constructs (100 ng) together with increasing amounts of ASC-HA (0, 0.78, 1.56, 3.13, 6.25, 12.5, 25 and 50 ng). 24h after transfection, cells were imaged by epifluorescence microscopy. Cluster formation of the PYD-CFP fusion constructs were quantified using ImageJ. The detected protein clusters of above-threshold fluorescence intensity are highlighted in red color and overlaid on greyscale images of below threshold fluorescence intensity (non-clustered protein) (**a**). The absolute count of PYD-CFP clusters per visual field of a 20X objective as analyzed by ImageJ is shown in (**b**). One representative experiment out of three independent experiments is shown.

Supplementary Figure 5 | Only full length AIM2 induces complex formation of ASC and ASC-dependent NF-kB activation. a, Stable HEK293-ASC-YFP (green) cells were transiently transfected with CFP-tagged IFIX, IFI16, MNDA, AIM2 or NLRP3 (all in red), the membrane was stained with choleratoxin (blue) and cells were then imaged by confocal microscopy and the percentage of ASC-YFP speckles per transfected cells was assessed **(b)**.

c, 293T cells were transfected with a multimerized NF-κB luciferase reporter construct together with fixed amounts of constructs as in **(a)** alone or together with increasing amounts of ASC. Cellular NF-κB activation was quantified in cell lysates 24 hours after transfection. Data of one representative experiment out of two (a and b) or three (c) are depicted.

Supplementary Figure 6 | AIM2 is not involved in IFN induction. a, 293T cells grown in well plates were transfected with a pIFNβ luciferase reporter construct (p125-LUC) together with fixed amounts of NLRP3-PYD or IFIX, IFI16 or MNDA-PYD CFP fusion constructs, AIM2- PYD, AIM2 HIN domain, AIM2 full length or RIG-I (100 ng) alone or together with increasing amounts of ASC. Transactivation of the IFNβ promoter was quantified in cell lysates 24 hours after transfection. **b,** 293T cells were transfected with either AIM2-PYD, AIM2 HIN domain or AIM2 full length (100 ng) together with p125-LUC. 24h after transfection cells were retransfected with 200 ng poly(dA-dT) and after an additional period of 24h, transactivation of the IFNβ promoter was quantified in cell lysates by luminometry. Data of one representative experiment out of three are depicted as mean values ± s.d.

Supplementary Figure 7 | Low level expression of full length AIM2 induces robust cleavage of IL-1β. a, 293T cells were transfected with caspase-1 (12.5 ng), ASC (3.1 or 6.25 ng), pro-IL-1β (100 ng) and ascending amounts of AIM2 full length (1.56, 3.12, 6.25, 12.5 ng). Cell lysates were immunoblotted for ASC expression (HA epitope), AIM2 expression (CFP tag) and the C-terminally epitope tagged IL-1β, recognizing both the pro-IL-1β form (>) and the cleaved IL-1β form (-) 24h after transfection. **b,** 293T cells were transfected with caspase-1 (12.5 ng), ASC (6.25 ng), pro-IL-1β (100 ng) and either full length IFIX, IFI16, MDNA or AIM2 (81.25 ng) and analyzed as in **(a)**. One representative experiment out of two is depicted (a and b).

Supplementary Figure 8 | Knock down of AIM2 expression strongly enhances poly(dAdT) triggered type I IFN production. a, Macrophages from wild type mice were transfected with poly(dA-dT) or stimulated with Sendai virus (300 HAU/ml). After 5h, AIM2, NLRP3 and HPRT1 mRNA expression was determined by real time PCR. The expression levels were normalized to HPRT1 expression. Murine macrophage cells (B6-MCLs) were

transduced with lentiviral vectors encoding shRNAs targeting AIM2 (AIM2#1, AIM2#2, AIM2#3) or an irrelevant control gene (Ctrl.) and were stimulated with either poly(dA-dT) (**b**) or Sendai virus (300 HAU/ml) (**c**) and IFNβ/HPRT1 expression was determined after 5h. d, siRNAs targeting human AIM2, ASC or TLR8 (Control siRNA) were contransfected into 293T cells with expression plasmids coding for either AIM2-CFP or ASC-CFP, whereas MNDA-CFP served as a control target (Control). 24h after transfection, CFP expression was assessed by FACS and is depicted as percent expression in relation to the control siRNA. **e,** THP1 cells were transfected with siRNA targeting TLR8 (Control), AIM2 or ASC. 48h after transfection, cells were stimulated with 200 or 100ng poly(dA-dT) or 125 µg/ml MSU crystals. 6h after stimulation IL-1β production was assessed by ELISA. One representative experiment out of two (a, d and e) or four (b and c) independent experiments is depicted as mean values ± s.d.

References

[1] H. K. Schachman, J. Adler, C. M. Radding et al., *The Journal of biological chemistry* **235**, 3242 (1960).

[2] T. D. Kanneganti, M. Body-Malapel, A. Amer et al., *The Journal of biological chemistry* **281** (48), 36560 (2006).

[3] R. C. Edgar, *Nucleic acids research* **32** (5), 1792 (2004).

[4] A. Natarajan, R. Ghose, and J. M. Hill, *The Journal of biological chemistry* **281** (42), 31863 (2006).

[5] D. R. Caffrey, P. H. Dana, V. Mathur et al., *BMC bioinformatics* **8**, 381 (2007).

[6] M. Severa, E. M. Coccia, and K. A. Fitzgerald, *The Journal of biological chemistry* **281** (36), 26188 (2006).

[7] G. Szentesi, G. Horvath, I. Bori et al., *Computer methods and programs in biomedicine* **75** (3), 201 (2004).

[8] V. Hornung, F. Bauernfeind, A. Halle et al., *Nat Immunol* **9** (8), 847 (2008).

[9] K. S. Cresswell, C. J. Clarke, J. T. Jackson et al., *Biochemical and biophysical research communications* **326** (2), 417 (2005).

3. Danksagung

Für die Überlassung des Themas und die herzliche Aufnahme in die Arbeitsgruppe möchte ich mich bei Herrn Professor Dr. Stefan Endres und Herrn Prof. Dr. Gunther Hartmann bedanken. Ferner gilt mein Dank Ihrer außerordentlichen Unterstützung und der Möglichkeit zum Besuch internationalen Kongressen. Auch möchte ich mich für die Aufnahme in das Graduiertenkolleg 1202 *Oligonukleotide in Zellbiologie und Therapie* der Deutschen Forschungsgemeinschaft bedanken.

Für die außergewöhnliche Betreuung und die herausragende Anleitung zum wissenschaftlichen Arbeiten möchte ich mich bei meinem Betreuer Professor Dr. Veit Hornung bedanken.

Bei Herrn Professor Dr. Dr. Jürgen Heesemann möchte ich mich für das Stipendium im Rahmen des Graduiertenprogramms *Molekulare Medizin* der LMU bedanken.

Ferner gilt mein Dank den Mitdoktoranden Michael Berger und Franz Bauernfeind für die herzliche Zusammenarbeit und tatkräftige Unterstützung.

4. Veröffentlichungen

4.1. Originalarbeiten:

1. **Ablasser A**, Bauernfeind F, Hartmann G, Latz E, Fitzgerald KA, Hornung V.
RIG-I-dependent sensing of poly(dA:dT) through the induction of an RNA polymerase III-transcribed RNA intermediate.
Nature Immunology. 2009; [Epub ahead of print]

2. **Ablasser A**, Poeck H, Anz D, Berger M, Schlee M, Kim S, Bourquin C, Goutagny N, Jiang Z, Fitzgerald KA, Rothenfusser S, Endres S, Hartmann G, Hornung V.
Selection of molecular structure and delivery of RNA oligonucleotides to activate TLR7 versus TLR8 and to induce high amounts of IL-12p70 in primary human monocytes.
Journal of Immunology. 2009 Jun 1;182(11):6824-33.

3. Berger M, **Ablasser A**, Kim S, Bekeredjian-Ding I, Giese T, Endres S, Hornung V, Hartmann G.
TLR8-driven IL-12-dependent reciprocal and synergistic activation of NK cells and monocytes by immunostimulatory RNA.
Journal of Immunotherapy. 2009 Apr;32(3):262-71.

4. Hornung V, **Ablasser A**, Charrel-Dennis M, Bauernfeind F, Horvath G, Caffrey DR, Latz E, Fitzgerald KA.
AIM2 recognizes cytosolic dsDNA and forms a caspase-1-activating inflammasome with ASC.
Nature. 2009 Mar 26;458(7237):514-8.

5. Bekeredjian-Ding I, Roth SI, Gilles S, Giese T, **Ablasser A**, Hornung V, Endres S, Hartmann G.
T cell-independent, TLR-induced IL-12p70 production in primary human monocytes.
Journal of Immunology. 2006 Jun 15;176(12):7438-46.

6. Hornung V, Guenthner-Biller M, Bourquin C, **Ablasser A**, Schlee M, Uematsu S, Noronha A, Manoharan M, Akira S, de Fougerolles A, Endres S, Hartmann G.
Sequence-specific potent induction of IFN-alpha by short interfering RNA in plasmacytoid dendritic cells through TLR7.
Nature Medicine. 2005 Mar;11(3):263-70.

4.2. Kongressabstracts (Erstautor):

1. **Ablasser A**, Hornung V, Endres S, Hartmann G.
Differential delivery agents modulate the fate of RNA to induce reciprocal cytokine responses.
2nd annual meeting of the Oligonucleotide Therapeutic Society, Rockefeller University, New York 2006, Abstract 12.

2. **Ablasser A**, Hornung V, Berger M, Kim S, Bekeredjian-Ding I, Endres S, Hartmann G.
Single-stranded RNA as potent TLR8 Ligand in humans.
1st meeting of the Oligonucleotide Therapeutic Society, Rockefeller University, New York 2005, Abstract 2.

3. **Ablasser A**, Hornung V, Berger M, Kim S, Bekeredjian-Ding I, Endres S, Hartmann G.
Single-stranded RNA as potent TLR8 Ligand in humans.
Crossroads between Innate and adaptive Immunity, Rhodes, Greece 2005, Abstract 46.

4.3. Buchkapitel:

Ablasser A, Hartmann G, Hornung V.
RNA interference in the scope of the immune system.
Nucleic acids in innate immunity, edited by Ishii, Akira; *CRC Press* 2008

5. Lebenslauf

Andrea Ablasser

geboren am 13.07.1983 in Bad Friedrichshall als Tochter von Dipl.-Math. Irmgard Ablasser und Dr. med. Ambros Ablasser.

Schulische Ausbildung:

1989-1993	Grundschule Buchloe
1993-1997	Joseph-Bernhart-Gymnasium Türkheim
1997-2001	Gymnasium mit Schülerheim Hohenschwangau
2001	Abitur (Note: 1,1)

Studium:

2001	Beginn des Studiums für Humanmedizin an der Ludwig-Maximilians-Universität München
10/2002-03/2003	Kursus der Makroskopischen Anatomie, Universidad Miguel Hernández de Elche, Alicante, Spanien
10/2003	Physikum (Note: 2,0)
2007-2008	Praktisches Jahr: 1. Innere Medizin am Beth Israel Deaconess Medical Center, Harvard Medical School, Boston, USA 2. Pädiatrie am Dr. von Haunerschen Kinderspital, LMU München und am John Radcliffe Hospital, University of Oxford, Oxford, England 3. Chirurgie am Klinikum Großhadern, LMU München
2008	Staatsexamen Medizin (Gesamtnote: 1,0) Approbation als Arzt

Promotion:

2004-2007	Doktorarbeit in der Abteilung für Klinische Pharmakologie, Leiter: Prof. Dr. Stefan Endres Medizinische Klinik Innenstadt, Klinikum der Universität München
08/2005-09/2005	Forschungsaufenthalt in der Arbeitsgruppe von Katherine A. Fitzgerald, University of Massachusetts, Worcester, USA

Stipendien:

02/2004-08/2006:	Promotionsstudium „Molekulare Medizin“, LMU München
2005:	Studienstiftung des deutschen Volkes
08/2005:	Reisestipendium der Boehringer-Ingelheim-Foundation

10/2005-04/2006:	Graduiertenkolleg 1201 *Oligonucleotides in cell biology and therapy* der Deutschen Forschungsgemeinschaft (DFG)
03/2007-07/2007:	Reisestipendium des Deutschen Akademischen Austauschdienst (DAAD)
03/2007-07/2007:	PJ-Stipendium im Rahmen der München-Harvard-Allianz

Beruf:

08/2008-11/2008:	Forschungsaufenthalt bei Eicke Latz und Katherine A. Fitzgerald, University of Massachusetts, Worcester, USA
seit 11/2008:	Assistenzarzt am Institut für Klinische Chemie und Pharmakologie, Rheinische Friedrich-Wilhelms-Universität Bonn